Supporting in information

Novel Quinazolinone Inhibitors of ALK2 Flip between Alternate Binding Modes: SAR, Structural Characterization, Kinase Profiling and Cellular Proof of Concept

Liam Hudson[§], James Mui[§], Santiago Vázquez[†], Diana M. Carvalho[§], Eleanor Williams[‡], Chris Jones[§], Alex N. Bullock[‡], Swen Hoelder[§]*

[§] Institute of Cancer Research, 15 Cotswold Road, Sutton, Surrey, SM2 5NG, United Kingdom

[‡] Structural Genomics Consortium, University of Oxford, Old Road Campus Research Building, Roosevelt Drive, Oxford OX3 7DQ, United Kingdom

[†] Laboratori de Química Farmacèutica (Unitat Associada al CSIC), Facultat de Farmàcia i Ciències de l'Alimentació, and Institute of Biomedicine (IBUB), Universitat de Barcelona, Av. Joan XXIII s/n, Barcelona E-08028, Spain

Contents

1. 16 and 21 kinome selectivity data

Table S1: DiscoverX selectivity data for compounds **16** and **21**

(P – phosphorylated; nP – nonphosphorylated; % Ctrl values show the % of DNA-tagged kinase which was not displaced from a solid supported ligand by a test compound relative to untreated control, quantified by qPCR).

Please note: ALKs 1, 2, 3, 4, 5 and 6 are listed by their gene symbols: ACVRL1 (ALK1), ACVR1 (ALK2), BMPR1A (ALK3), ACVR1B (ALK4), TGFBR1 (ALK5) and BMPR1B (ALK6)

Cmpd	DiscoverX Gene Symbol	Entrez Gene Symbol	% Ctrl	Cmpd Conc (nM)
16	KIT	KIT	1.8	1000
	BMPR1B	BMPR1B	4.1	1000
	PDGFRA	PDGFRA	8.7	1000
	ACVR1	ACVR1	17	1000
	PDGFRB	PDGFRB	20	1000
	ACVRL1	ACVRL1	44	1000
	MINK	MINK1	51	1000
	PAK2	PAK2	54	1000
	BRAF(V600E)	BRAF	58	1000
	EGFR(L858R)	EGFR	63	1000
	BMPR2	BMPR2	64	1000
	BRAF	BRAF	65	1000
	CDK11	CDK19	68	1000
	CSNK1D	CSNK1D	68	1000
	EGFR	EGFR	71	1000
	PAK1	PAK1	71	1000
	ABL1-nP	ABL1	76	1000
	TRKA	NTRK1	76	1000
	ABL1-P	ABL1	77	1000
	BMPR1A	BMPR1A	77	1000
	TNK1	TNK1	78	1000
	SRPK3	SRPK3	79	1000
	MET	MET	80	1000

	FLT3	FLT3	83	1000
	ABL1(E255K)-P	ABL1	84	1000
	IKK-beta	IKBKB	84	1000
	PDPK1	PDPK1	84	1000
	MEK2	MAP2K2	85	1000
	AKT2	AKT2	86	1000
	IKK-alpha	CHUK	86	1000
	PLK1	PLK1	86	1000
	YANK3	STK32C	86	1000
	PCTK1	CDK16	87	1000
	RAF1	RAF1	88	1000
	RIPK2	RIPK2	88	1000
	SRC	SRC	88	1000
	MEK1	MAP2K1	89	1000
	PIM2	PIM2	89	1000
	PKAC-alpha	PRKACA	89	1000
	CSNK1G2	CSNK1G2	90	1000
	DYRK1B	DYRK1B	90	1000
	MARK3	MARK3	90	1000
	PLK3	PLK3	90	1000
	CSF1R	CSF1R	91	1000
	DCAMKL1	DCLK1	92	1000
	MKNK1	MKNK1	92	1000
	PIM1	PIM1	92	1000
	PRKCE	PRKCE	92	1000
	RET	RET	92	1000
	TYK2(JH1domain)	TYK2	92	1000
	ULK2	ULK2	93	1000
	AKT1	AKT1	94	1000
	CDK9	CDK9	94	1000
	CDK2	CDK2	95	1000
	GSK3B	GSK3B	95	1000
	VEGFR2	KDR	95	1000
	AXL	AXL	96	1000
	LKB1	STK11	96	1000

	MAPKAPK2	MAPKAPK2	96	1000
	SIK2	SIK2	96	1000
	TGFBR1	TGFBR1	96	1000
	ABL2	ABL2	97	1000
	AURKB	AURKB	97	1000
	CDK7	CDK7	97	1000
	ERK1	MAPK3	97	1000
	FAK	PTK2	97	1000
	MLK1	MAP3K9	97	1000
	NEK7	NEK7	97	1000
	PAK4	PAK4	97	1000
	ACVR2B	ACVR2B	98	1000
	JAK3(JH1domain)	JAK3	98	1000
	JNK3	MAPK10	98	1000
	LCK	LCK	98	1000
	ALK	ALK	99	1000
	BTK	BTK	99	1000
	JAK2(JH1domain)	JAK2	99	1000
	TIE2	TEK	99	1000
	ABL1(T315I)-P	ABL1	100	1000
	ACVR1B	ACVR1B	100	1000
	ACVR2A	ACVR2A	100	1000
	ADCK3	CABC1	100	1000
	AURKA	AURKA	100	1000
	CDK3	CDK3	100	1000
	CHEK1	CHEK1	100	1000
	EPHA2	EPHA2	100	1000
	ERBB2	ERBB2	100	1000
	ERBB4	ERBB4	100	1000
	FGFR2	FGFR2	100	1000
	FGFR3	FGFR3	100	1000
	FYN	FYN	100	1000
	IGF1R	IGF1R	100	1000
	INSR	INSR	100	1000
	JNK1	MAPK8	100	1000

	JNK2	MAPK9	100	1000
	KIT(D816H)	KIT	100	1000
	KIT(V559D,T670I)	KIT	100	1000
	MAP3K4	MAP3K4	100	1000
	MKNK2	MKNK2	100	1000
	NEK6	NEK6	100	1000
	p38-alpha	MAPK14	100	1000
	p38-beta	MAPK11	100	1000
	PIK3C2B	PIK3C2B	100	1000
	PIK3CA	PIK3CA	100	1000
	PIK3CG	PIK3CG	100	1000
	PIM3	PIM3	100	1000
	PLK4	PLK4	100	1000
	RIOK2	RIOK2	100	1000
	ROCK2	ROCK2	100	1000
	RSK2(Kin.Dom.1-N-terminal)	RPS6KA3	100	1000
	SNARK	NUAK2	100	1000
	TSSK1B	TSSK1B	100	1000
	ZAP70	ZAP70	100	1000
21	BMPR1B	BMPR1B	1.6	1000
	ACVR1	ACVR1	5.5	1000
	BRAF(V600E)	BRAF	11	1000
	ACVRL1	ACVRL1	16	1000
	BRAF	BRAF	17	1000
	ACVR1B	ACVR1B	18	1000
	RAF1	RAF1	25	1000
	TGFBR1	TGFBR1	30	1000
	PIM1	PIM1	60	1000
	PAK4	PAK4	62	1000
	BMPR1A	BMPR1A	65	1000
	ACVR2B	ACVR2B	67	1000
	RIPK2	RIPK2	68	1000
	JAK2(JH1domain)	JAK2	75	1000
	PLK1	PLK1	75	1000
	BMPR2	BMPR2	76	1000

	PAK2	PAK2	77	1000
	ULK2	ULK2	77	1000
	JNK3	MAPK10	79	1000
	MEK2	MAP2K2	79	1000
	PDGFRB	PDGFRB	81	1000
	ACVR2A	ACVR2A	83	1000
	MARK3	MARK3	83	1000
	MEK1	MAP2K1	85	1000
	DCAMKL1	DCLK1	87	1000
	CSNK1D	CSNK1D	88	1000
	MET	MET	88	1000
	MINK	MINK1	89	1000
	TIE2	TEK	89	1000
	CDK11	CDK19	90	1000
	KIT(D816H)	KIT	90	1000
	MAP3K4	MAP3K4	90	1000
	p38-alpha	MAPK14	90	1000
	TNK1	TNK1	90	1000
	ABL1-nP	ABL1	91	1000
	JNK1	MAPK8	91	1000
	JNK2	MAPK9	91	1000
	MLK1	MAP3K9	91	1000
	PRKCE	PRKCE	91	1000
	CSNK1G2	CSNK1G2	92	1000
	DYRK1B	DYRK1B	92	1000
	FLT3	FLT3	92	1000
	MKNK2	MKNK2	92	1000
	ABL2	ABL2	93	1000
	AKT2	AKT2	93	1000
	INSR	INSR	93	1000
	MKNK1	MKNK1	93	1000
	PDGFRA	PDGFRA	93	1000
	TRKA	NTRK1	93	1000
	AURKB	AURKB	94	1000
	CDK3	CDK3	94	1000

	IGF1R	IGF1R	94	1000
	JAK3(JH1domain)	JAK3	94	1000
	PCTK1	CDK16	94	1000
	ABL1(E255K)-P	ABL1	95	1000
	CSF1R	CSF1R	95	1000
	IKK-beta	IKBKB	95	1000
	PDPK1	PDPK1	95	1000
	TYK2(JH1domain)	TYK2	95	1000
	YANK3	STK32C	95	1000
	LCK	LCK	96	1000
	PAK1	PAK1	96	1000
	PIM2	PIM2	96	1000
	PLK3	PLK3	96	1000
	SRPK3	SRPK3	96	1000
	ABL1(T315I)-P	ABL1	97	1000
	ABL1-P	ABL1	97	1000
	ADCK3	CABC1	97	1000
	GSK3B	GSK3B	97	1000
	KIT	KIT	97	1000
	RIOK2	RIOK2	97	1000
	RSK2(Kin.Dom.1-N-terminal)	RPS6KA3	97	1000
	AXL	AXL	98	1000
	EGFR	EGFR	98	1000
	EGFR(L858R)	EGFR	98	1000
	ERK1	MAPK3	98	1000
	FAK	PTK2	98	1000
	KIT(V559D,T670I)	KIT	98	1000
	PIK3C2B	PIK3C2B	98	1000
	PIK3CG	PIK3CG	98	1000
	PIM3	PIM3	98	1000
	SRC	SRC	98	1000
	p38-beta	MAPK11	99	1000
	RET	RET	99	1000
	VEGFR2	KDR	99	1000
	ZAP70	ZAP70	99	1000

	AKT1	AKT1	100	1000
	ALK	ALK	100	1000
	AURKA	AURKA	100	1000
	BTK	BTK	100	1000
	CDK2	CDK2	100	1000
	CDK7	CDK7	100	1000
	CDK9	CDK9	100	1000
	CHEK1	CHEK1	100	1000
	EPHA2	EPHA2	100	1000
	ERBB2	ERBB2	100	1000
	ERBB4	ERBB4	100	1000
	FGFR2	FGFR2	100	1000
	FGFR3	FGFR3	100	1000
	FYN	FYN	100	1000
	IKK-alpha	CHUK	100	1000
	LKB1	STK11	100	1000
	MAPKAPK2	MAPKAPK2	100	1000
	NEK6	NEK6	100	1000
	NEK7	NEK7	100	1000
	PIK3CA	PIK3CA	100	1000
	PKAC-alpha	PRKACA	100	1000
	PLK4	PLK4	100	1000
	ROCK2	ROCK2	100	1000
	SIK2	SIK2	100	1000
	SNARK	NUAK2	100	1000
	TSSK1B	TSSK1B	100	1000

2. Crystallographic data

Table S2: Crystallographic table for the structures of 11, 16 and 21.

	5-Methyl-6-(quinolin-5-yl)quinazolin-4(3H)-one (11)	**3-(4-Morpholinophenyl)-6-(quinolin-4-yl)quinazolin-4(3H)-one (16)**	**2,5-Dimethyl-6-(quinolin-4-yl)quinazolin-4(3H)-one (21)**
PDB ID	6GI6	6GIN	6GIP
Wavelength (Å)	0.9795	0.9795	0.9763
Resolution range	53.33 - 1.98 (2.06 - 1.98)	73.42 - 2.20 (2.28 - 2.20)	57.89 - 2.17 (2.24 – 2.17)
Space group	P 32 2 1	P 2 21 21	P 32 2 1
a b c (Å)	66.15, 66.15, 146.00	59.08, 86.39, 139.29	66.85, 66.85, 139.93
α β γ (°)	90, 90, 120	90, 90, 90,	90, 90, 120,
Total reflections	50508 (5016)	72347 (7162)	39652 (3882)
Unique reflections	26281 (2603)	36780 (3651)	19839 (1943)
Multiplicity	4.2 (4.4)	4.6 (4.1)	7.5 (7.7)
Completeness (%)	99.59 (99.62)	99.76 (99.78)	100.00 (100.00)
Mean I/sigma(I)	4.29 (1.68)	9.10 (3.01)	8.0 (2.0)
Wilson B-factor	16.22	25.82	21.71
R-merge	0.141 (0.457)	0.051 (0.242)	0.245 (1.216)
Reflections used in refinement	26281 (2603)	36767 (3650)	30159 (2950)
Reflections used for R-free	1302 (125)	1916 (187)	1550 (136)
R-work	0.2233	0.1838	0.1945
R-free	0.2684	0.2323	0.2361
Number of non-hydrogen atoms	2605	5157	2518
macromolecules	2353	4676	2363
ligands	81	104	51
solvent	171	377	104
Protein residues	298	592	296
RMS(bonds, Å)	0.007	0.006	0.008
RMS(angles, °)	0.97	0.94	1.21
Ramachandran favored (%)	97.97	97.96	96.94
Ramachandran allowed (%)	2.03	1.87	3.06
Ramachandran outliers (%)	0	0.17	0
Rotamer outliers (%)	0	0.2	0.39
Average B-factor	16.47	33.39	22.2
macromolecules	15.9	32.94	21.7
ligands	24.72	29.42	37.6
solvent	20.36	40.13	24.7
Number of TLS groups	3	8	-

3. Experimental procedures

3.1. Co-crystal Structure Determination

The construct used runs from residue V204 to D499 (Uniprot ID, Q04771) which includes the kinase domain of ALK2, and was prepared as detailed previously[1] concentrated to 10 mg/mL buffered in 50 mM HEPES, pH 7.5, 300 mM NaCl, 10 mM DTT. The construct contains the Q207D activating mutation; chosen to be a constitutively active mutation based upon the physiological Q207E mutation seen in the condition Fibrodysplasia Ossificans Progressiva. Mass spectrometry confirmed that the sample crystallised is un-phosphorylated, however upon addition of ATP autophosphorylate was observed (also by mass spectrometry) thus confirming that the kinase is still active. Crystallization was performed using the sitting drop vapor diffusion method at 4 °C. Viable crystals of ALK2 in complex with test compound grew as follows: Compound **11** in a 150 nL drop, mixing the protein, preincubated with 1 mM compound, with a reservoir solution containing 1.5 M ammonium sulfate, 0.1 M sodium chloride, 0.1 M bis-tris pH 6.5 at a 2:1 volume ratio. Compound **16** in a 150 nL drop, mixing the protein, preincubated with 1 mM compound, with a reservoir solution containing 1.6 M ammonium sulfate, 12% glycerol, 0.1 M tris pH 8.5 at a 1:1 volume ratio. Compound **21** in a 150 nL drop, mixing the protein, preincubated with 1 mM compound, with a reservoir solution containing 1.5 M ammonium sulfate, 0.1 M tris pH 8.5, 4% glycerol at a 2:1 volume ratio. Crystals were transferred into a cryoprotective solution prepared from the mother liquor supplemented with 25% ethylene glycol prior to vitrification in liquid nitrogen. Diffraction data were collected at Diamond Light Source (beamlines I02 (**11**), I04 (**16**) and I03 (**21**)), and were processed and scaled with MOSFLM[2] and AIMLESS from the CCP4 suite[3]. The structures were solved by molecular replacement using PHASER[4] and the structure of the ALK2-LDN-193189 complex (PDB 3Q4U) as a search model. Subsequent manual model building was performed using COOT[5] alternated with refinement in REFMAC[6] or PHENIX Refine[7]. TLS-restrained refinement was applied in the latter cycles using the input thermal motion parameters determined by the TLSMD server[8]. The final model was verified for geometry correctness with PHENIX validation tools[7] and MOLPROBITY[9]. Data collection and refinement statistics are summarized in **Table S2**.

3.2. Cell culture

Patient-derived culture HSJD-DIPG-007 (*H3F3A* K27M, *ACVR1* R206H) was grown in stem cell media consisting of Dulbecco's Modified Eagles Medium: Nutrient Mixture F12 (DMEM/F12), Neurobasal-A Medium, HEPES Buffer Solution 1 M, Sodium Pyruvate Solution 100 nM, Non-Essential Amino Acids Solution 10 mM, Glutamax-I Supplement and Antibiotic-Antimycotic solution (all Thermo Fisher, Loughborough, UK). The media was supplemented

with B-27 Supplement Minus Vitamin A, (Thermo Fisher), 20 ng/ml Human-EGF, 20 ng/ml Human-FGF-basic-154, 20 ng/ml Human-PDGF-AA, 20 ng/ml Human-PDGF-BB (all Shenandoah Biotech, Warwick, PA, USA) and 2 µg/ml Heparin Solution (0.2%, Stem Cell Technologies, Cambridge, UK). Cell authenticity was verified using short tandem repeat (STR) DNA fingerprinting.

3.3. Western blot analysis

For treatment with **24**, cells were incubated in complete media with vehicle or increasing concentrations of compounds (0.1, 1, 10 µM) and protein was collected at 18 hr post-treatment. Samples were lysed by using lysis buffer containing phosphatase inhibitor cocktail (Sigma, Poole, UK) and protease inhibitor cocktail (Roche Diagnostics, Burgess Hill, UK). Following quantification using Pierce BCA Protein Assay Kit (Thermo Fisher), equal amounts of cell extracts were loaded for western blot analysis. Membranes were incubated with primary antibody (1:1000) overnight at 4 °C, and horseradish peroxidase secondary antibody (Amersham Bioscience, Amersham, UK) for 1 hr at room temperature. Signal was detected with ECL Prime Western blotting detection agent (Amersham Biosciences), visualised using Hyperfilm ECL (Amersham Biosciences) and analysed using an x-ray film processor in accordance with standard protocols. Primary antibodies used were phospho-SMAD1/5/8 (CST#13820), SMAD1/5/8 (SC#6031), ID1 (SC#488) and GAPDH (CST#2118).

3.4. LCMS method details

LCMS analyses and high resolution mass spectrometry were performed on an Agilent 1200 series HPLC and diode array detector coupled to a 6210 time of flight mass spectrometer with dual multimode APCI/ESI source (Methods A and B) or a Waters Acquity UPLC and diode array detector coupled to a Waters G2 QToF mass spectrometer fitted with a multimode ESI/APCI source (Method C). Samples were supplied as approximately 1 mg/mL solutions in MeOH, acetone, CH_2Cl_2 or MeOH/H_2O with 0.5-10 µL injected on a partial loop fill. Method A: Analytical separation was carried out at 30 °C on a Merck Purospher STAR column (RP-18e, 30 x 4 mm) using a flow rate of 1.5 mL/min in a 4 minute gradient elution with detection at 254 nm. The mobile phase was a mixture of methanol (solvent A) and water containing formic acid at 0.1% (solvent B). Gradient elution was as follows: 1:9 (A/B) to 9:1 (A/B) over 2.5 min, 9:1 (A/B) for 1 min, and then reversion back to 1:9 (A/B) over 0.3 min, finally 1:9 (A/B) for 0.2 min. Method B: Analytical separation was carried out at 40 °C on a Merck Purospher STAR column (RP-18e, 30 x 4 mm) using a flow rate of 3 mL/min in a 2 minute gradient elution with detection at 254 nm. The mobile phase was a mixture of methanol (solvent A) and water containing formic acid at 0.1% (solvent B). Gradient elution was as follows: 1:9 (A/B) to 9:1 (A/B) over 1.25 min, 9:1 (A/B) for 0.5 min, and then reversion back to 1:9 (A/B) over 0.15 min, finally 1:9 (A/B) for 0.1 min. Method C: Analytical separation was carried out at 30 °C on a Phenomenex Kinetex XB-C18 column (30 x 2.1 mm, 1.7u, 100A) using a flow rate of 0.5 mL/min in a 2 minute gradient elution with detection at 254 nm. The mobile phase was a mixture of MeOH (solvent A) and water containing formic acid at 0.1% (solvent B). Gradient elution was as follows: 1:9 (A/B) to 9:1 (A/B) over 1.25 min, 9:1 (A/B) for 0.5 min, and then reversion back to 1:9 (A/B) over 0.15 min, finally 1:9 (A/B) for 0.1 min. UV absorbance spectra were collected at a wavelength of 254 nm. HRMS references: caffeine $[M+H]^+$ 195.08765; reserpine $[M+H]^+$ 609.28066 or hexakis (2,2-difluroethoxy)phosphazene $[M+H]^+$ 622.02896; and hexakis(1H,1H,3H-tetrafluoropentoxy)phosphazene $[M+H]^+$ 922.00980.

3.5. Preparative HPLC method details

For preparative HPLC, standard injections (with needle wash) of the sample were made onto a Phenomenex Gemini C18 column (250 x 21.2 Phenomenex, Torrence, CA, USA) or an ACE 5 C18-PFP column (250 x 21.2 mm Advanced Chromatography Technologies, Aberdeen, UK). UV-Vis spectra were acquired at 254 nm on a 1200 Series Prep Scale diode array detector (Agilent, Santa Clara, USA). Post-UV & pre-MS splitting was achieved using an Active Split (Agilent, Santa Clara, USA) before being infused into a 6120 Series Quad mass spectrometer fitted with an ESI/APCI Multimode ionisation source (Agilent, Santa

Clara, USA). LC eluent and nebulising gas was introduced into the grounded nebuliser with spray direction orthogonal to the capillary axis. 2 kV was applied to the charging electrode to generate a charged aerosol. The aerosol was dried by infrared emitters (200 °C) and heated drying gas (12 L/min of nitrogen at 350 °C, 60 psi), producing ions by ESI. Aerosol and ions were transferred by nebulising gas to the APCI zone where infrared emitters vaporized solvent and analyte. A corona discharge was produced between the corona needle and APCI counter electrode by applying a current of 4 μA, ionizing the solvent to transfer charge to analyte molecules, producing ions by APCI. ESI and APCI ions simultaneously entered the transfer capillary along which a potential difference of 4 kV was applied. The fragmentor voltage was set at 175 V and skimmer at 65 V. Signal was optimised by AutoTune.m. Profile mass spectrometry data was acquired in positive ionisation mode over a scan range of m/z 60-1000 (scan rate 1.0). Collection was triggered by UV signal and collected on a 1200 Series Fraction Collector (Agilent, Santa Clara, USA). Raw data was processed using Agilent Chemstation Software B.02.01. Chromatographic separation at room temperature was carried out using a 1200 Series Preparative HPLC (Agilent, Santa Clara, USA) over a 15 minute gradient elution (Grad15min20mls.m) from 90:10 to 0:100 water:methanol (both modified with 0.1% formic acid) at a flow rate of 20 mL/min.

4. NMR

6-Bromo-3-(4-morpholinophenyl)quinazolin-4(3H)-one, i

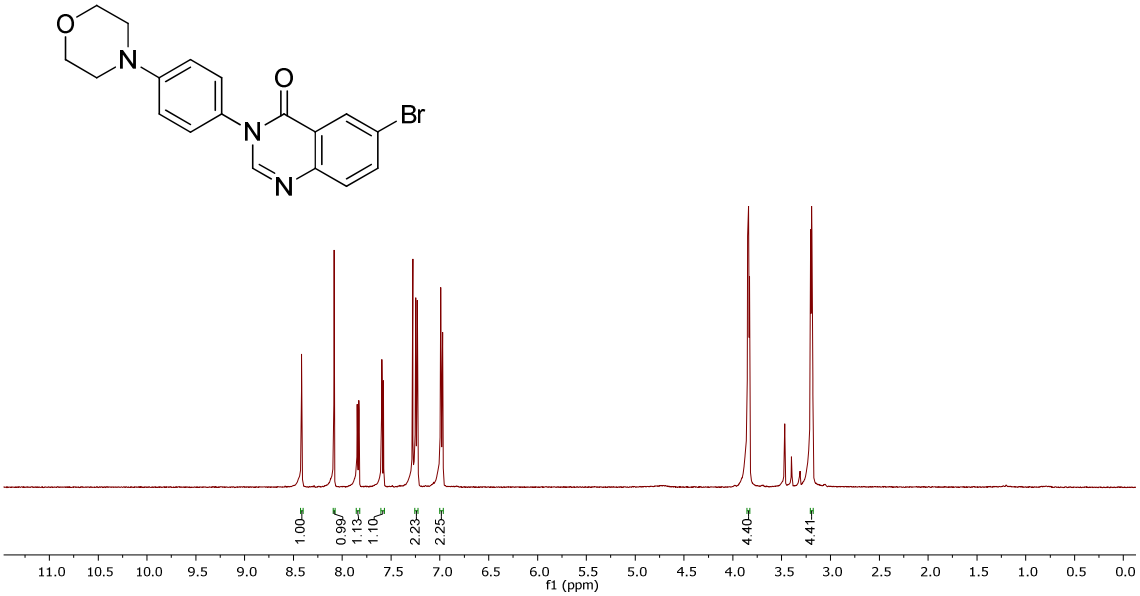

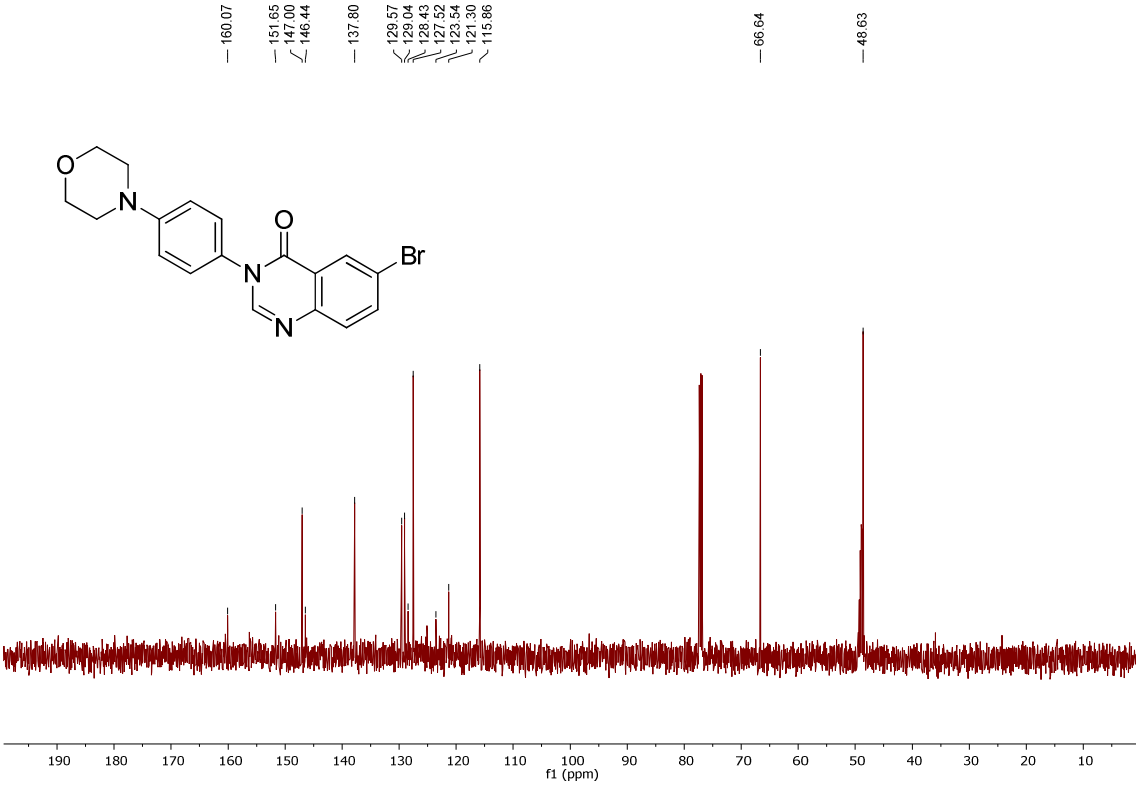

6-Bromo-3-phenylquinazolin-4(3*H*)-one, ii

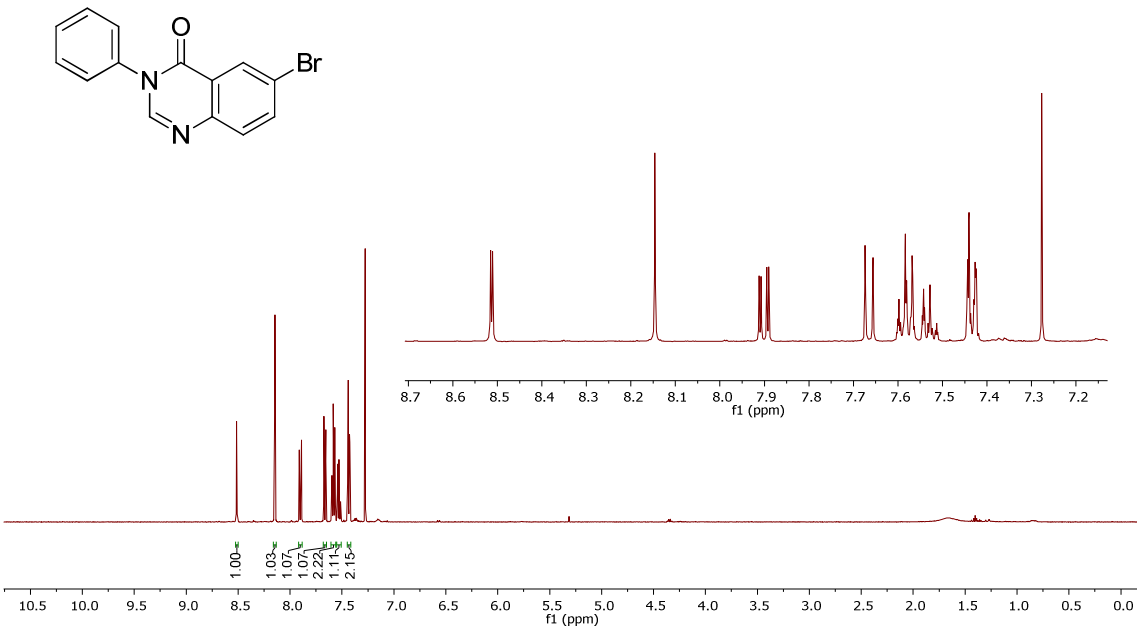

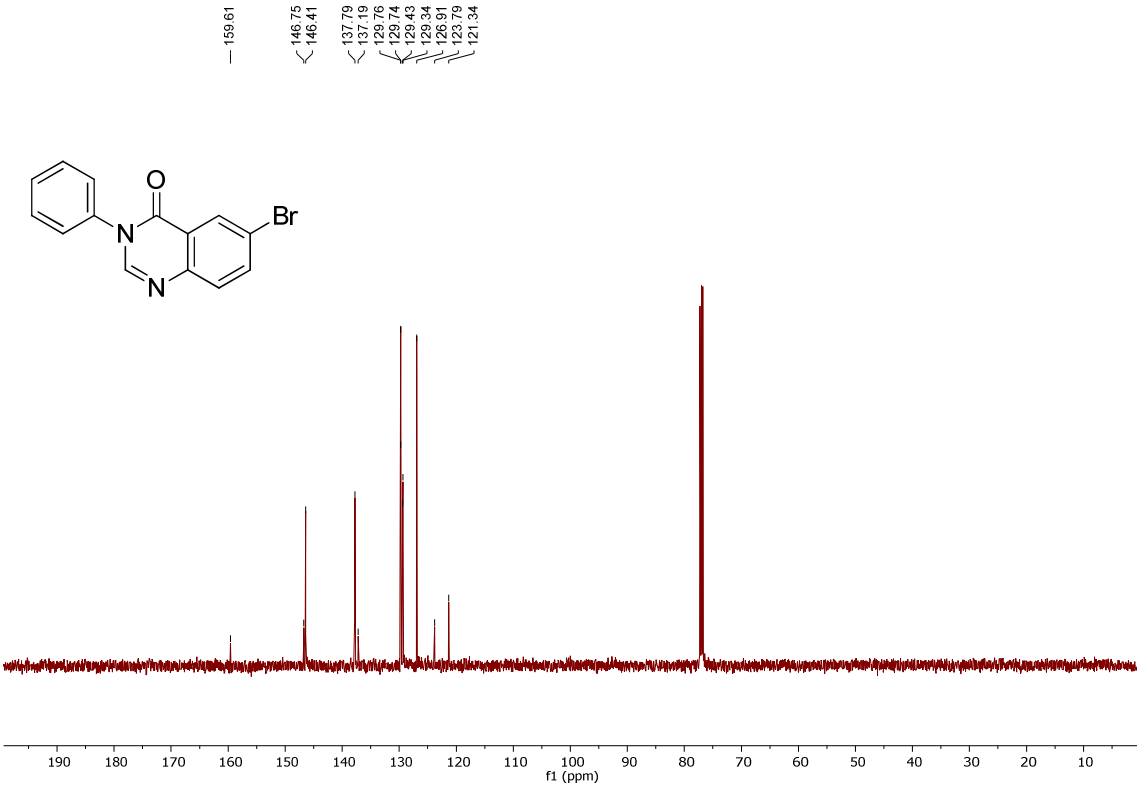

6-Bromo-3-cyclohexylquinazolin-4(3*H*)-one, iii

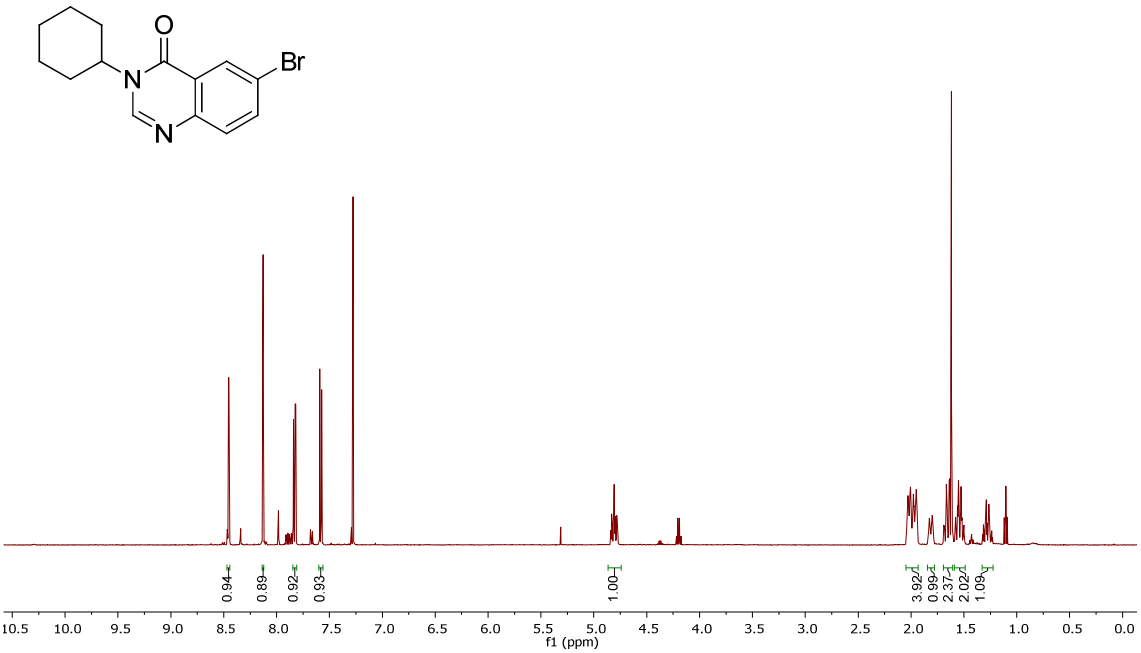

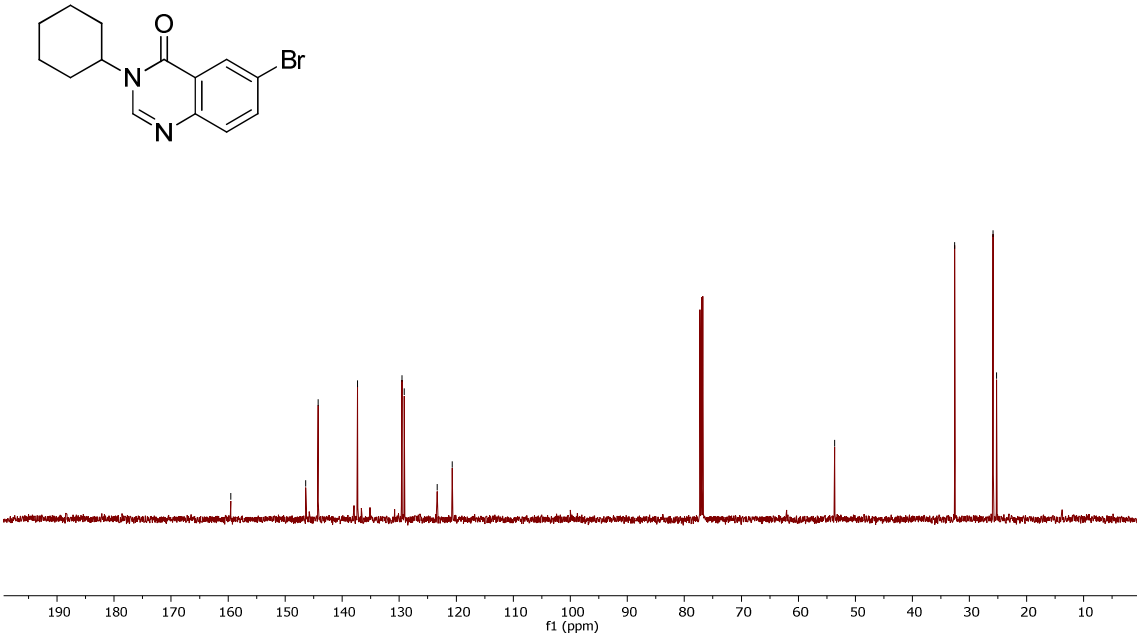

6-Bromo-3-(3-morpholinopropyl)quinazolin-4(3*H*)-one, iv

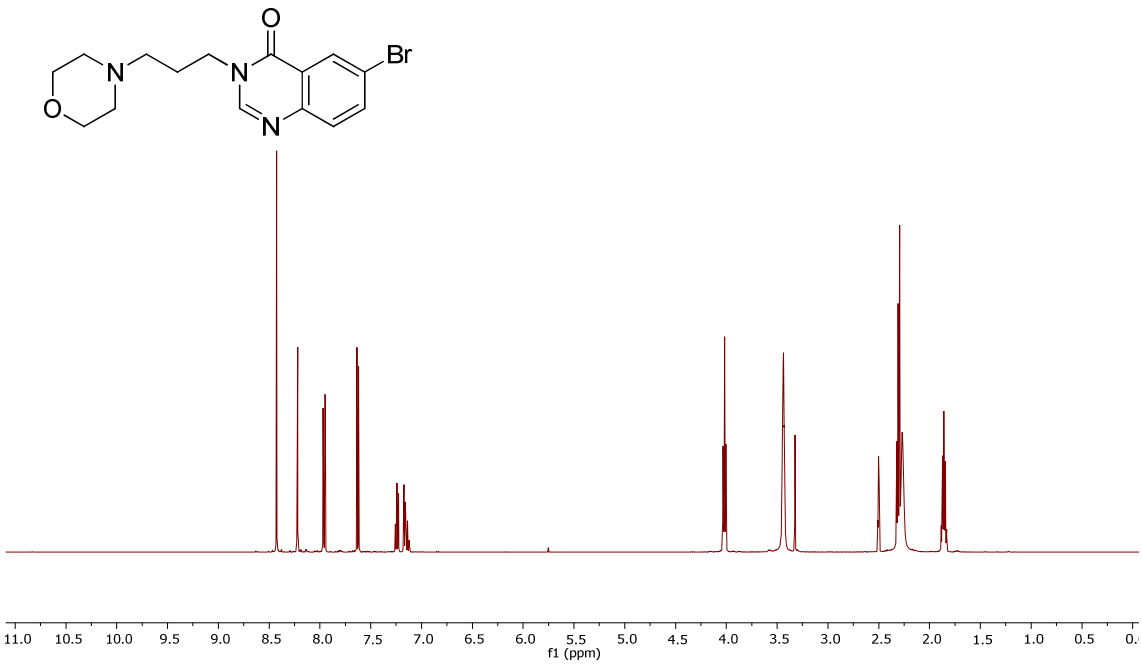

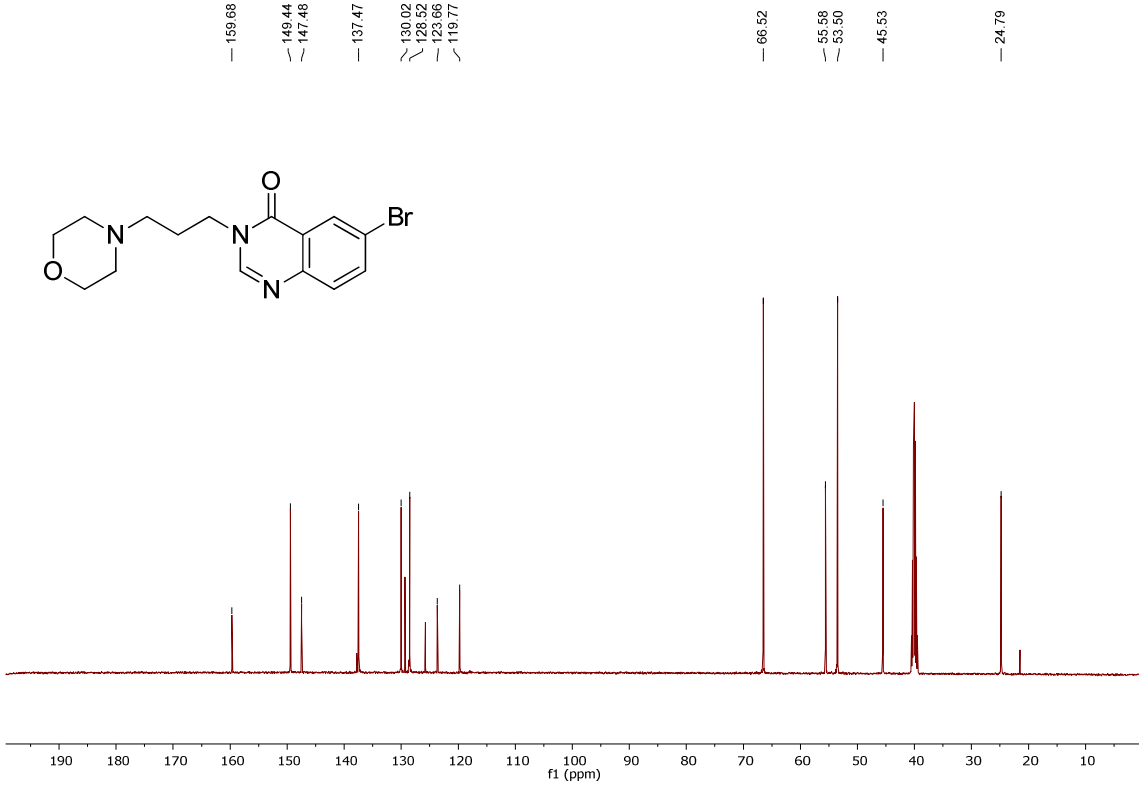

6-Bromo-3-(4-(dimethylamino)phenyl)quinazolin-4(3*H*)-one, v

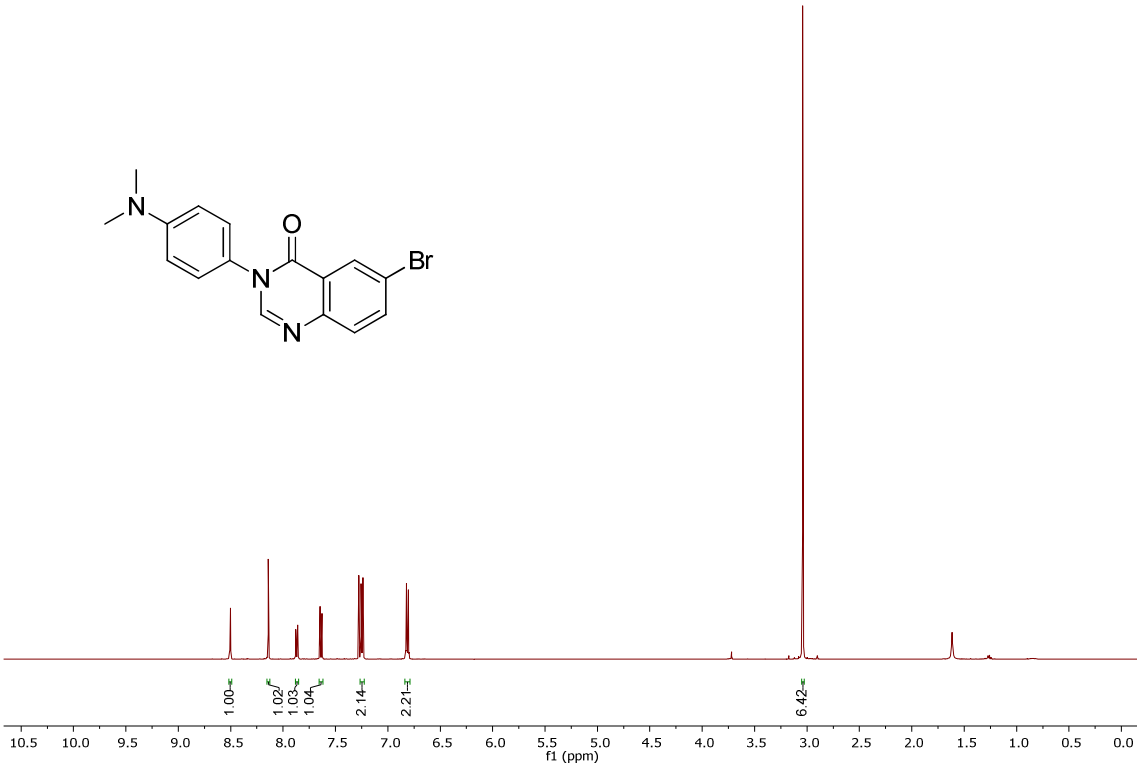

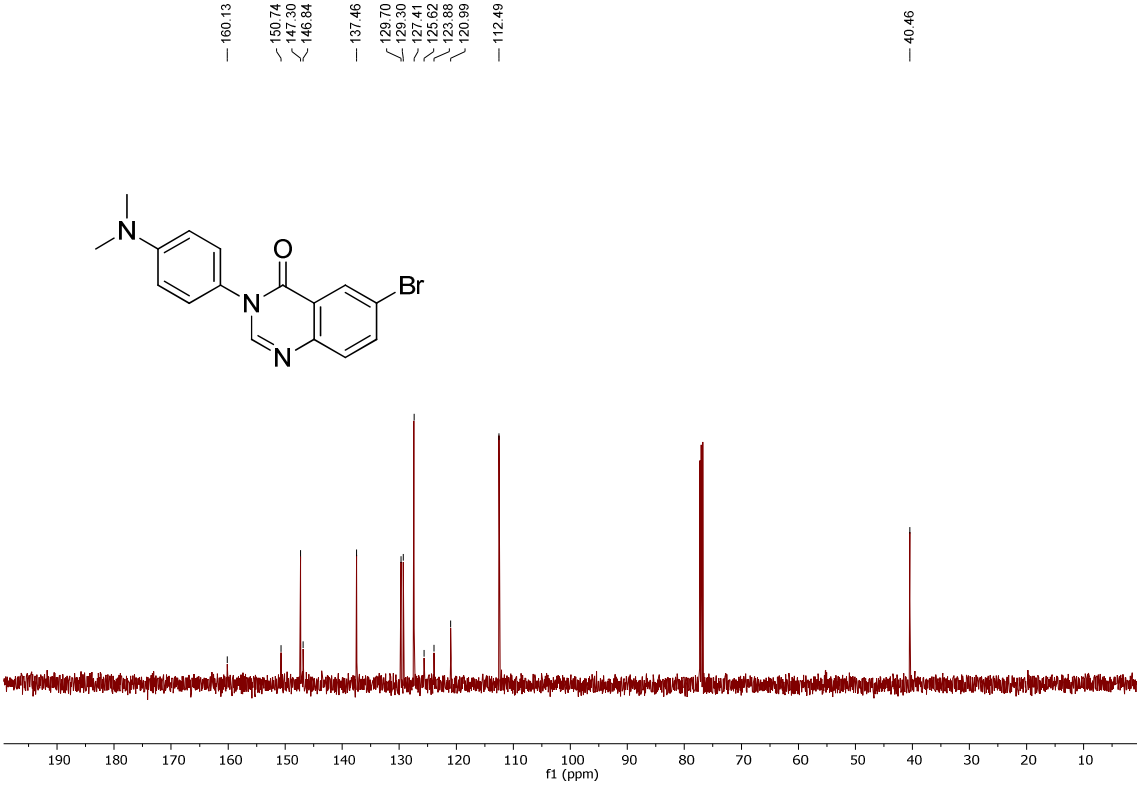

6-Bromo-2-methylquinazolin-4(3*H*)-one, vi

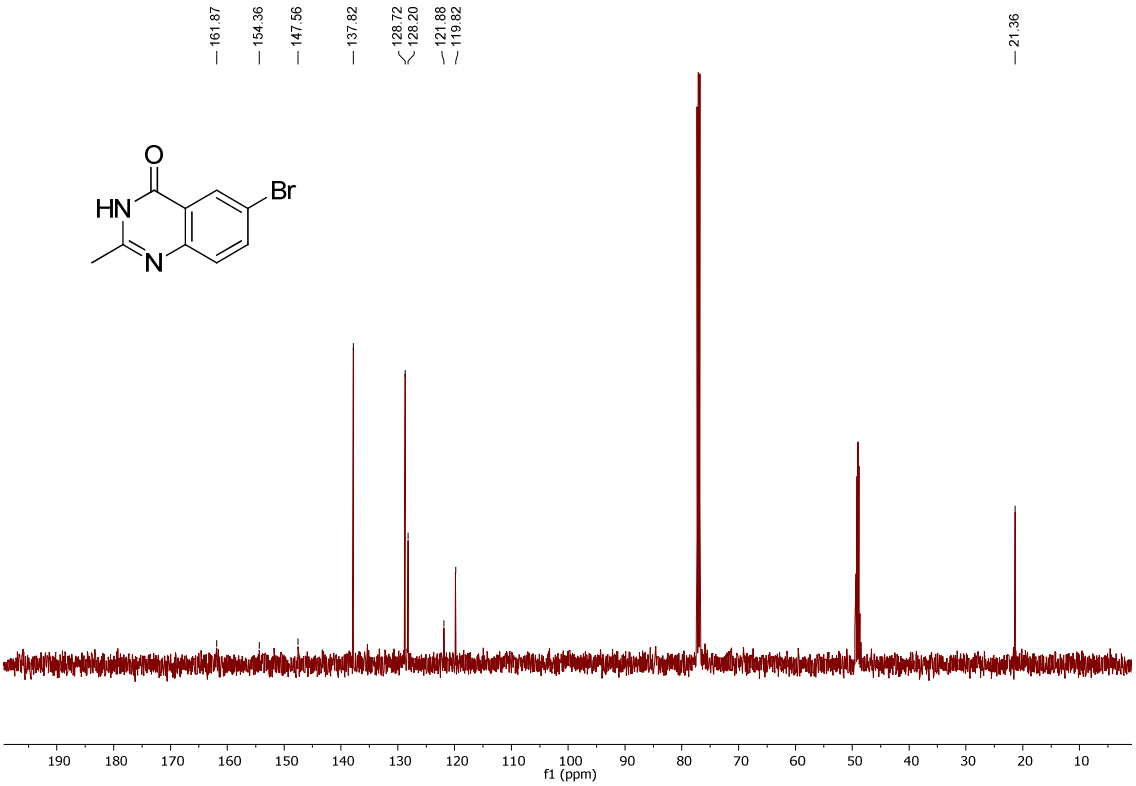

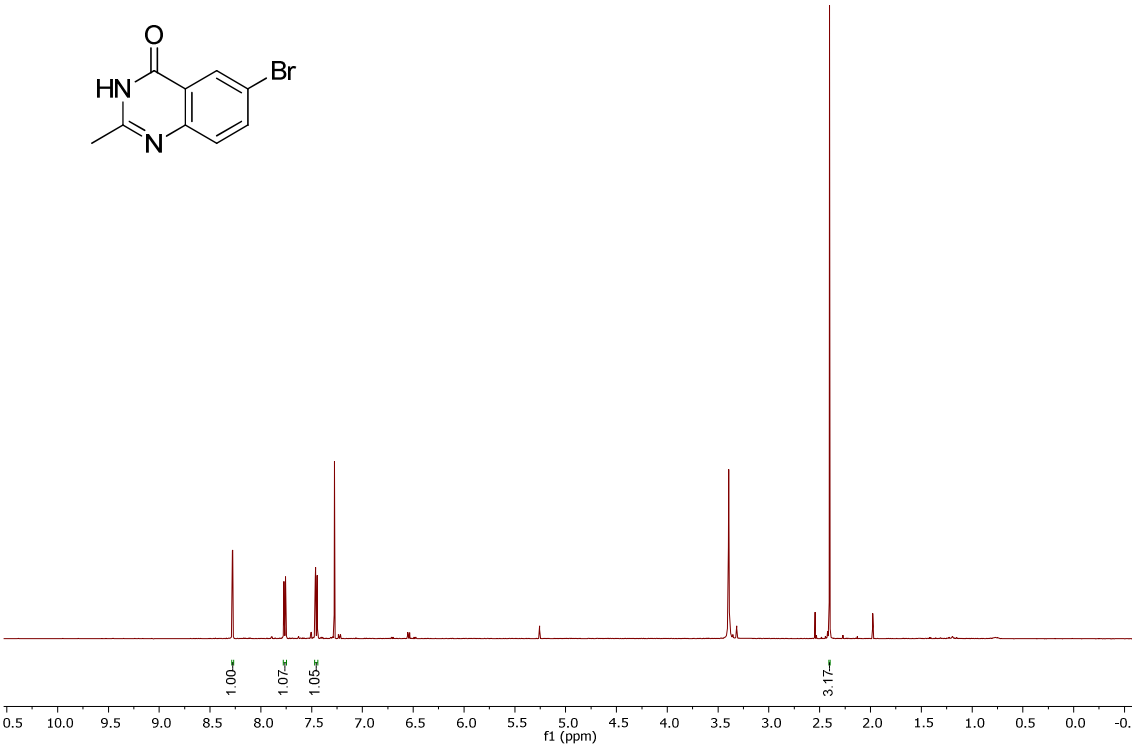

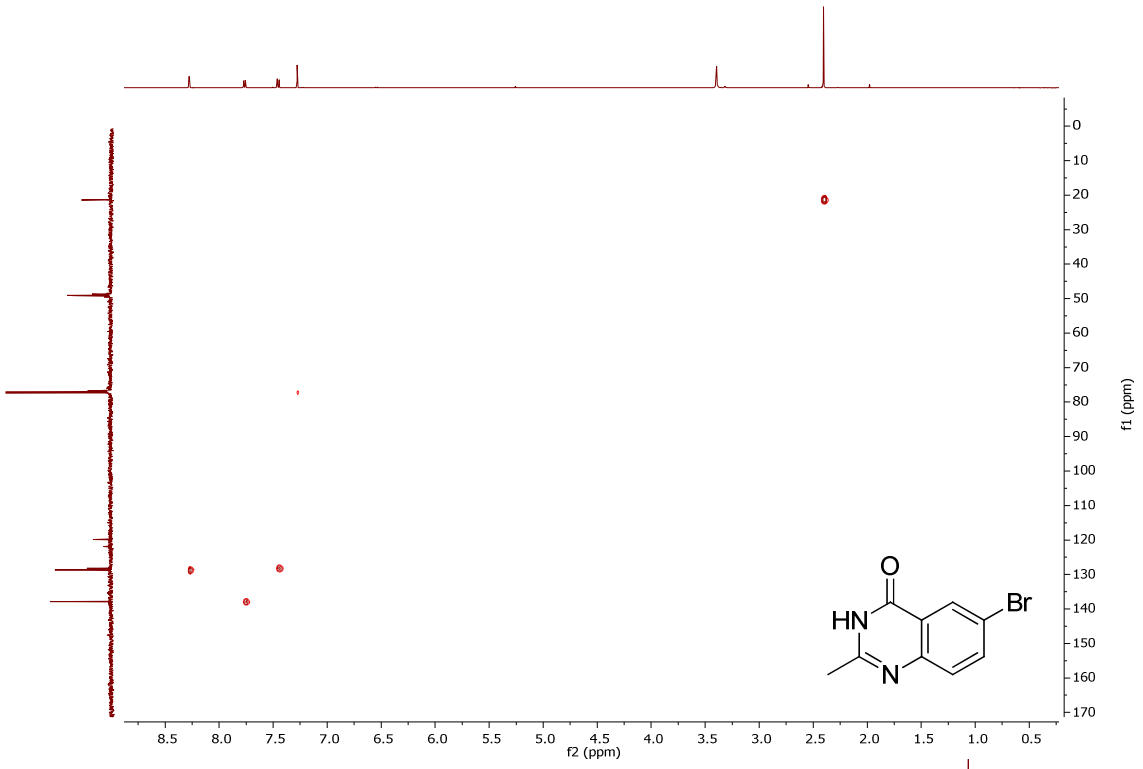
f2 (ppm)
f1 (ppm)
O
HN
N
Br

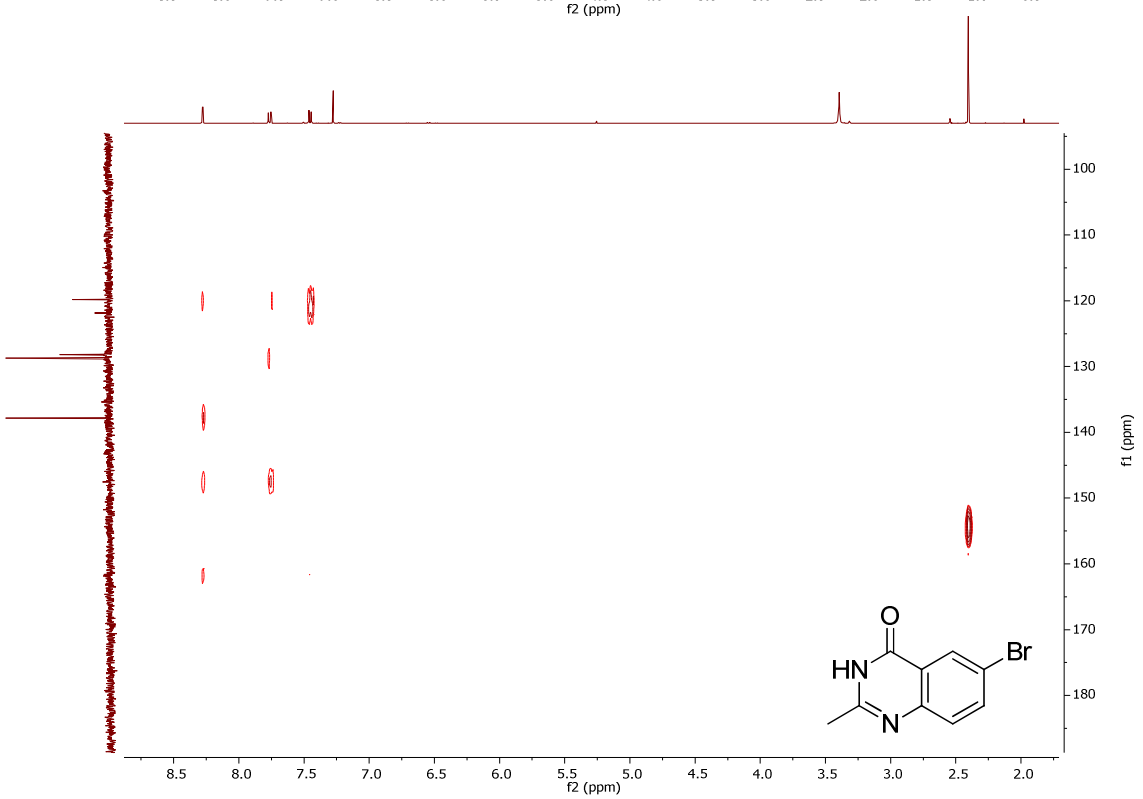
f2 (ppm)
f1 (ppm)
O
HN
N
Br

6-Bromo-2,5-dimethylquinazolin-4(3H)-one, vii

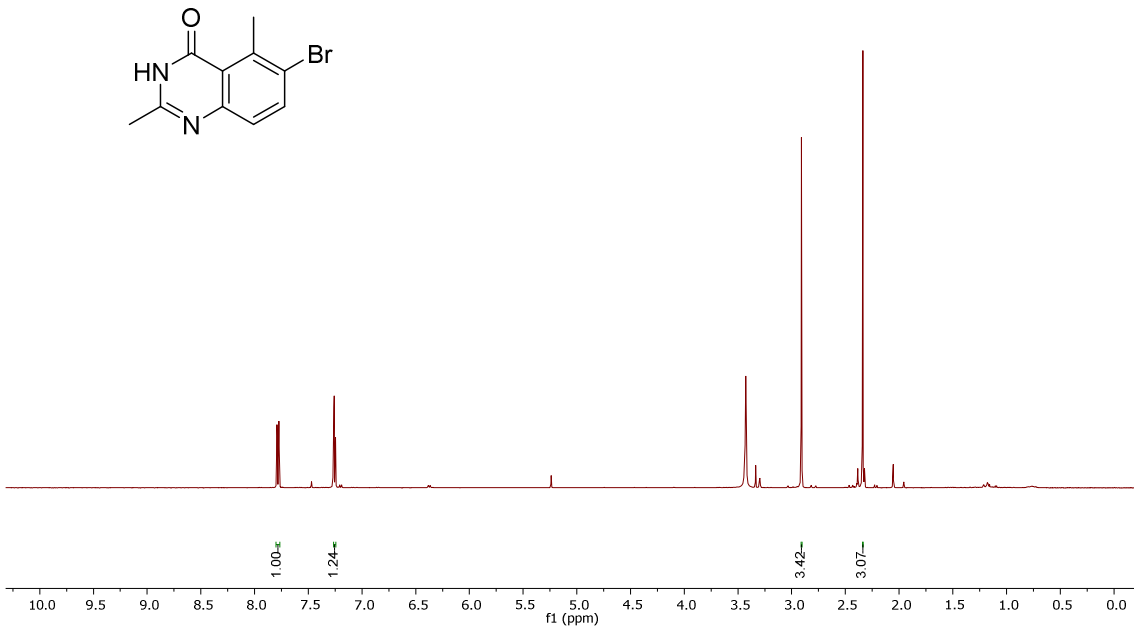

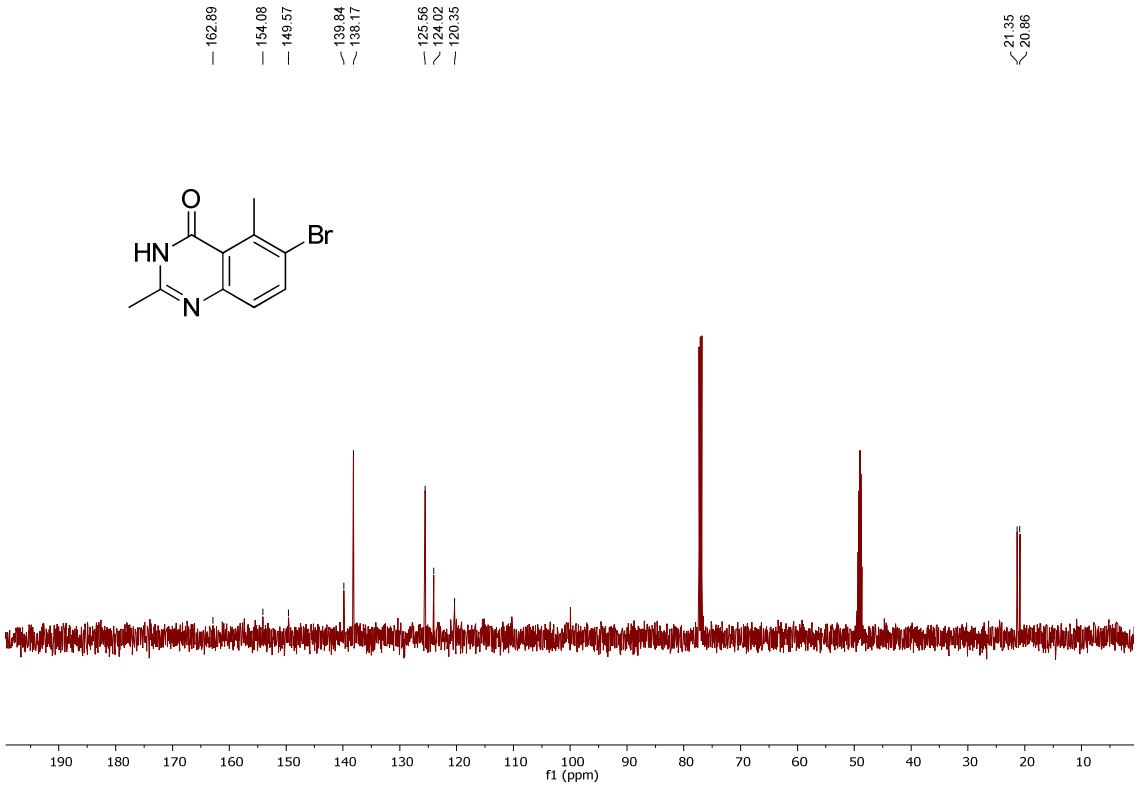

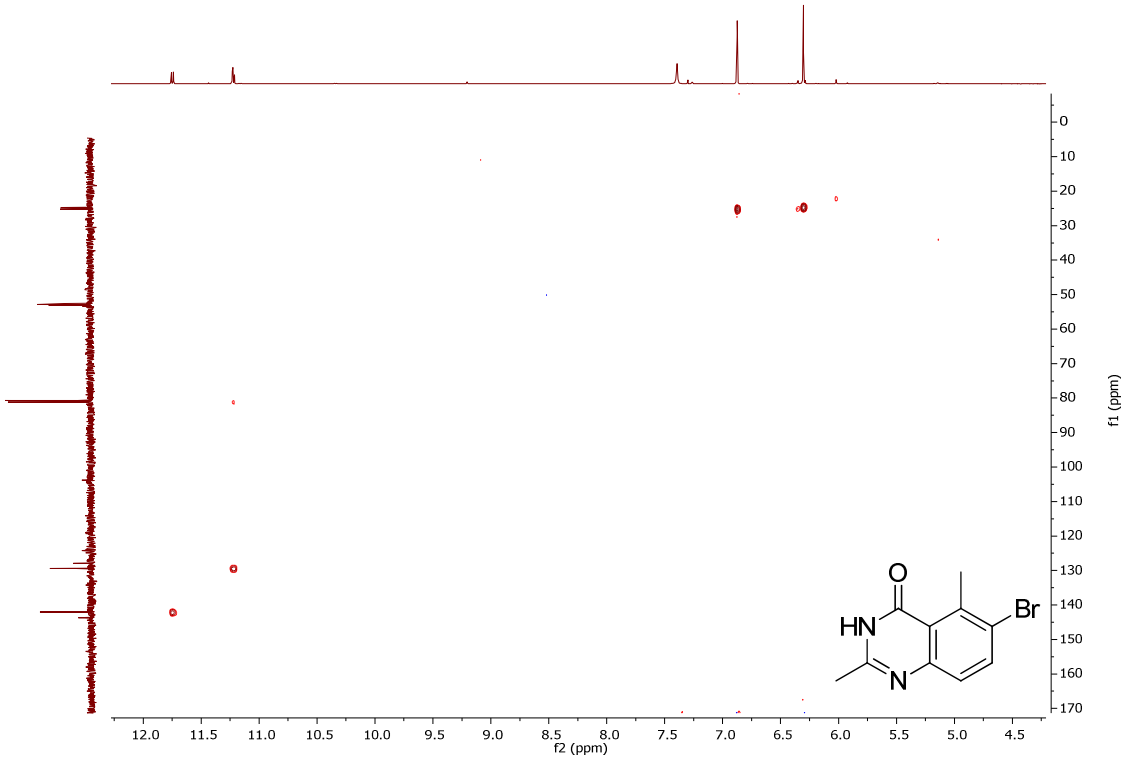
f2 (ppm)
f1 (ppm)
O
HN
N
Br

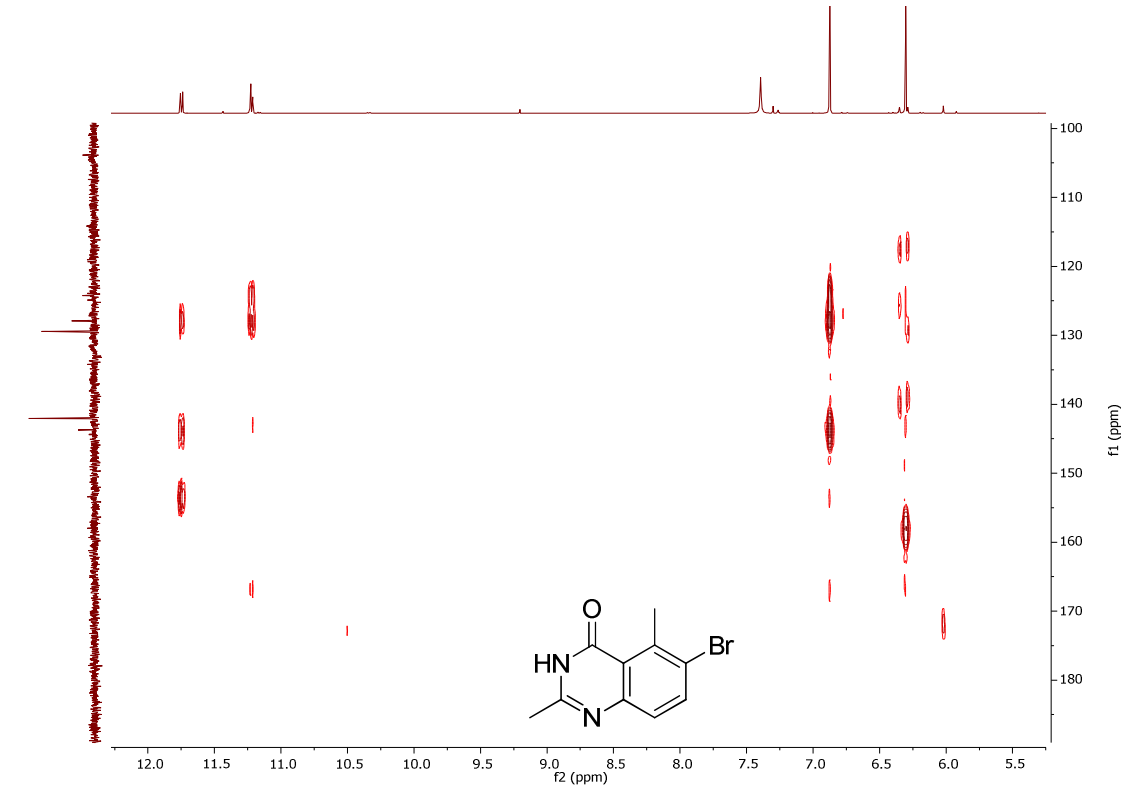
f2 (ppm)
f1 (ppm)
O
HN
N
Br

6-Bromo-2-ethyl-5-methylquinazolin-4(3*H*)-one, viii

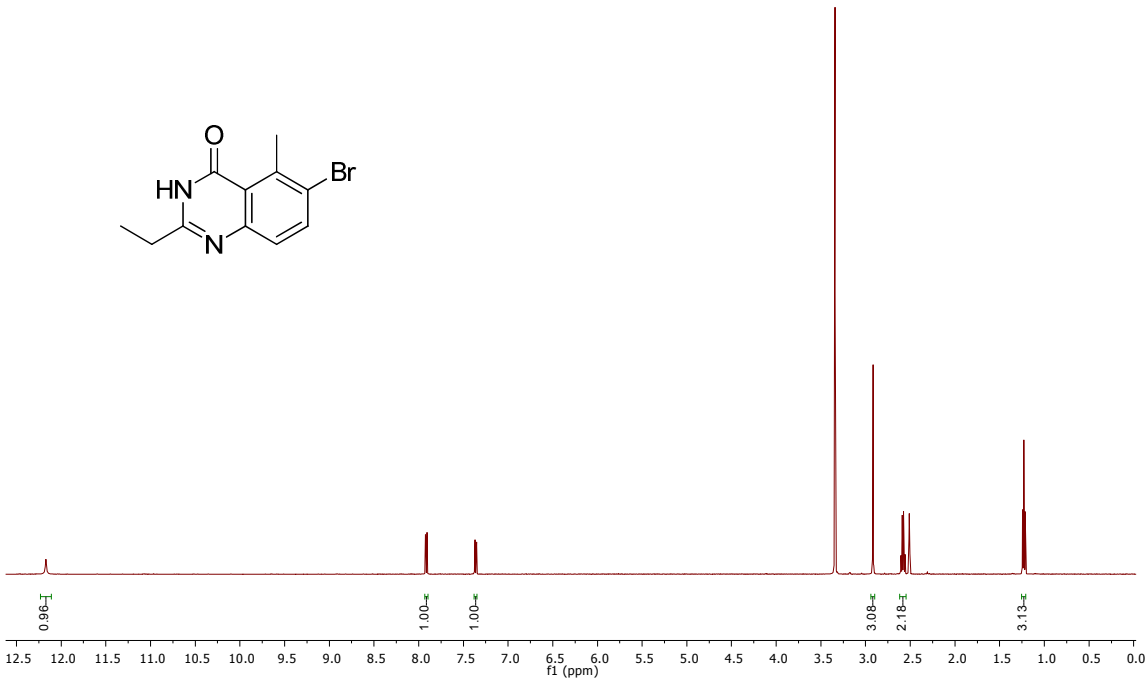

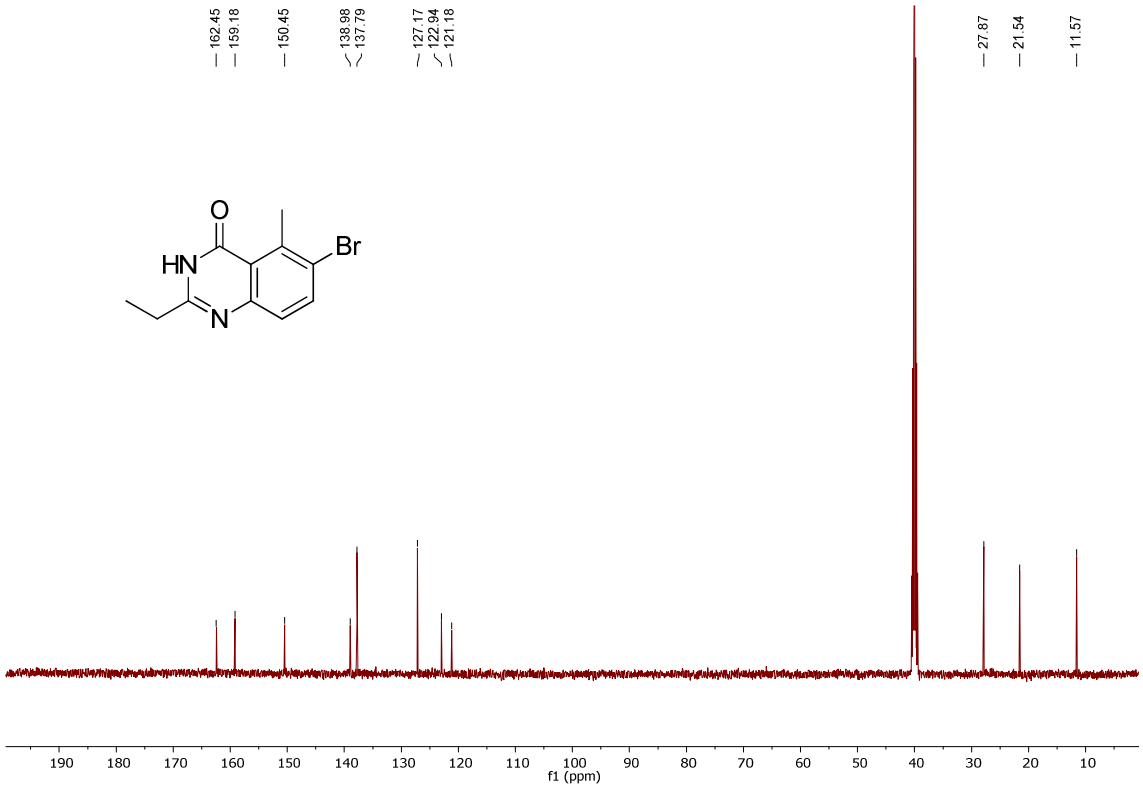

4-Bromo-3-cyclopropyl-1-tosyl-1*H*-pyrazole, ix

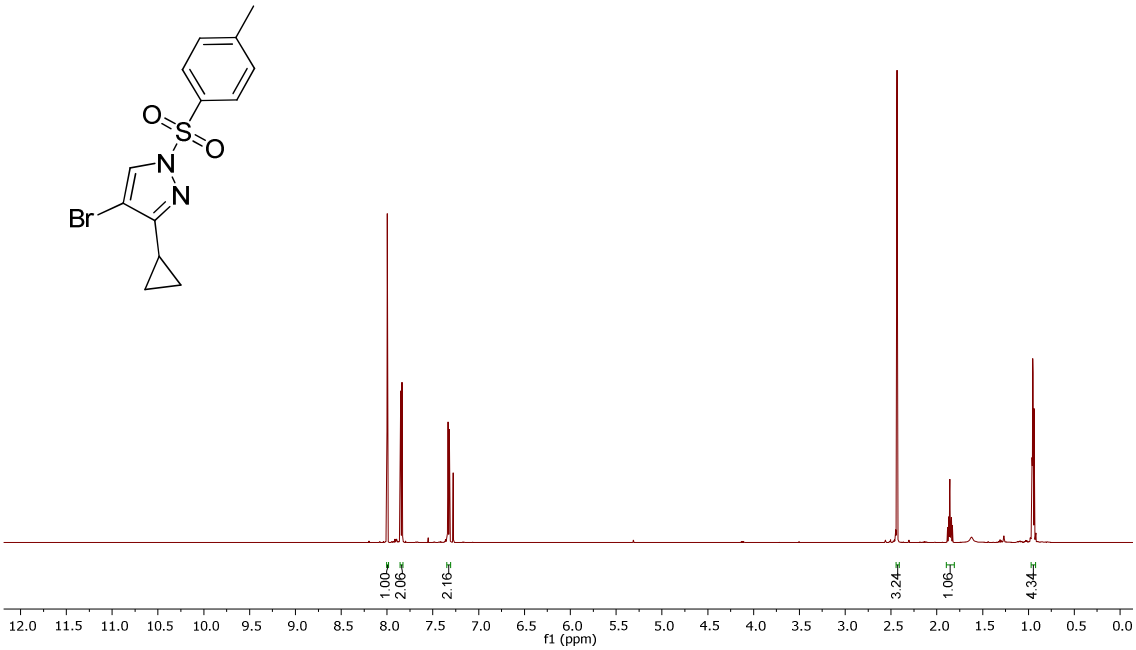

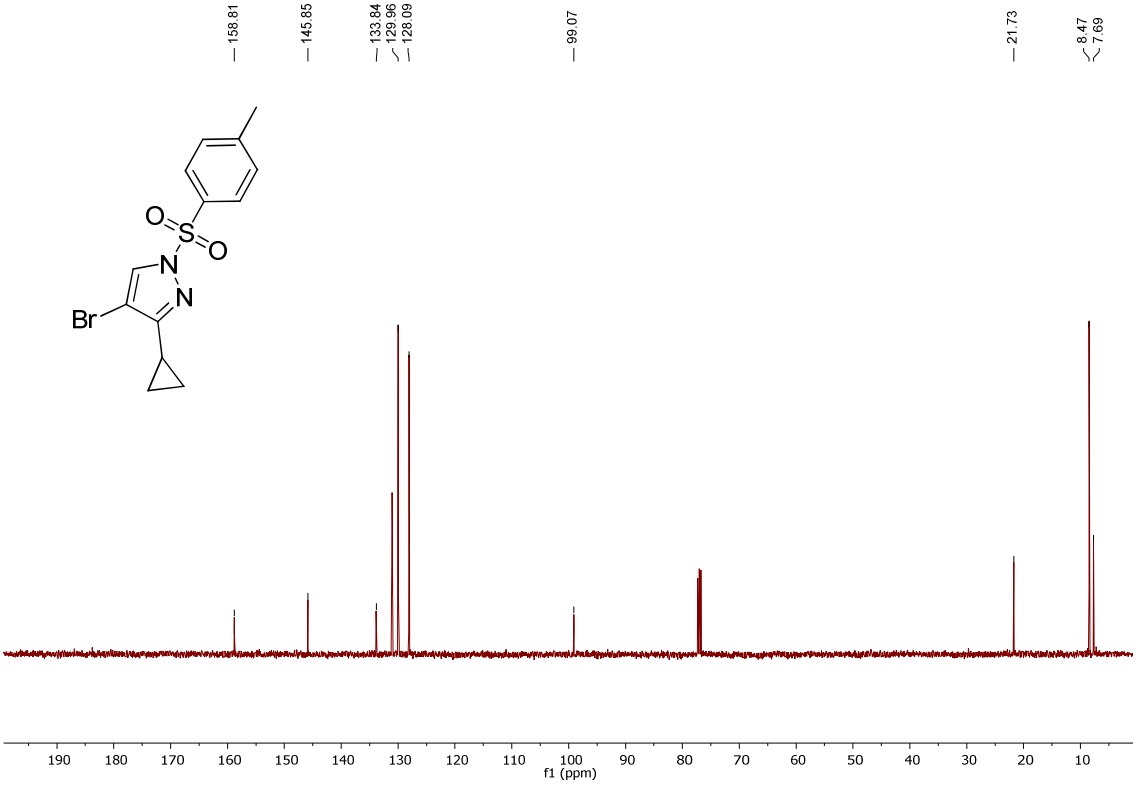

4-Bromo-3-ethyl-1-tosyl-1*H*-pyrazole, x

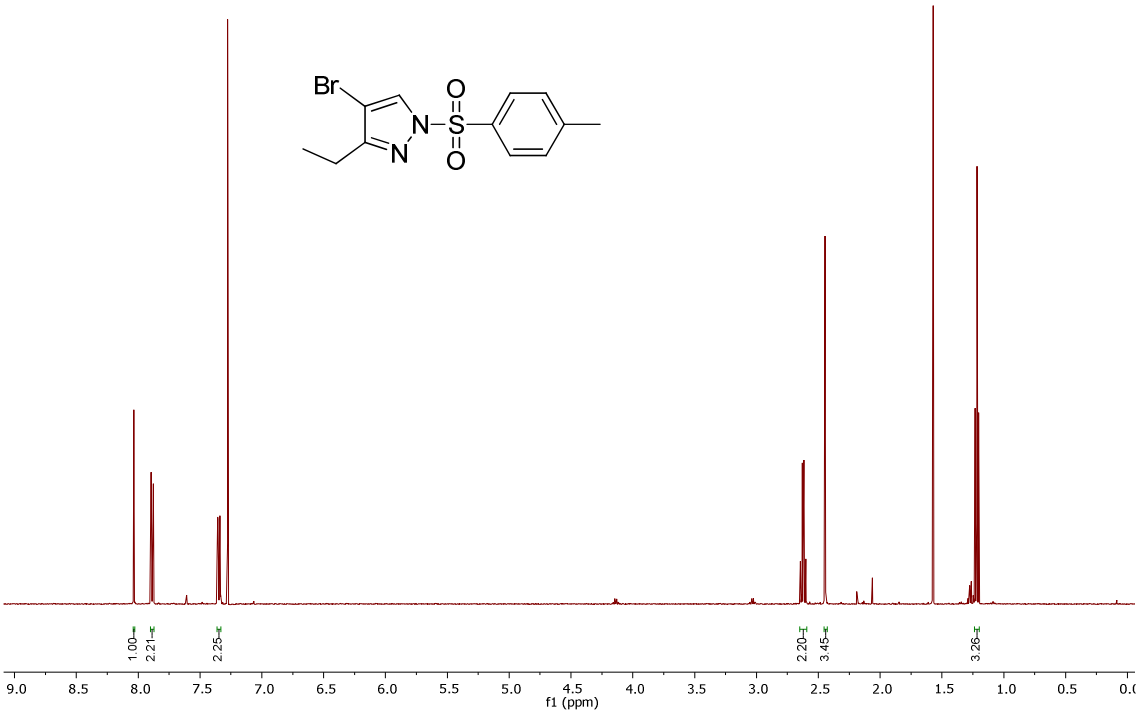

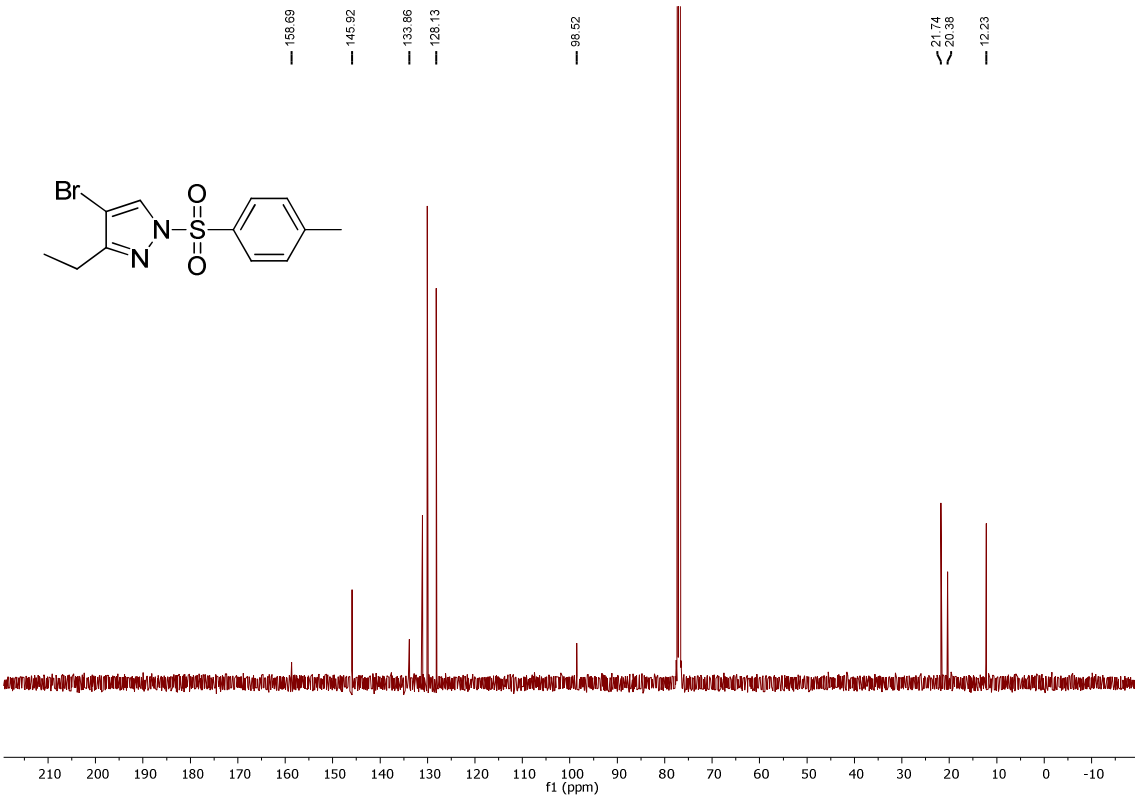

6-(1*H*-Pyrazol-4-yl)quinazolin-4(3*H*)-one, 1

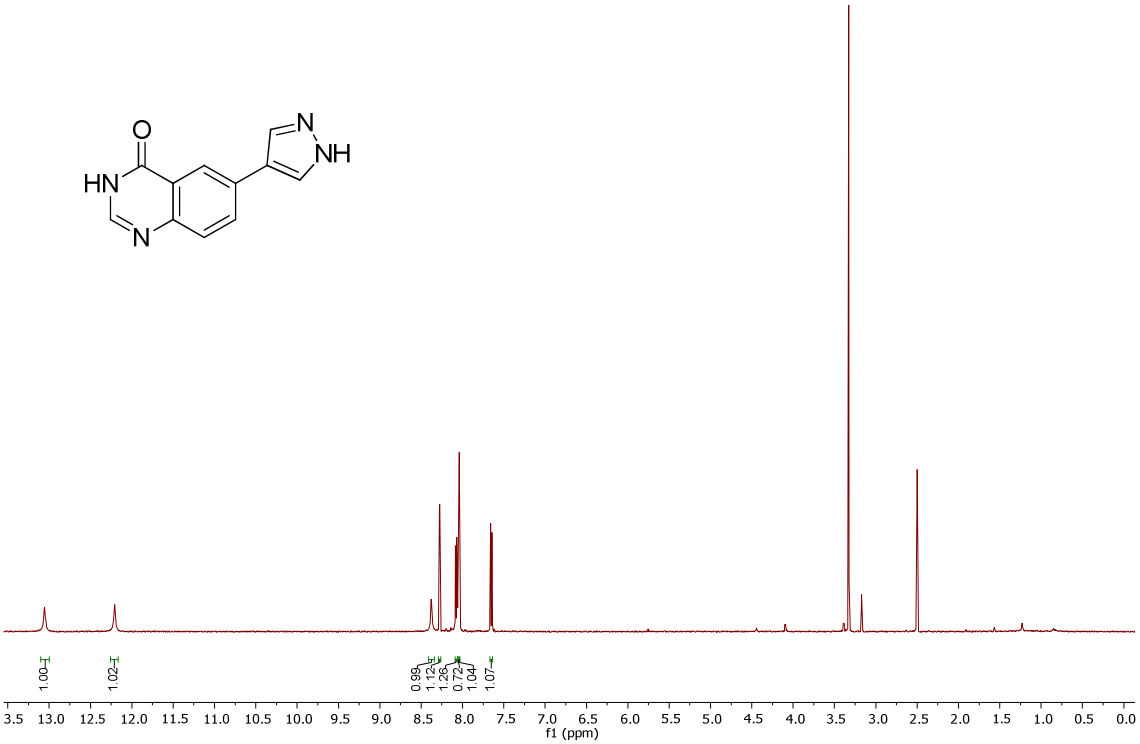

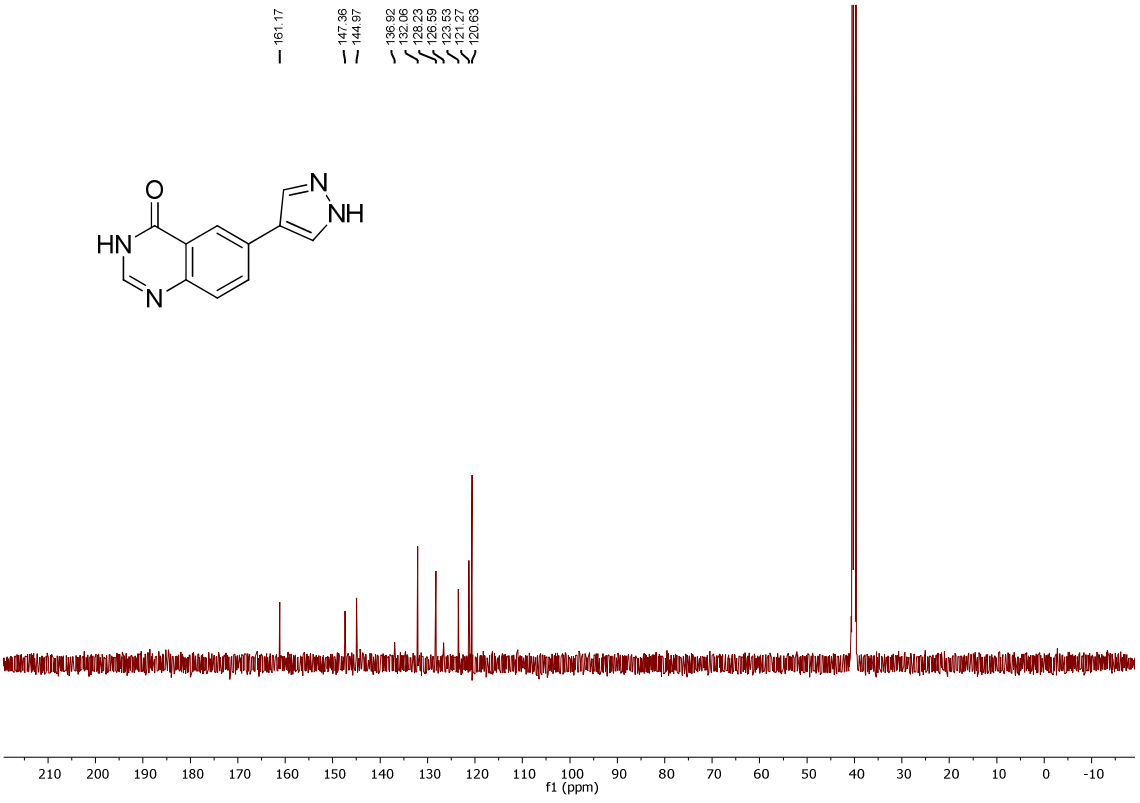

6-(1-Methyl-1*H*-pyrazol-4-yl)quinazolin-4(3*H*)-one, 2

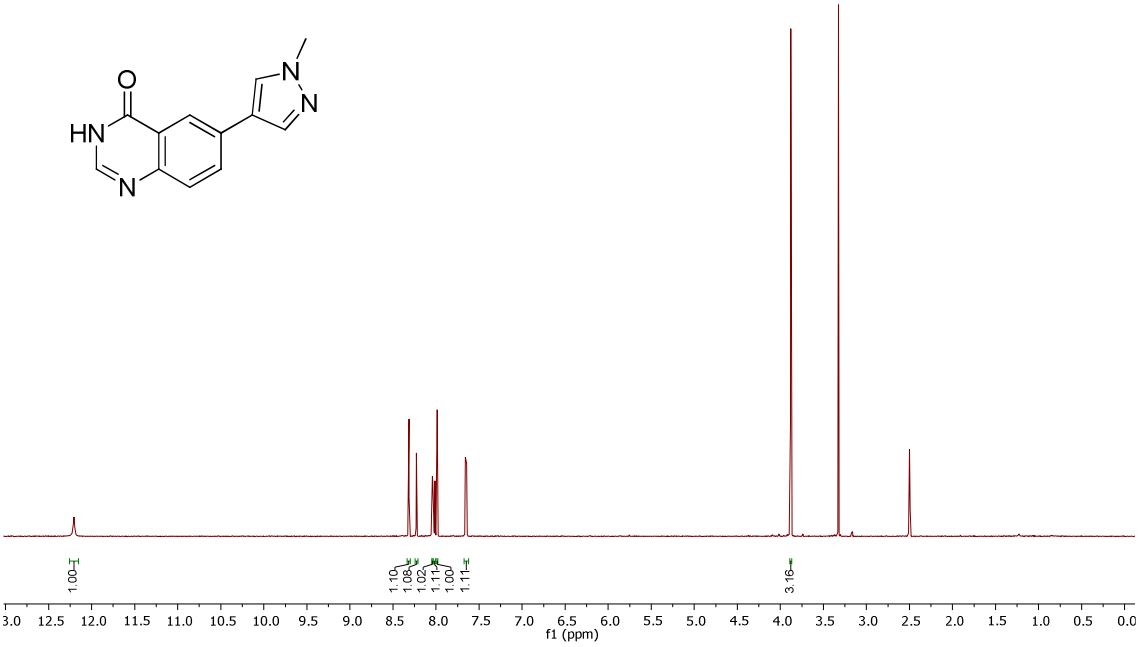

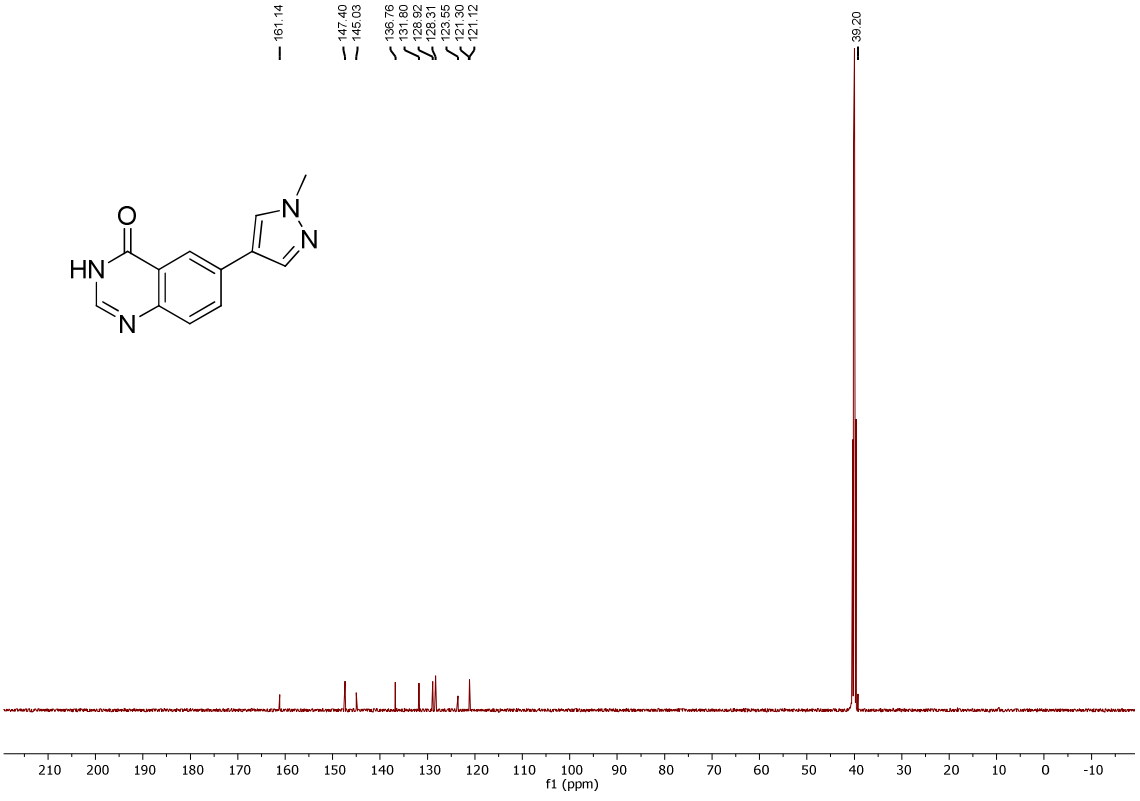

6-(3-Methyl-1*H*-pyrazol-4-yl)quinazolin-4(3*H*)-one, 3

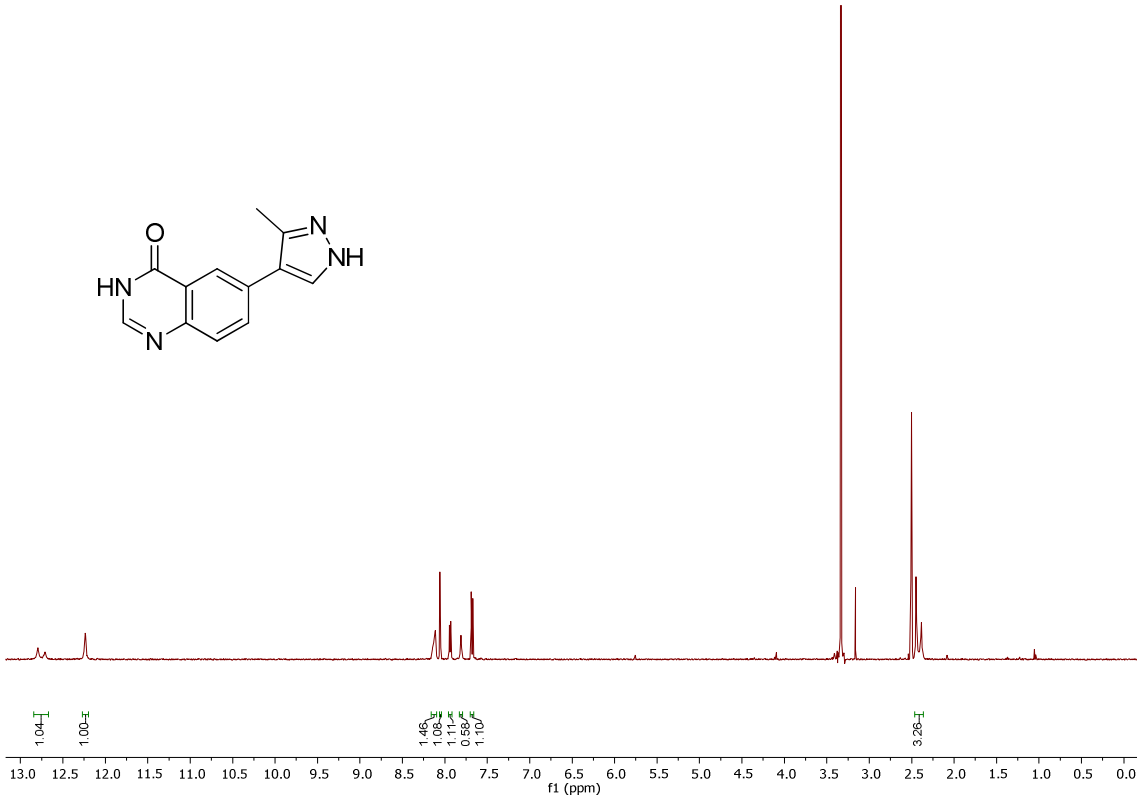

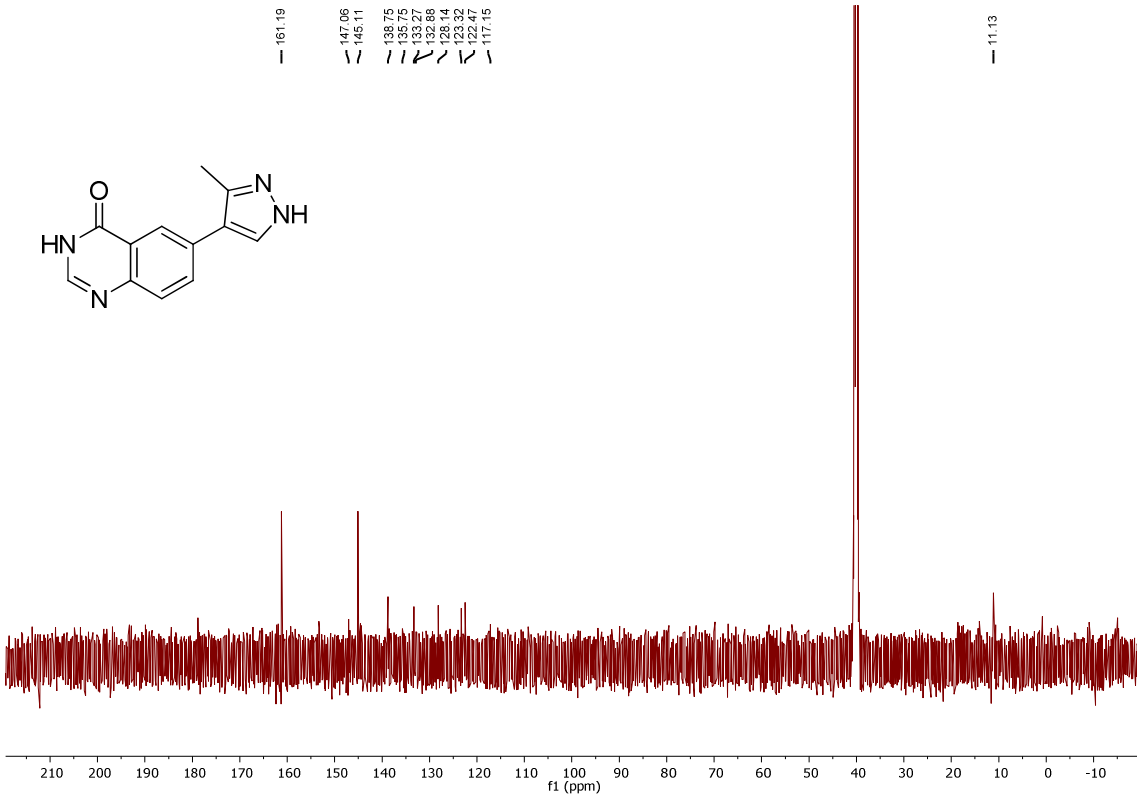

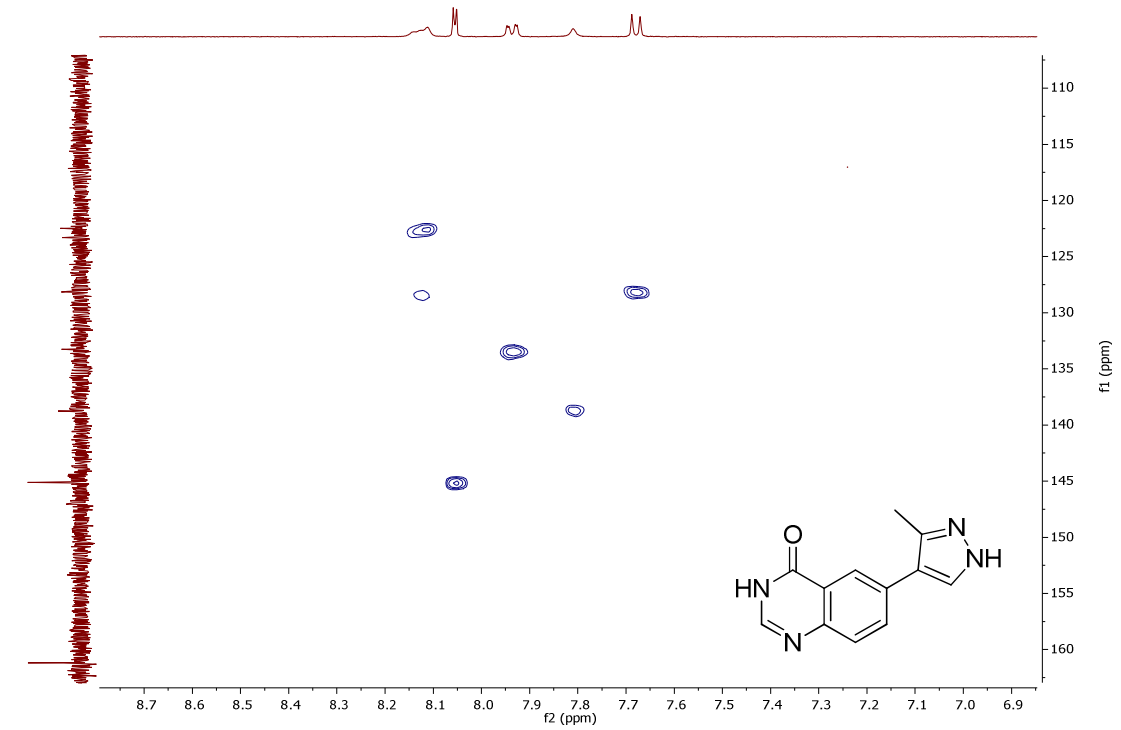
f2 (ppm)
f1 (ppm)
O
HN
N
N
NH

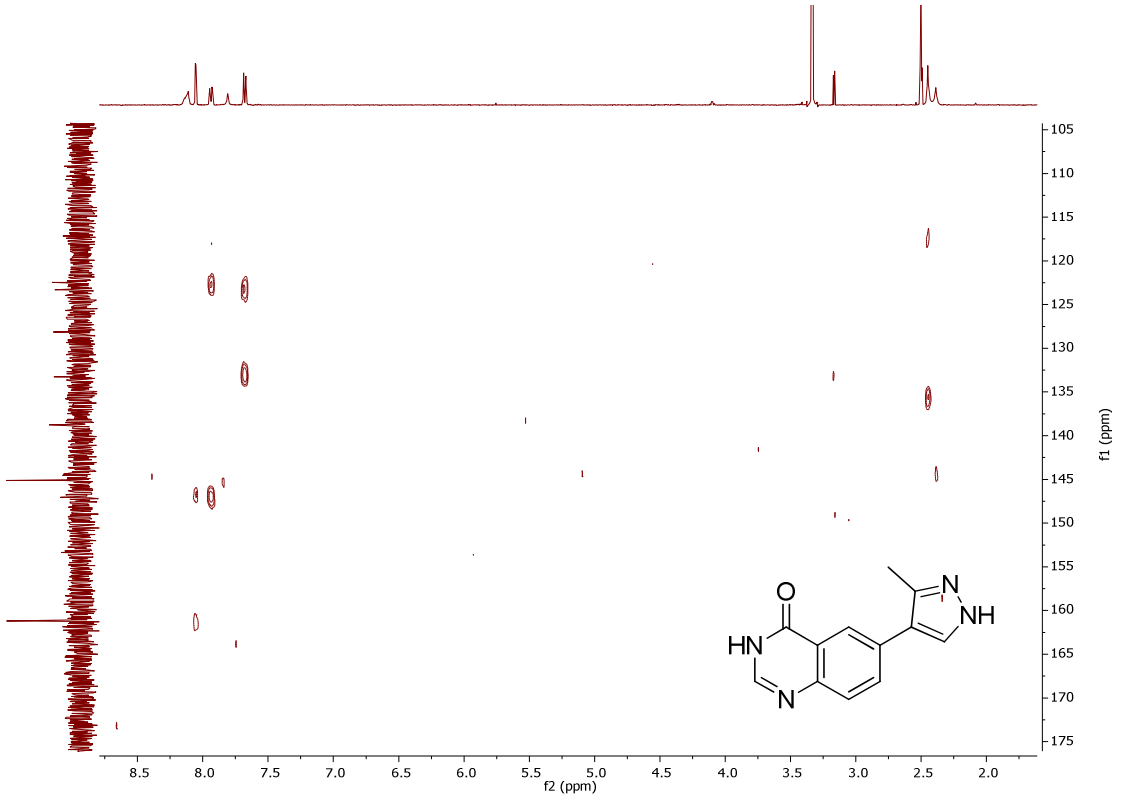
f2 (ppm)
f1 (ppm)
O
HN
N
N
NH

6-(3-Ethyl-1*H*-pyrazol-4-yl)quinazolin-4(3*H*)-one, 4

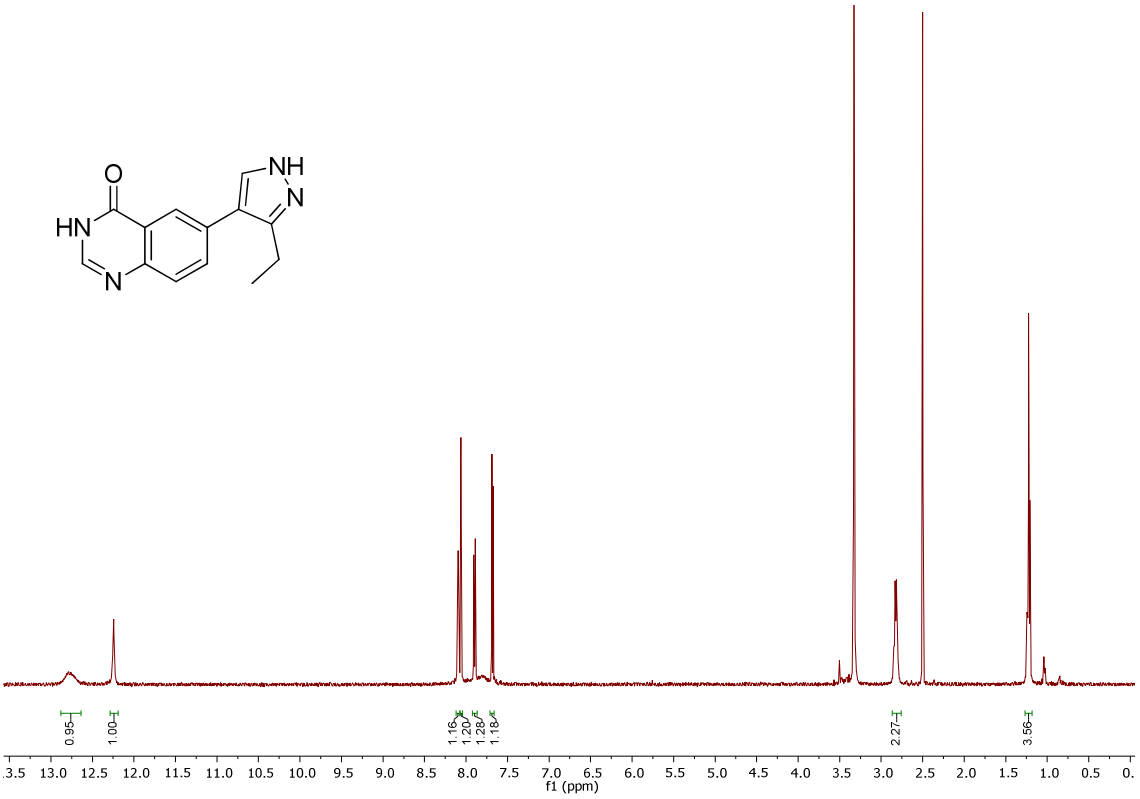

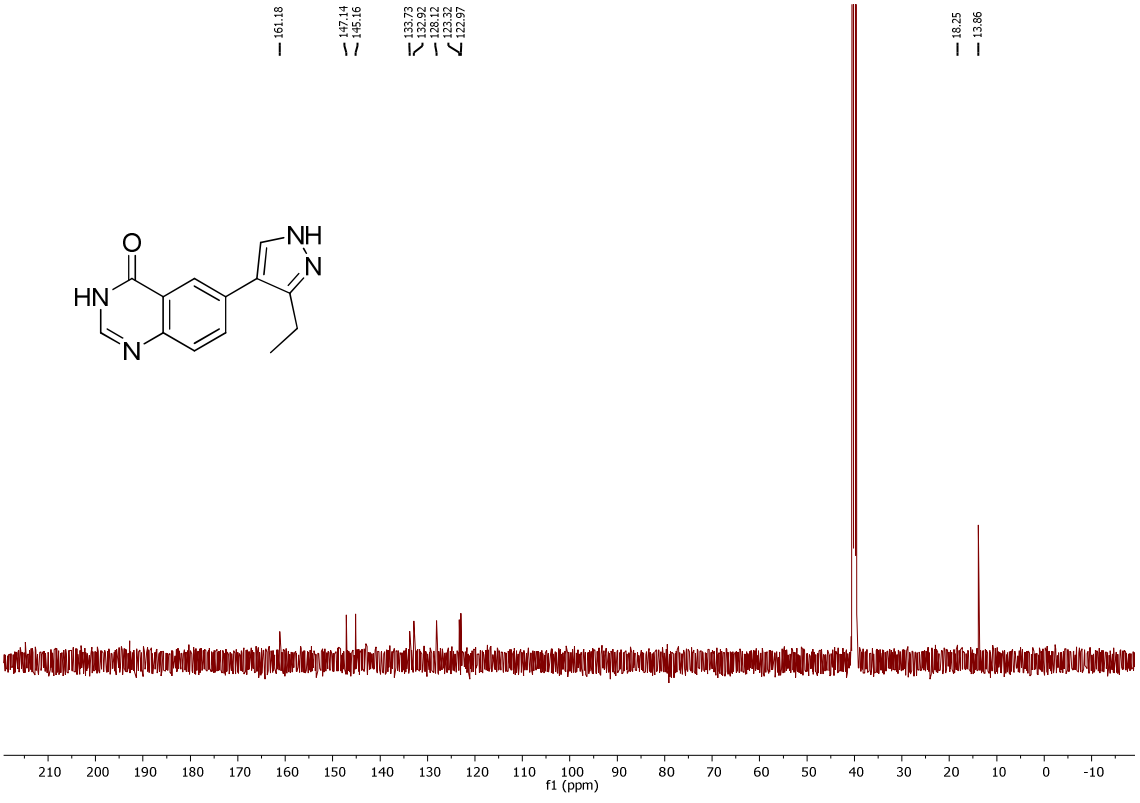

6-(3-Cyclopropyl-1*H*-pyrazol-4-yl)quinazolin-4(3*H*)-one, 5

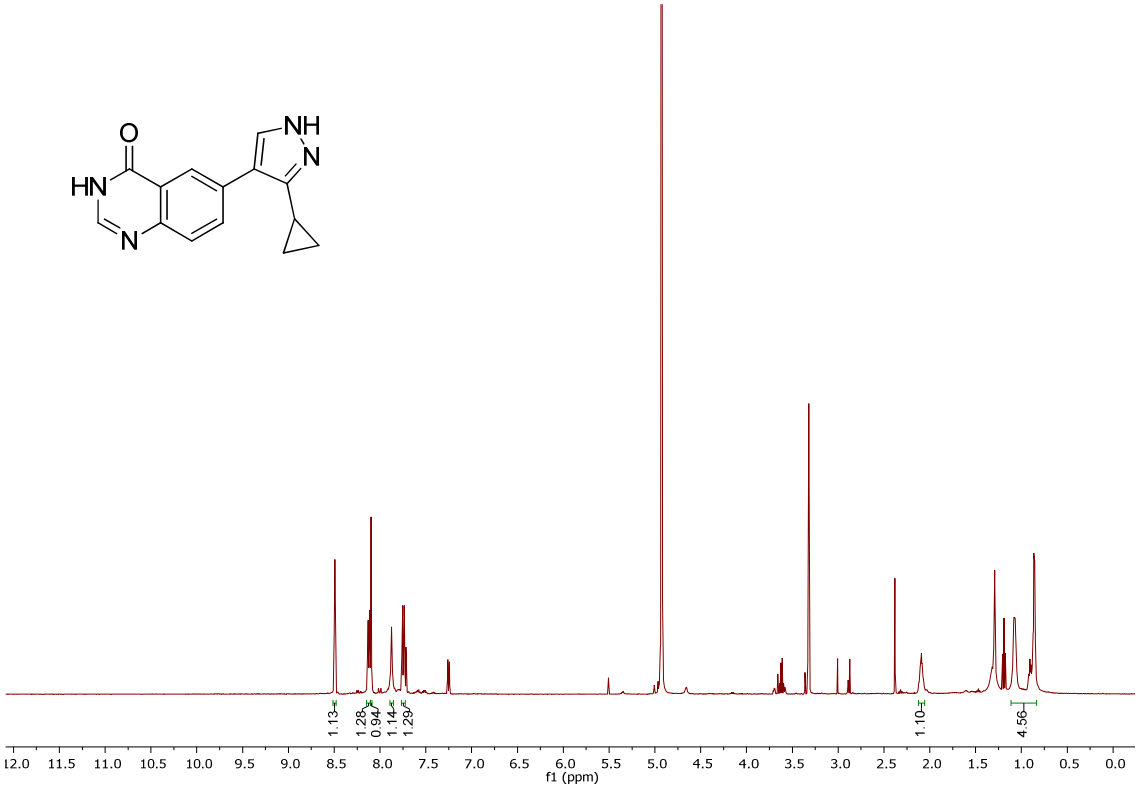

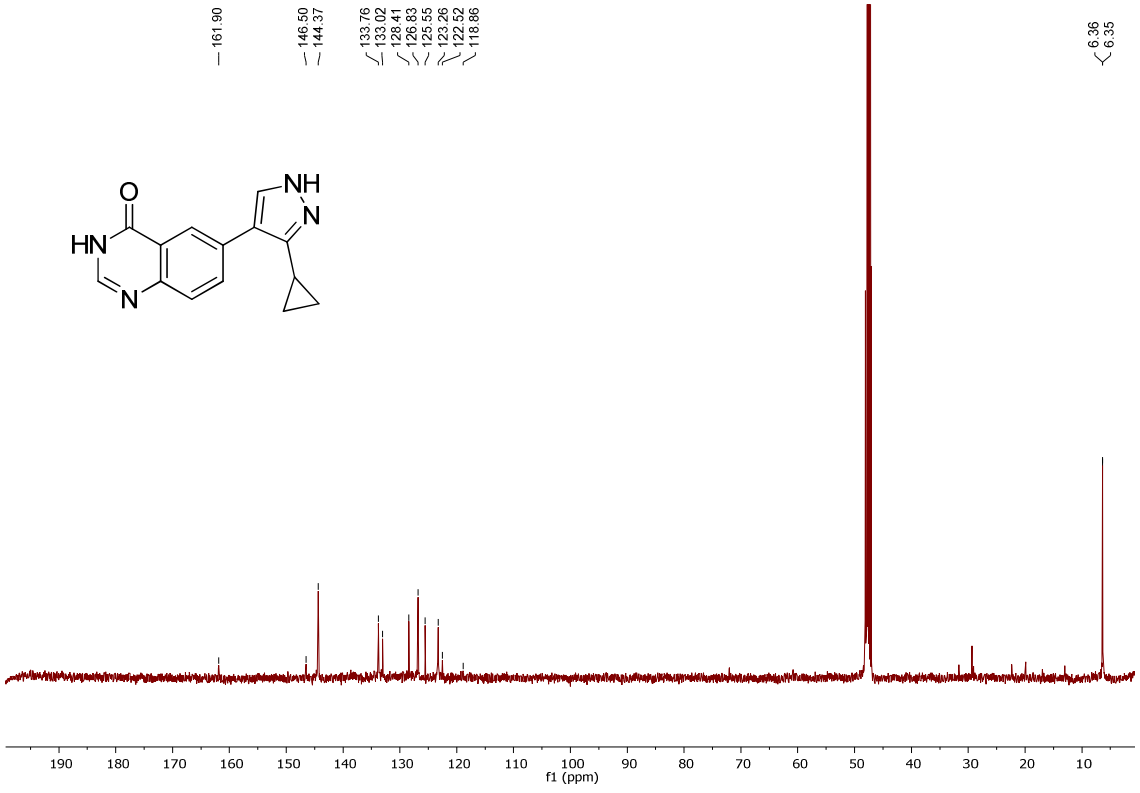

6-(3,5-Dimethyl-1*H*-pyrazol-4-yl)quinazolin-4(3*H*)-one, 6

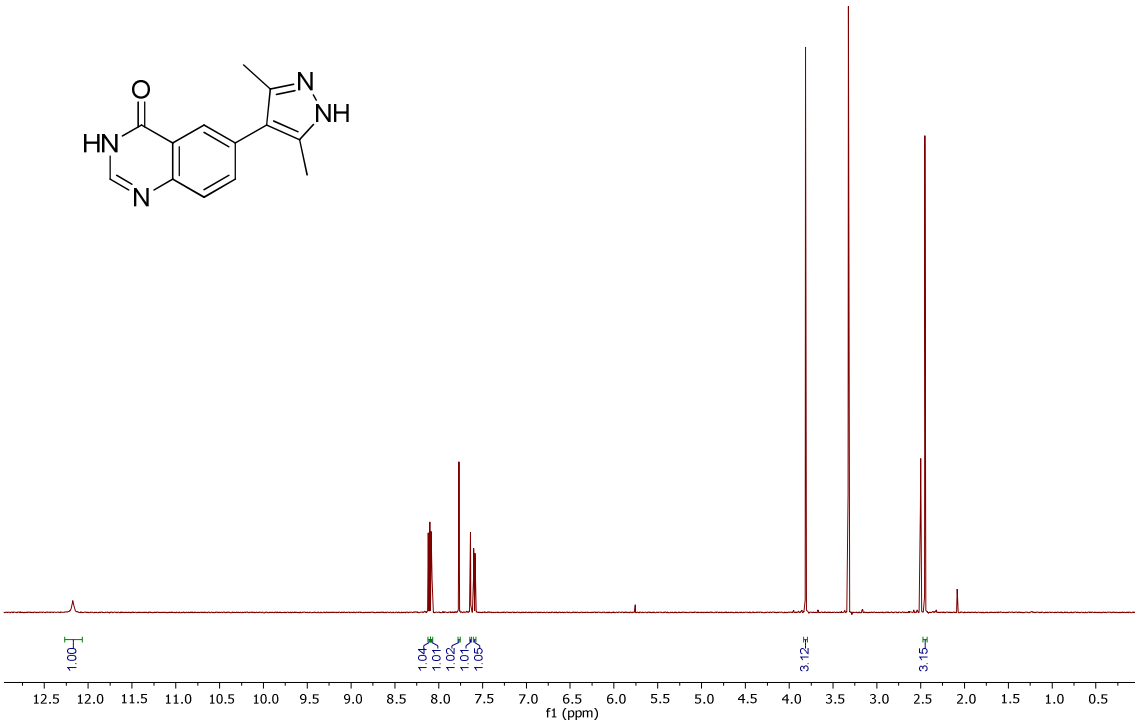

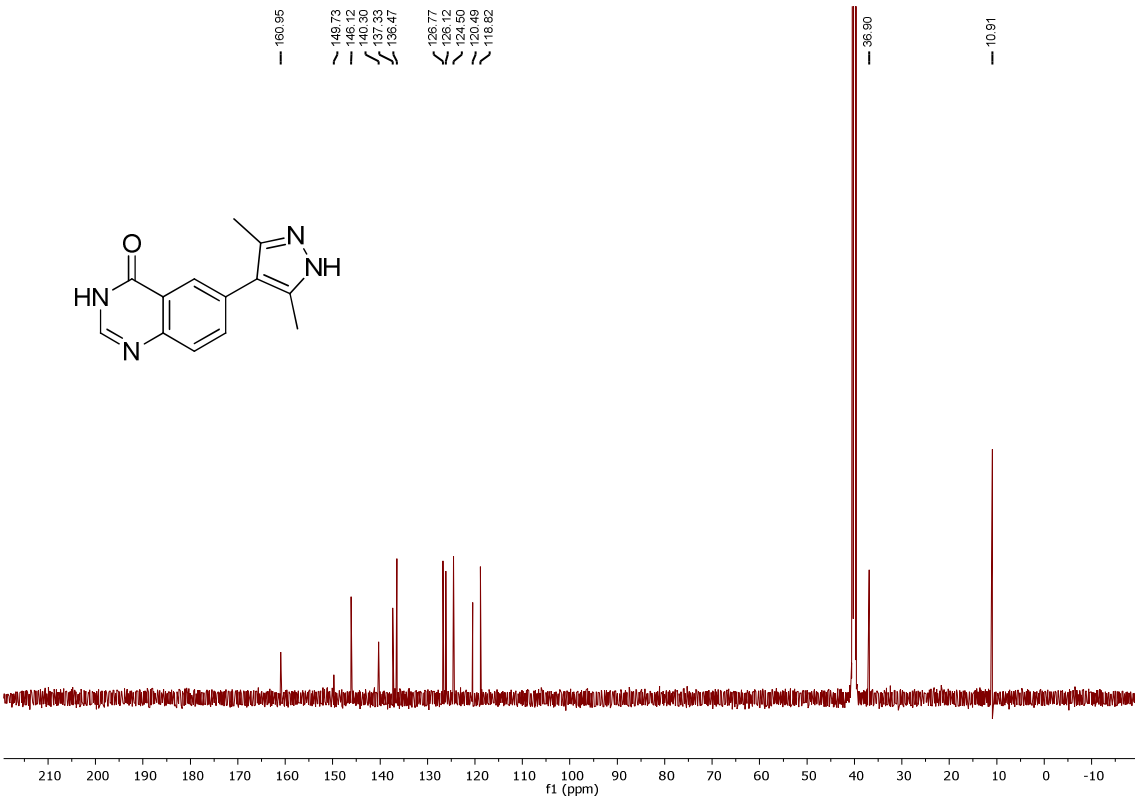

6-(Quinolin-4-yl)quinazolin-4(3*H*)-one, 7

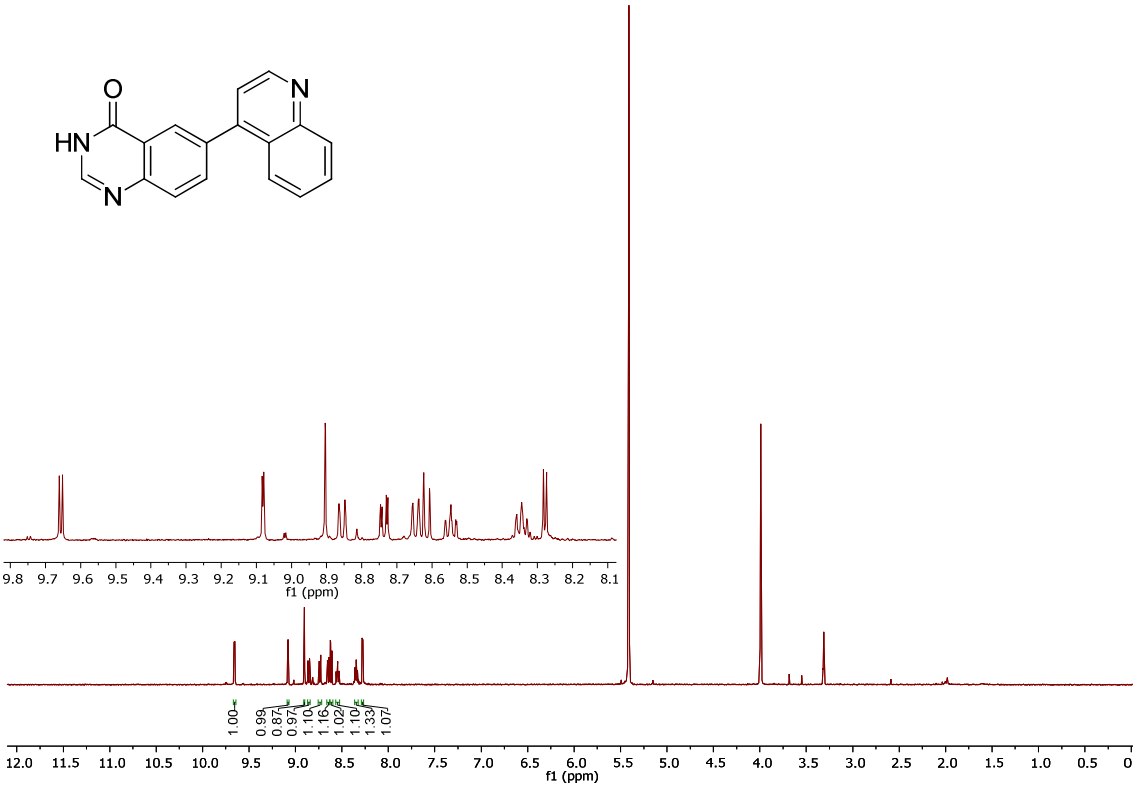

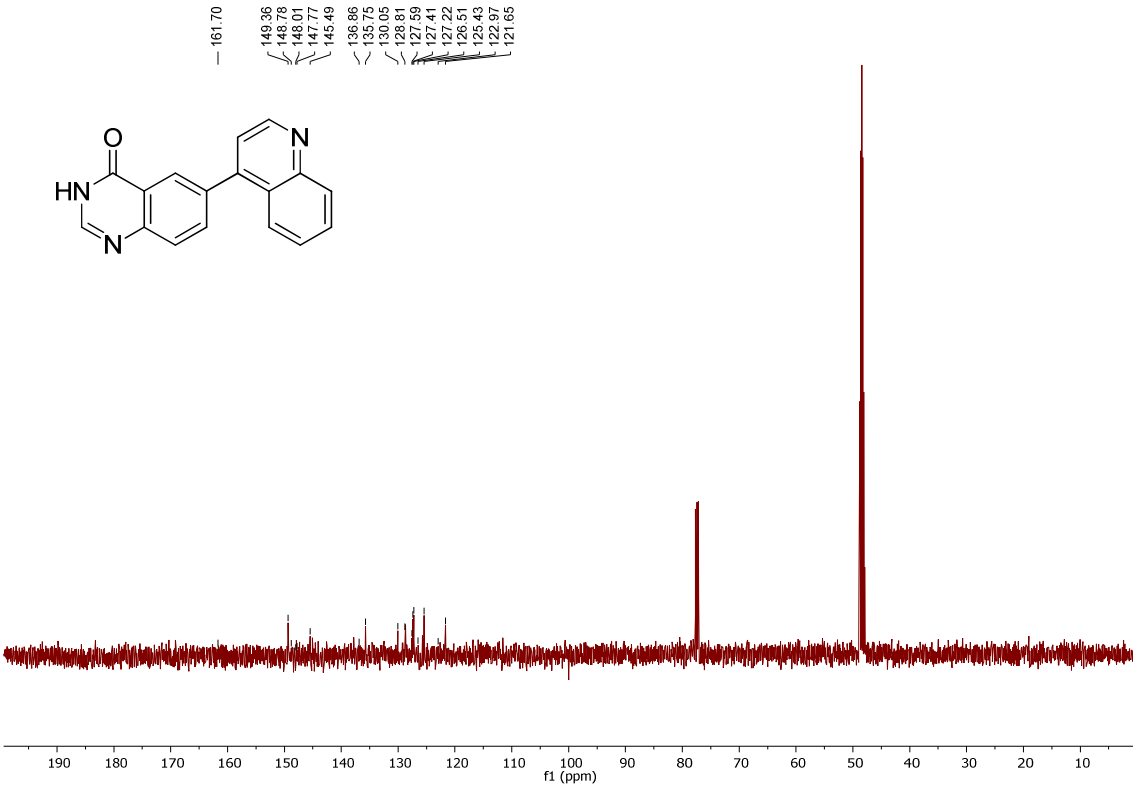

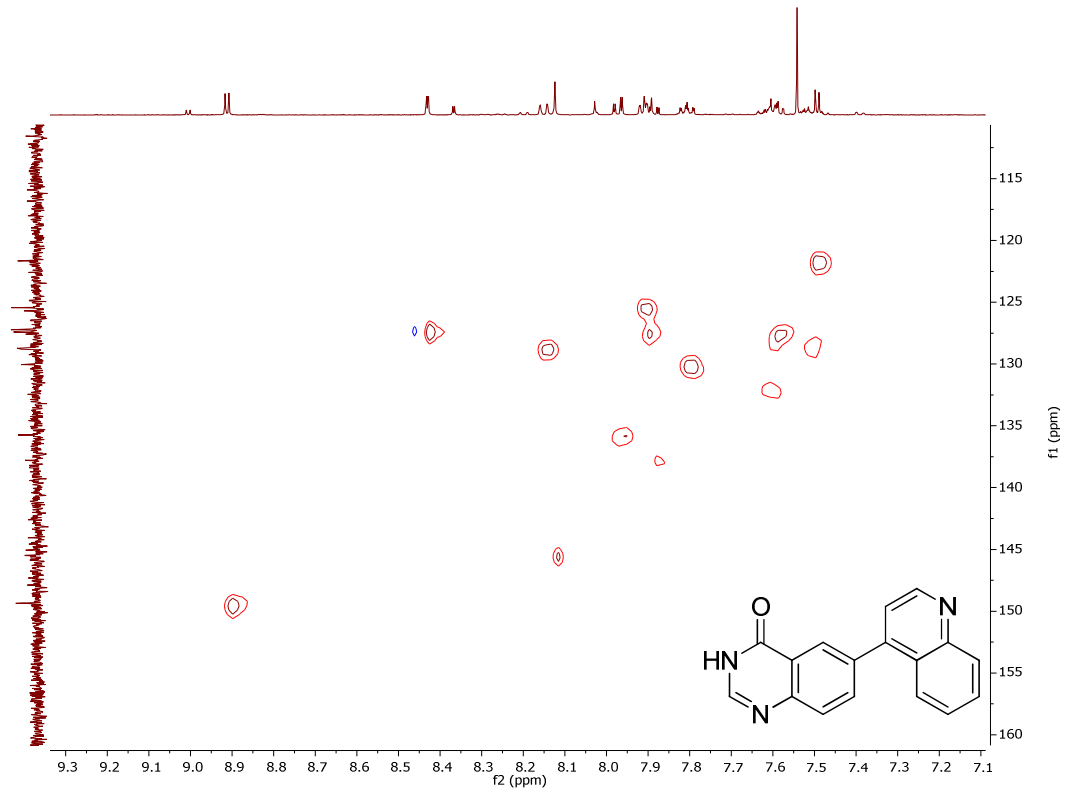
f2 (ppm)
f1 (ppm)
O
HN
N
N

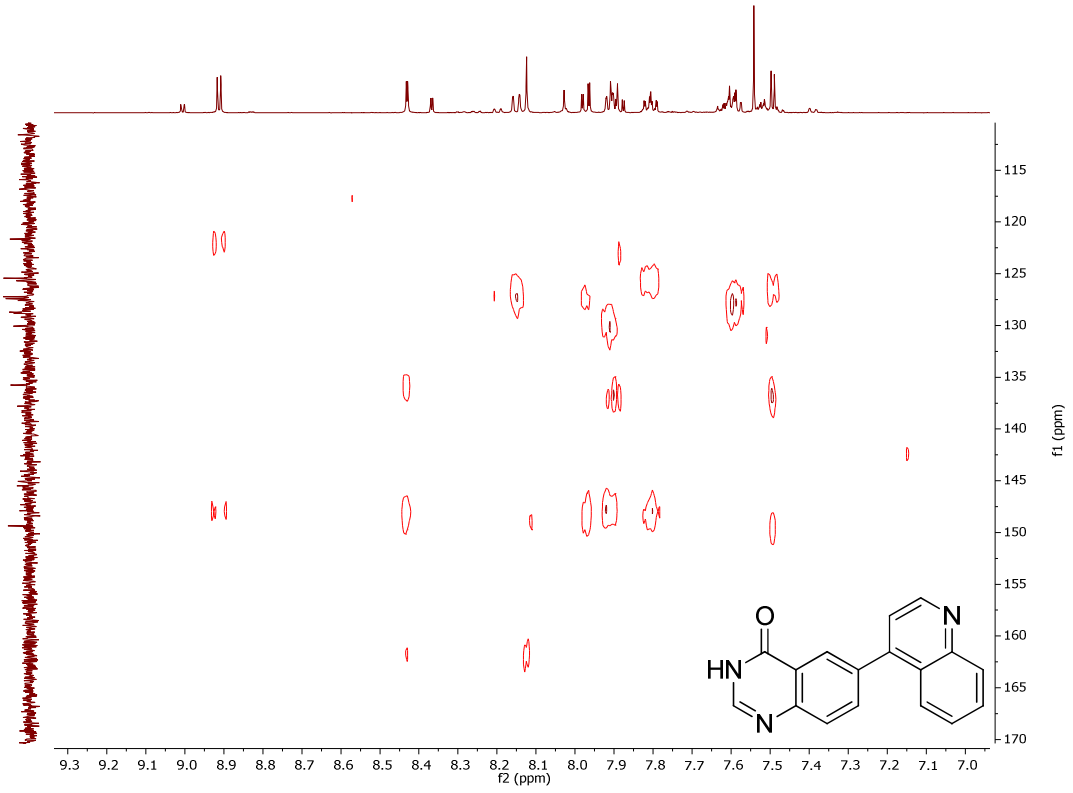
f2 (ppm)
f1 (ppm)
O
HN
N
N

6-(Quinolin-5-yl)quinazolin-4(3*H*)-one, 8

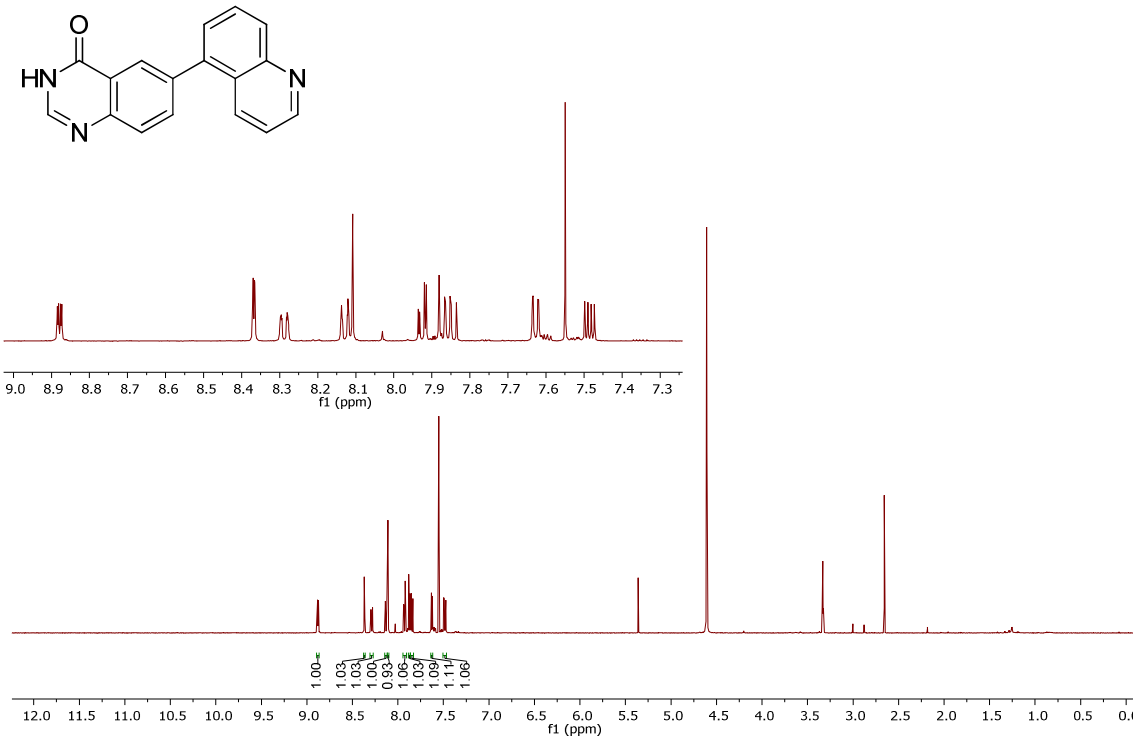

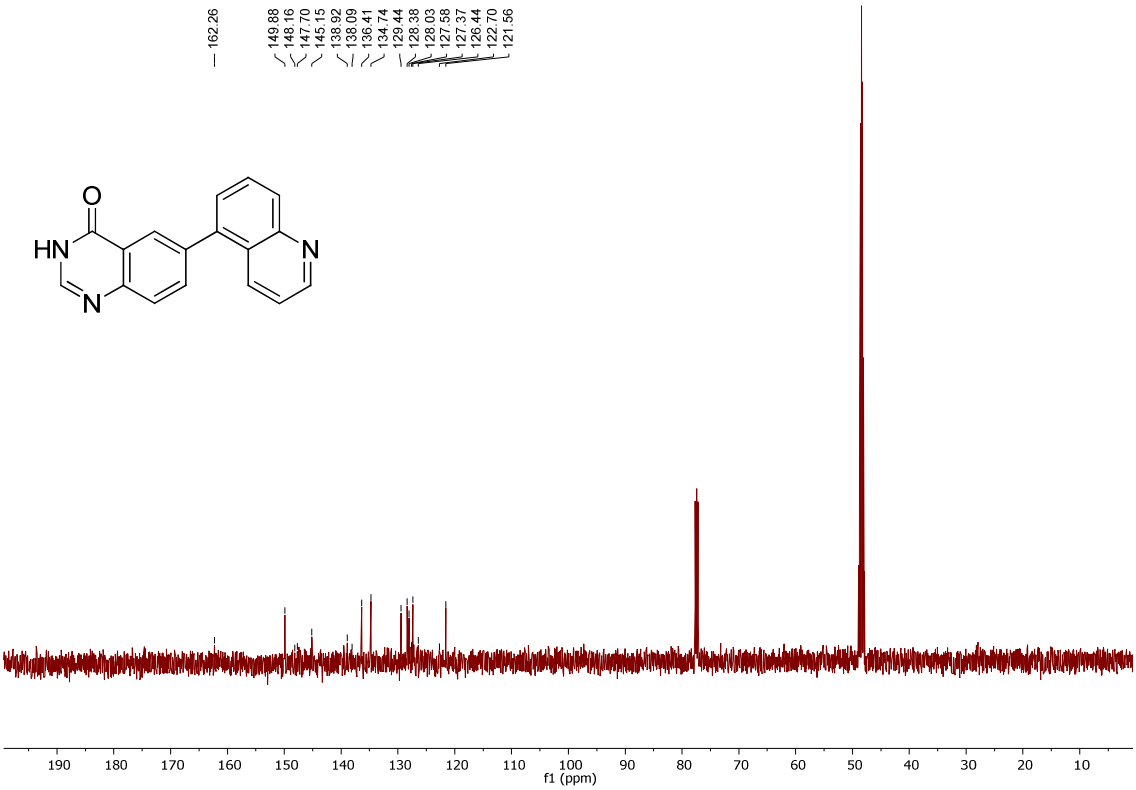

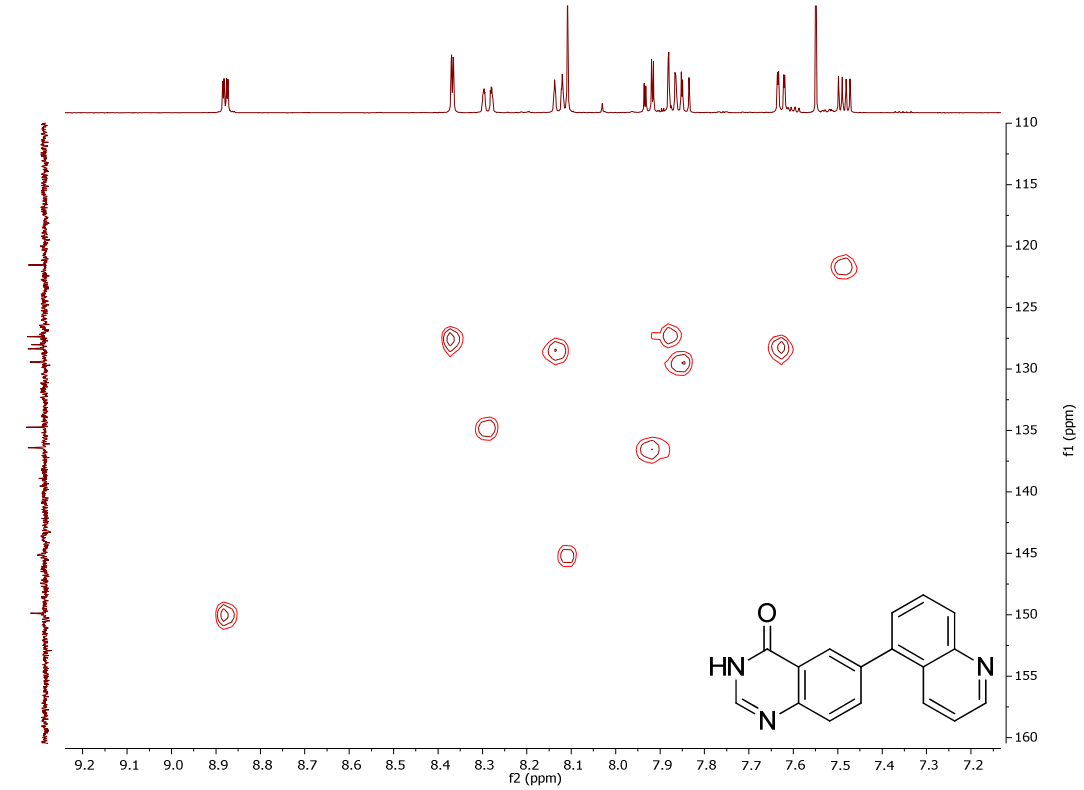
f2 (ppm)
f1 (ppm)
O
HN
N
N

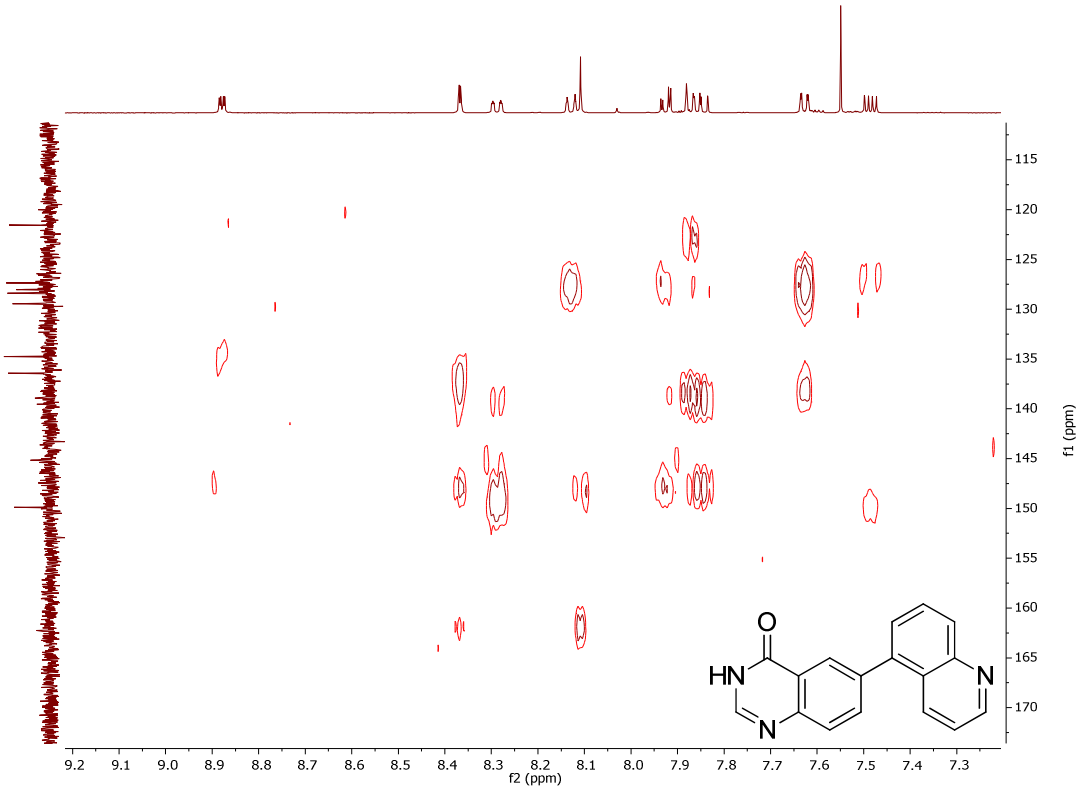
f2 (ppm)
f1 (ppm)
O
HN
N
N

6-(Pyrazolo[1,5-*a*]pyridin-3-yl)quinazolin-4(3*H*)-one, 9

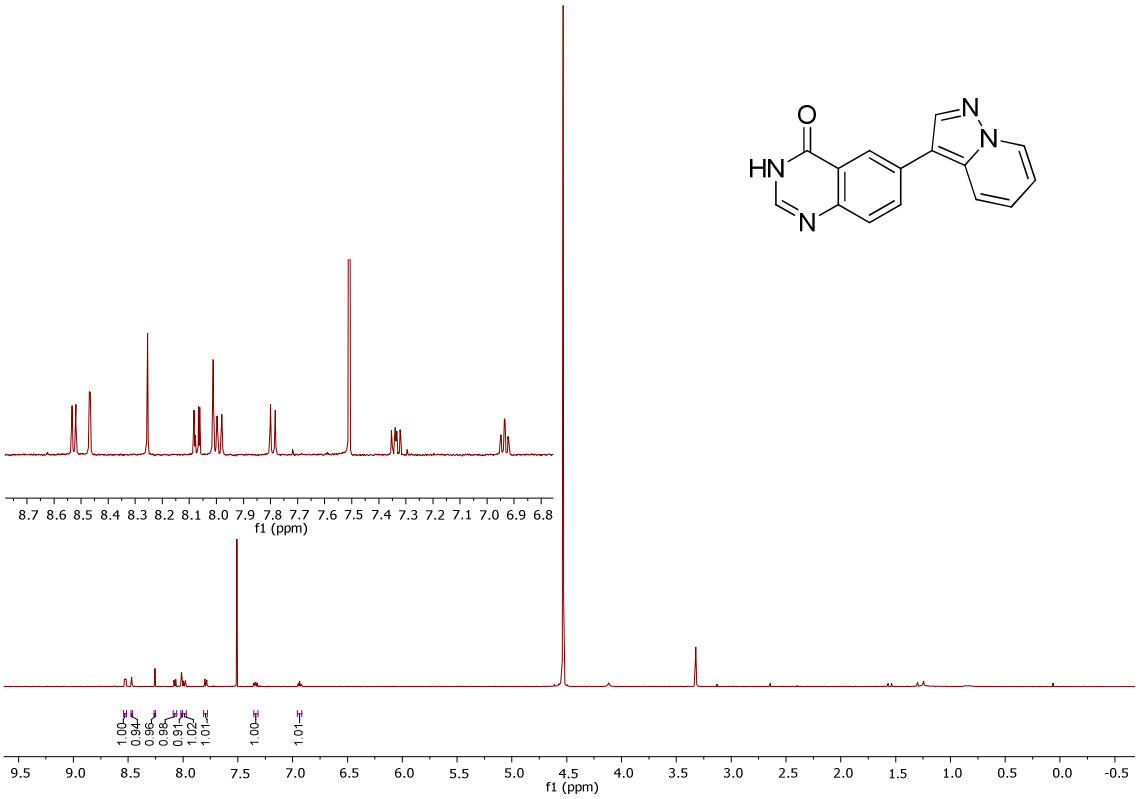

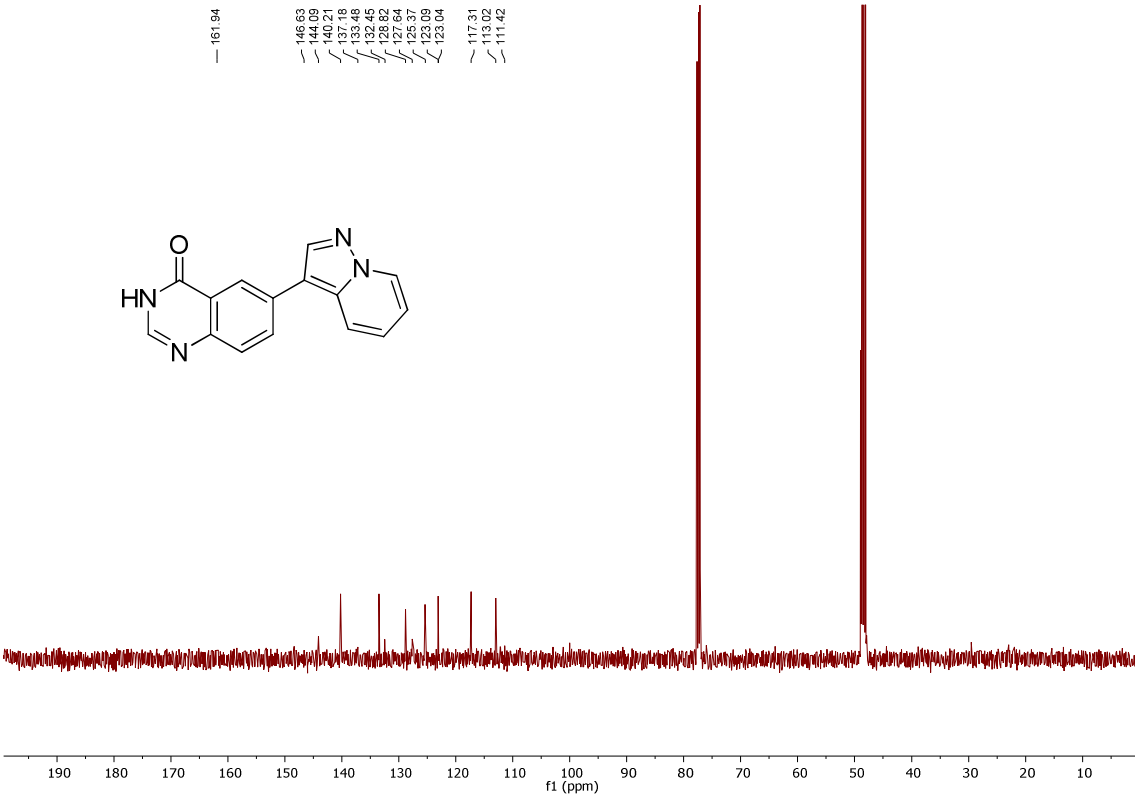

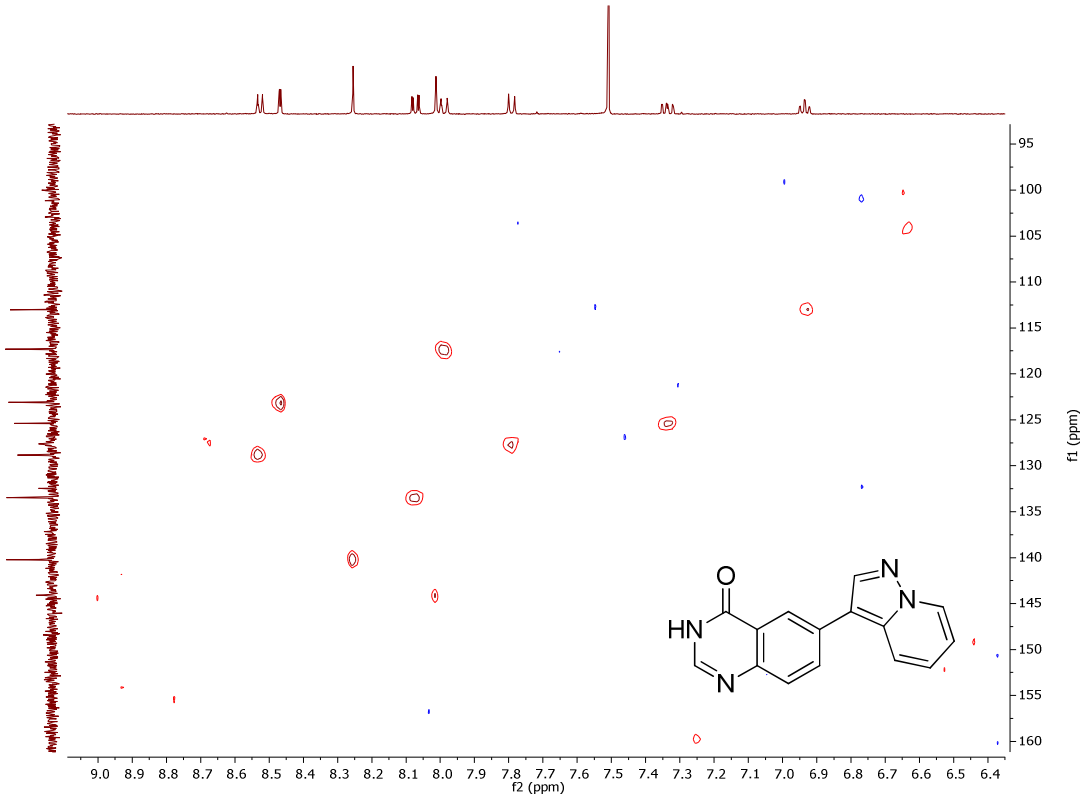
f1 (ppm)
f2 (ppm)
O
HN
N
N

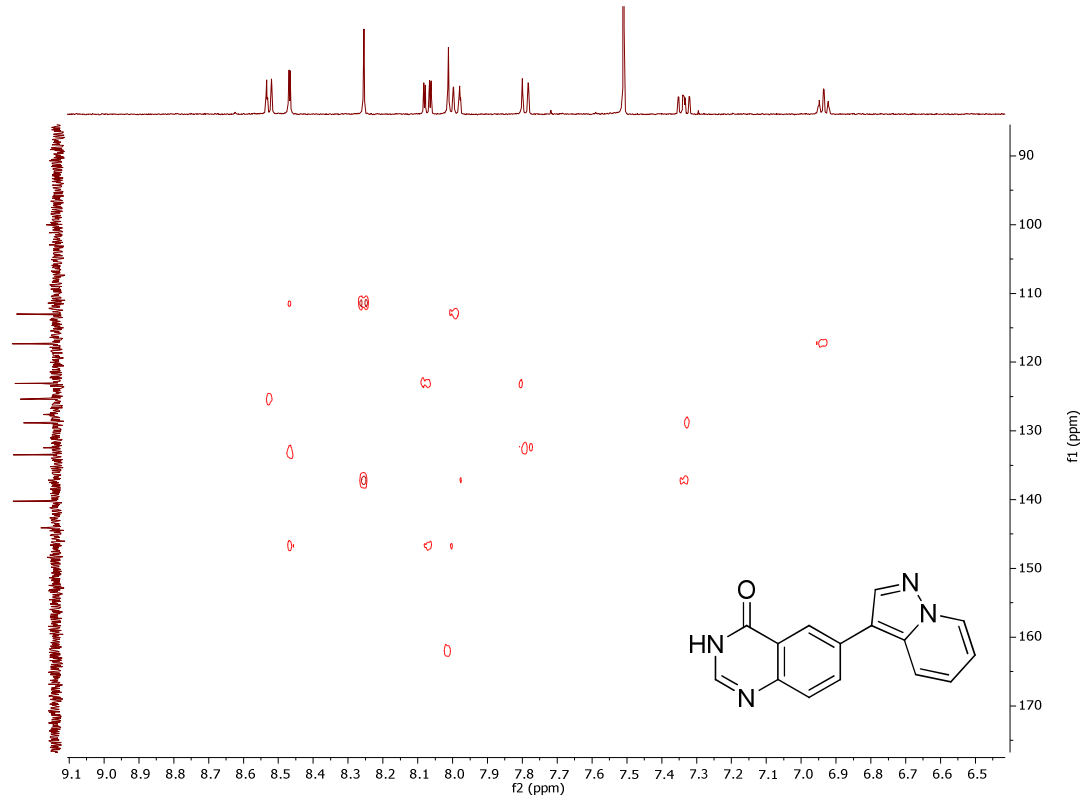
f1 (ppm)
f2 (ppm)
O
HN
N
N

5-Methyl-6-(quinolin-4-yl)quinazolin-4(3*H*)-one, 10

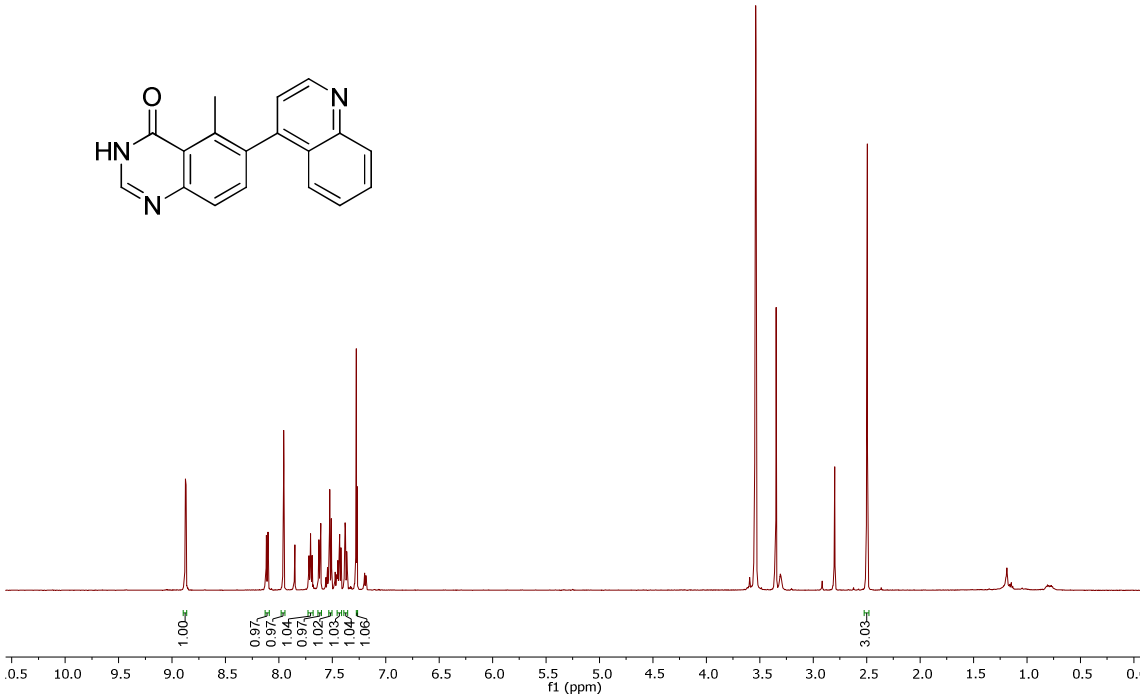

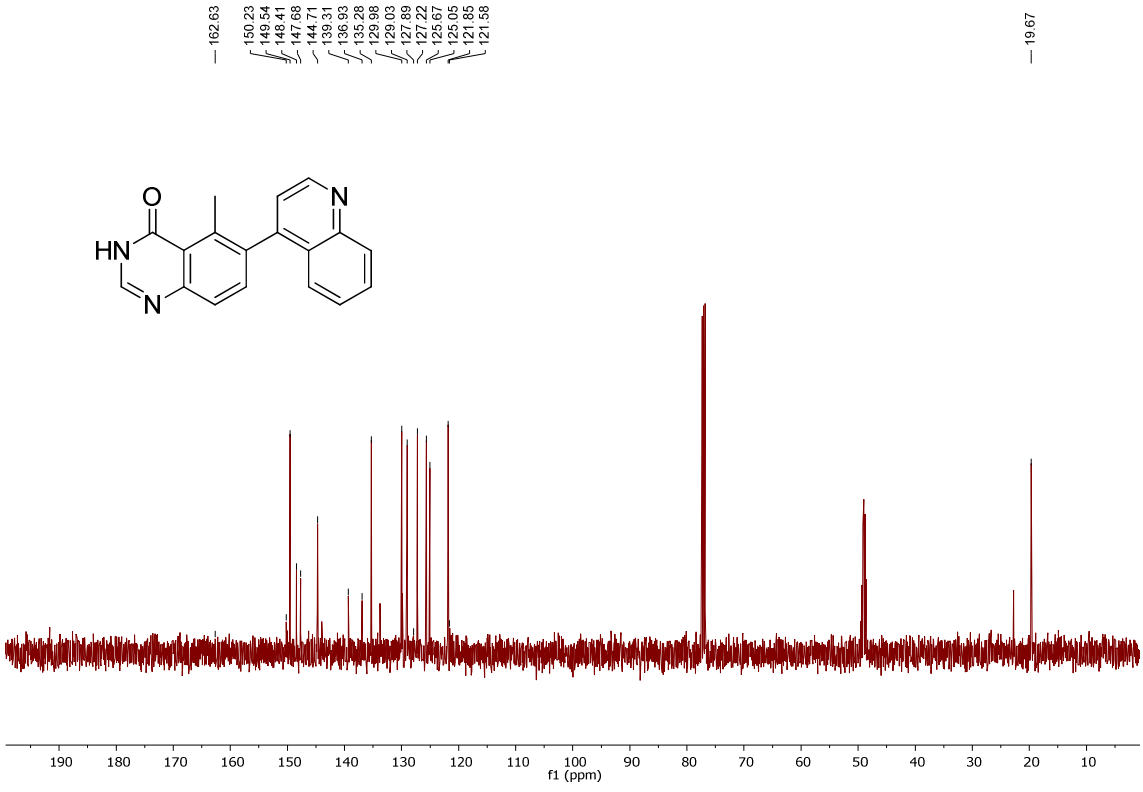

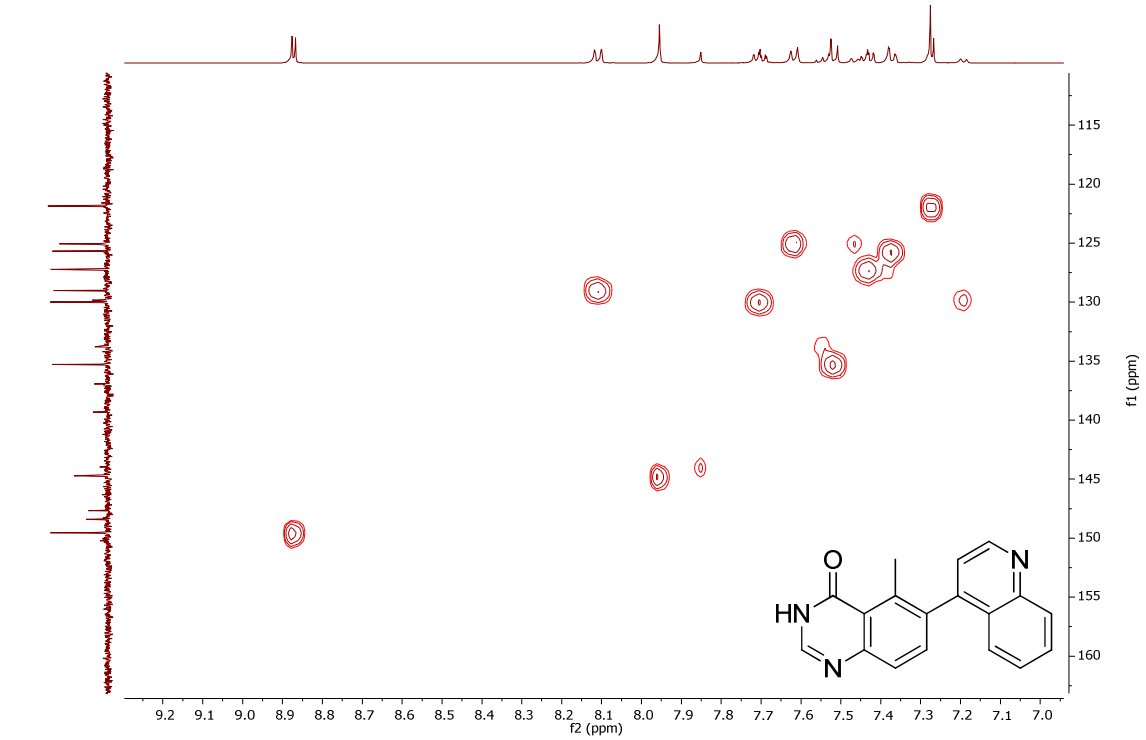
f1 (ppm)
f2 (ppm)
O
HN
N
N

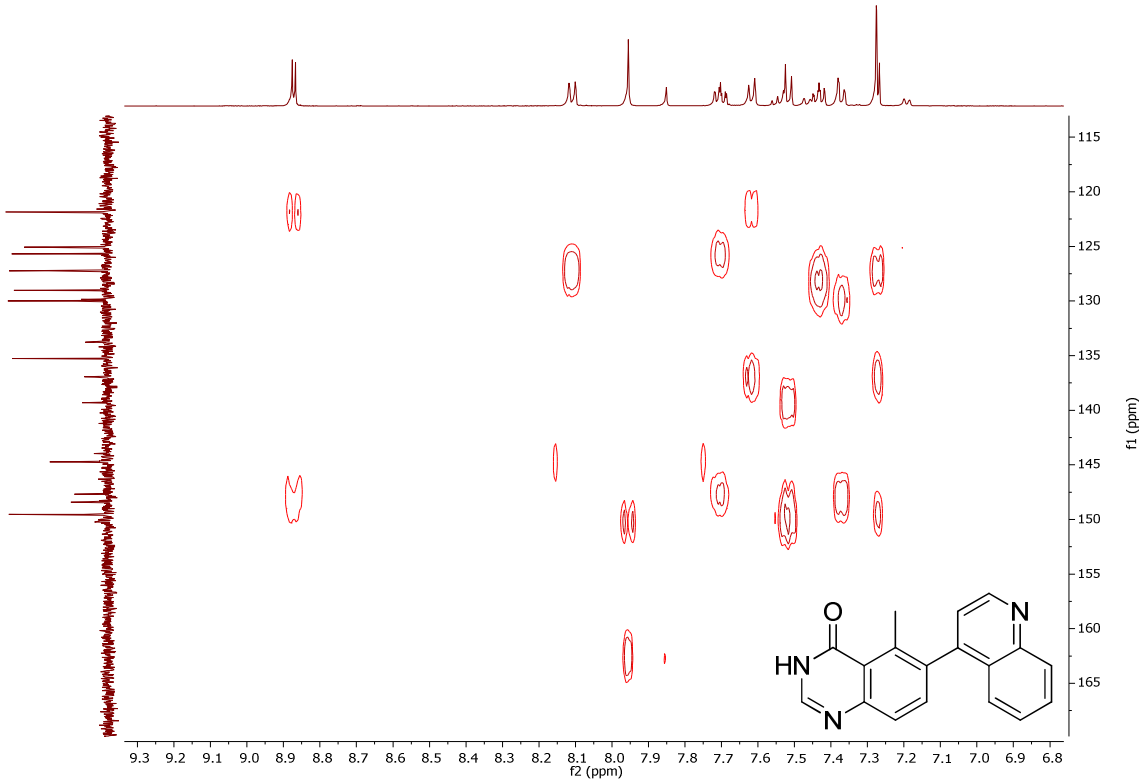
f1 (ppm)
f2 (ppm)
O
HN
N
N

5-Methyl-6-(quinolin-5-yl)quinazolin-4(3*H*)-one, 11

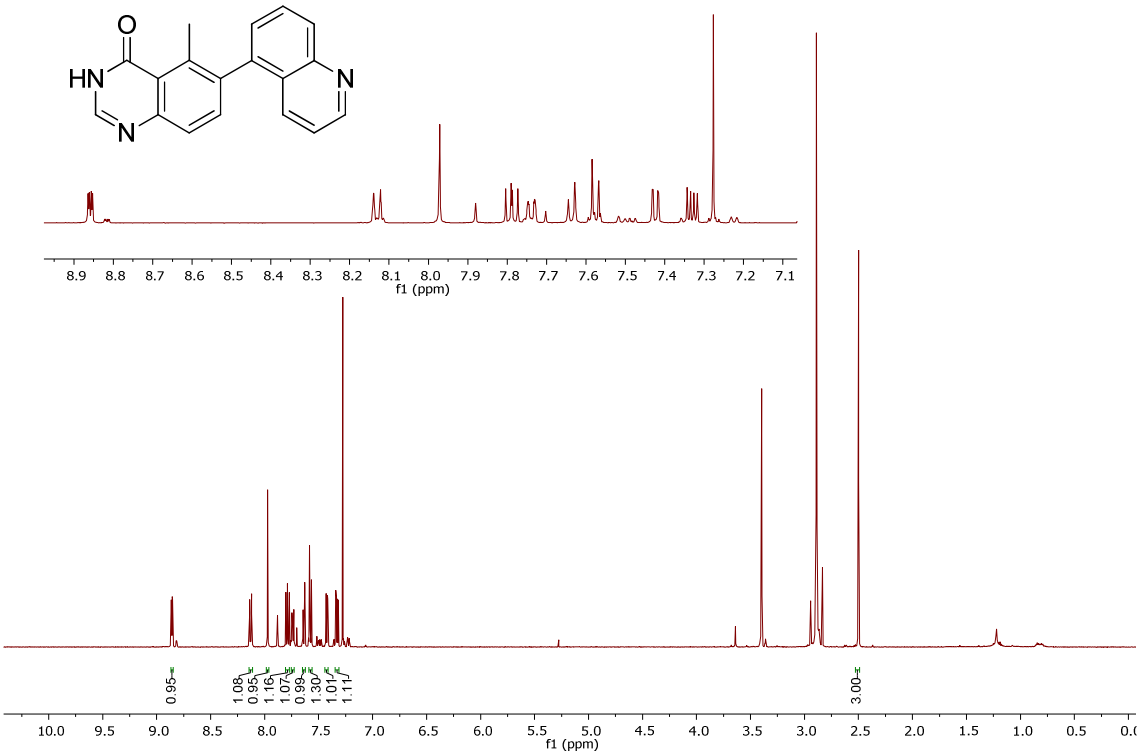

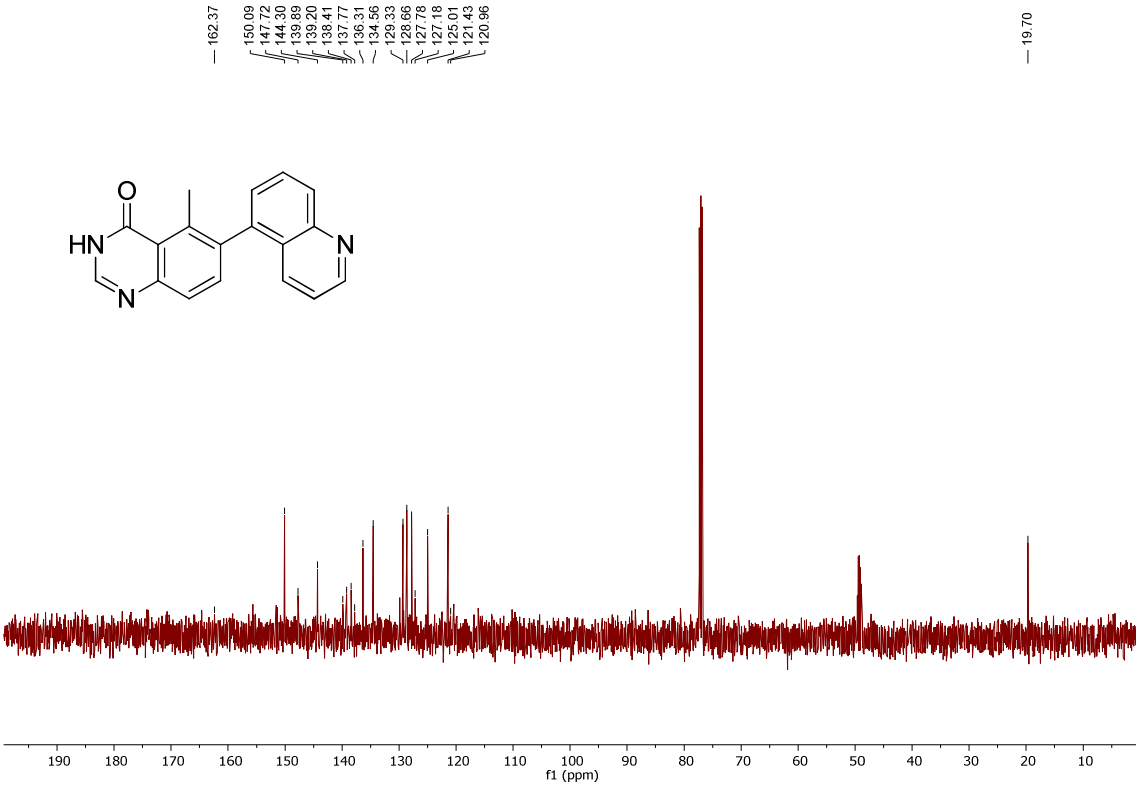

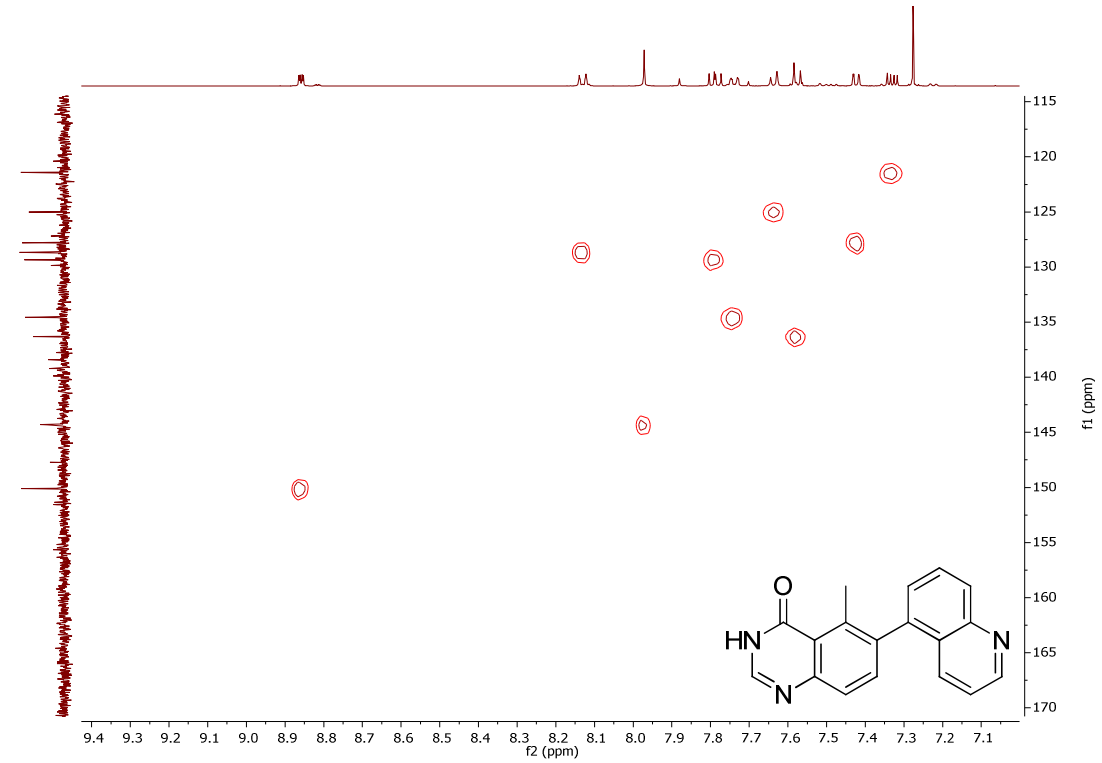
f2 (ppm)
f1 (ppm)
HN
O
N
N

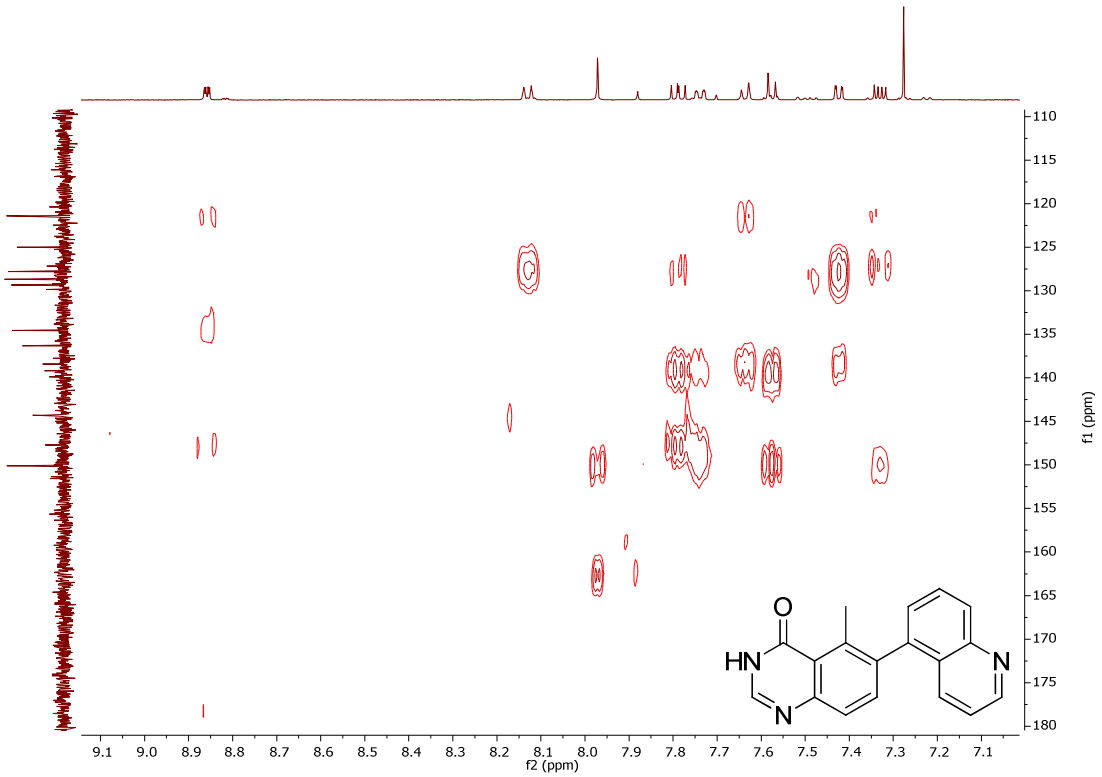
f2 (ppm)
f1 (ppm)
HN
O
N
N

3-Methyl-6-(quinolin-4-yl)quinazolin-4(3*H*)-one, 12

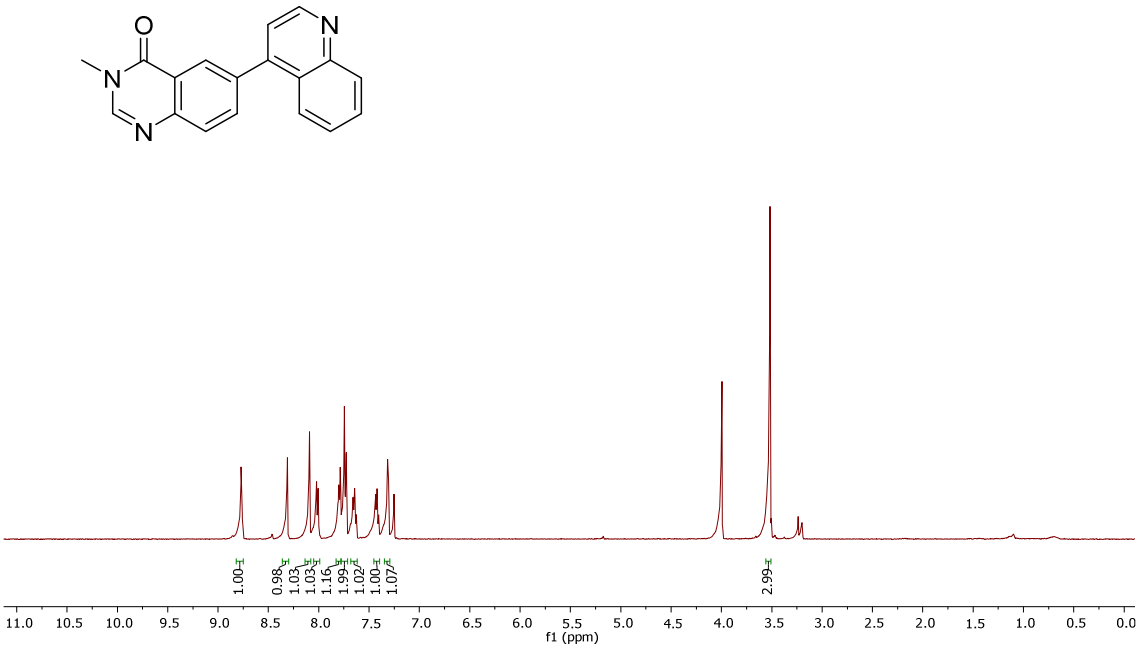

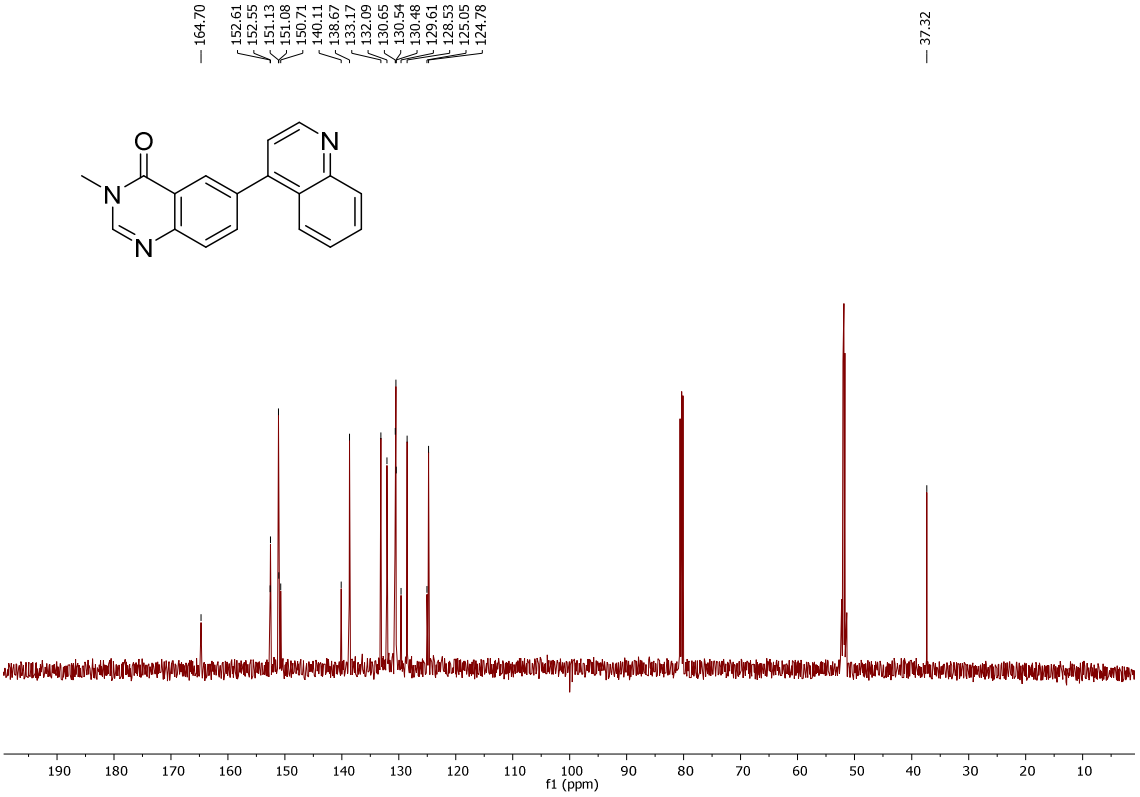

3-Methyl-6-(quinolin-5-yl)quinazolin-4(3*H*)-one, 13

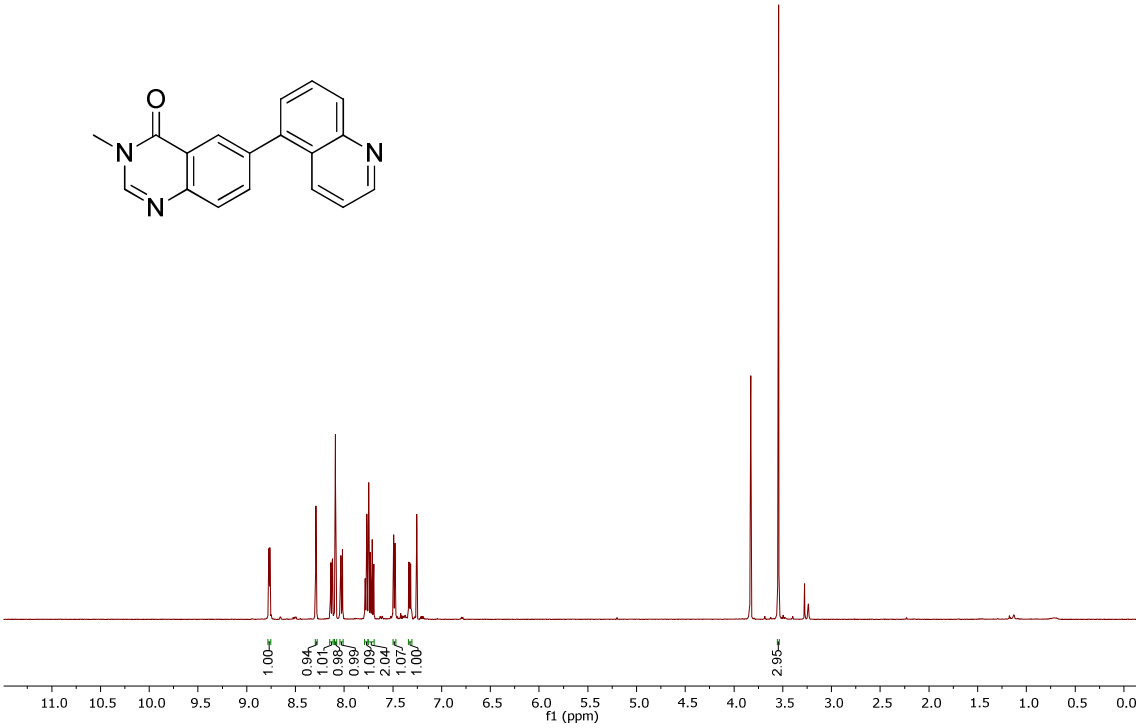

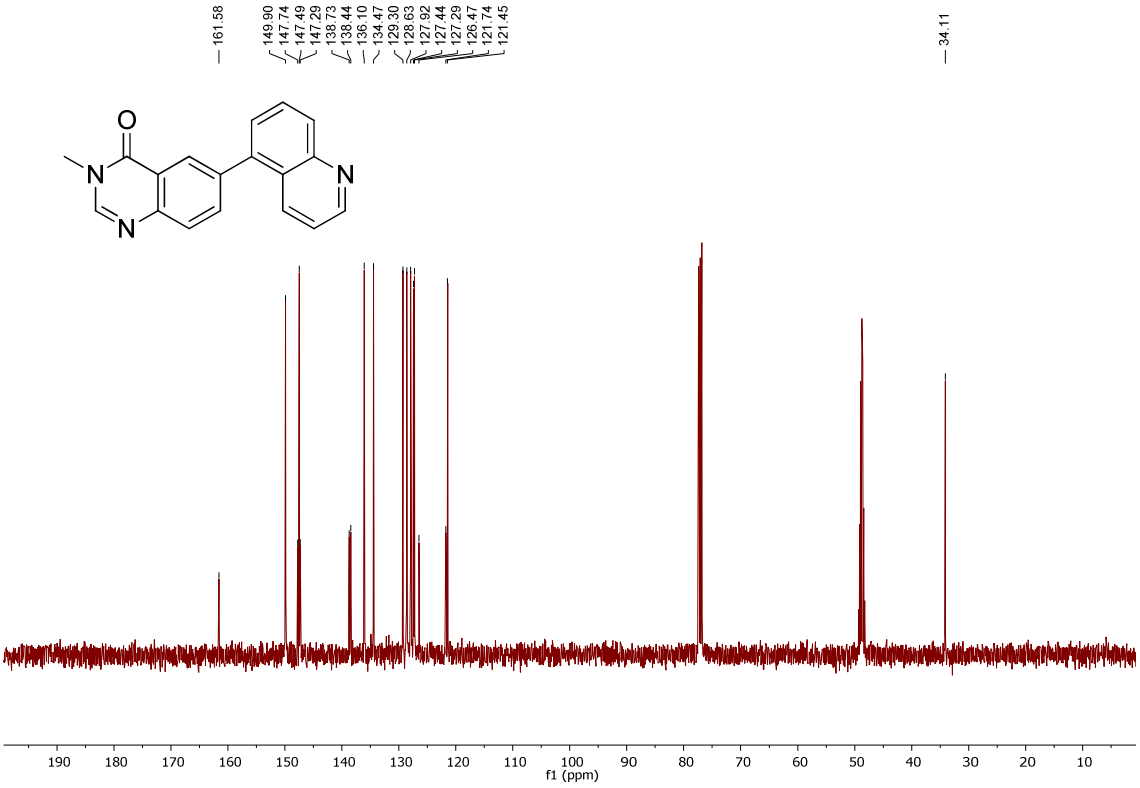

2-Methyl-6-(quinolin-4-yl)quinazolin-4(3*H*)-one, 14

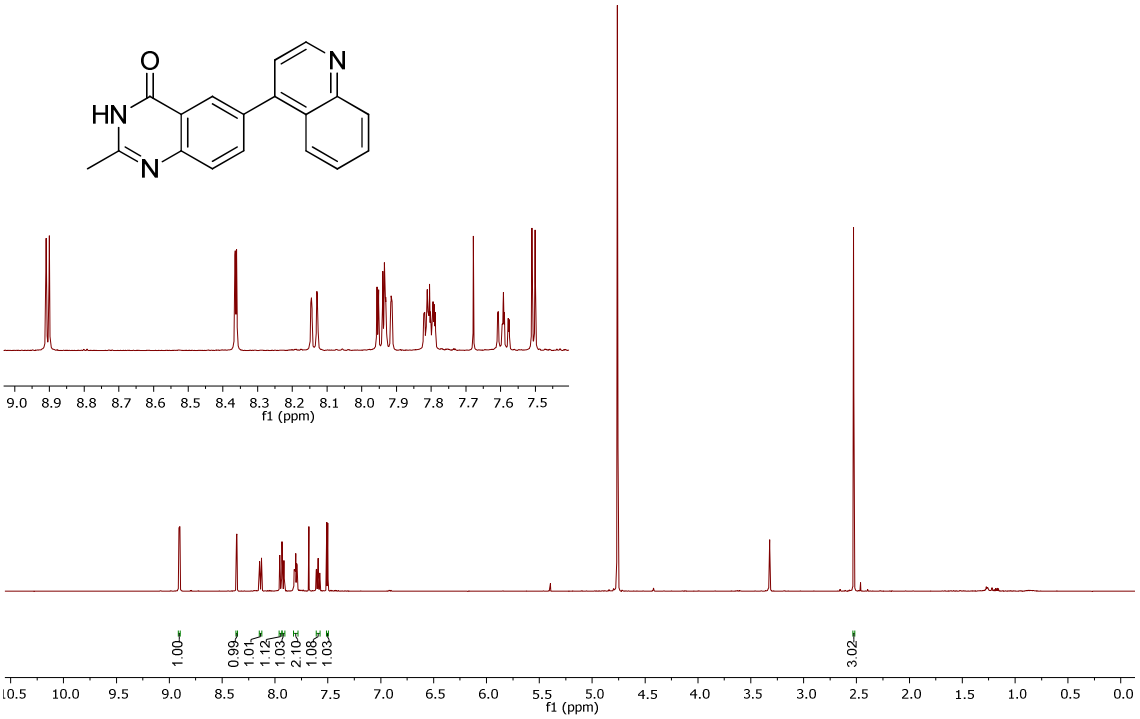

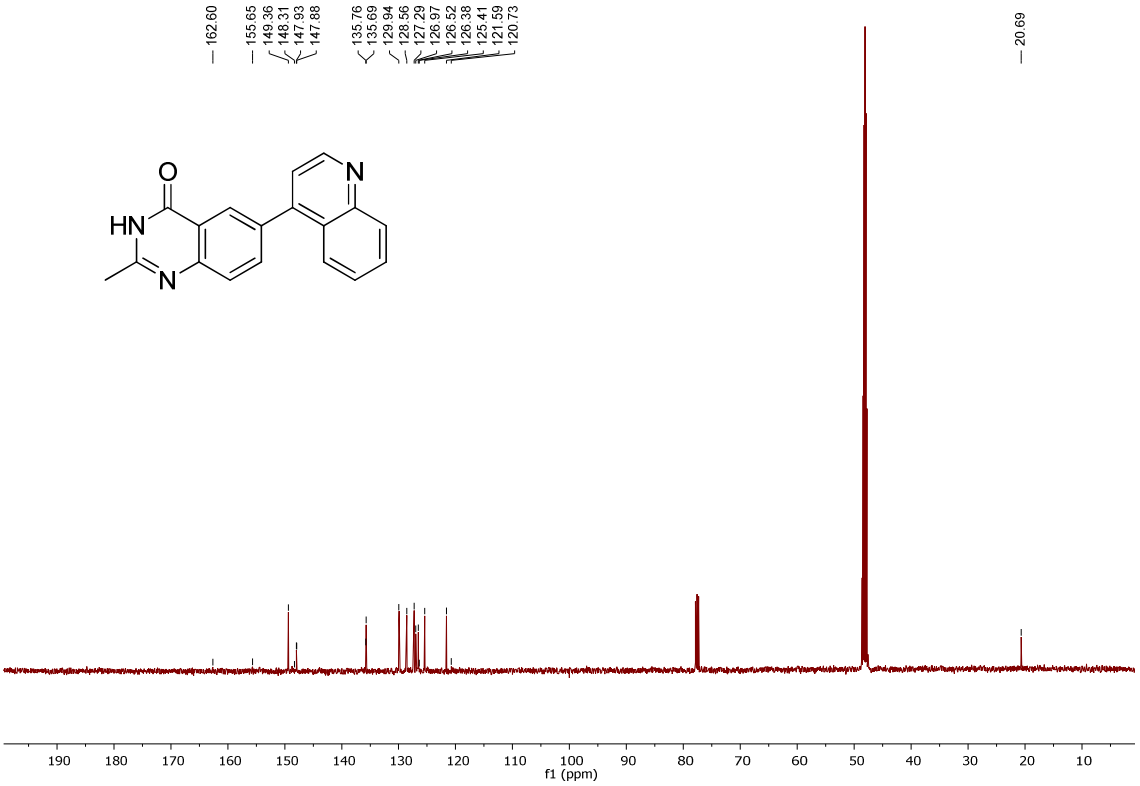

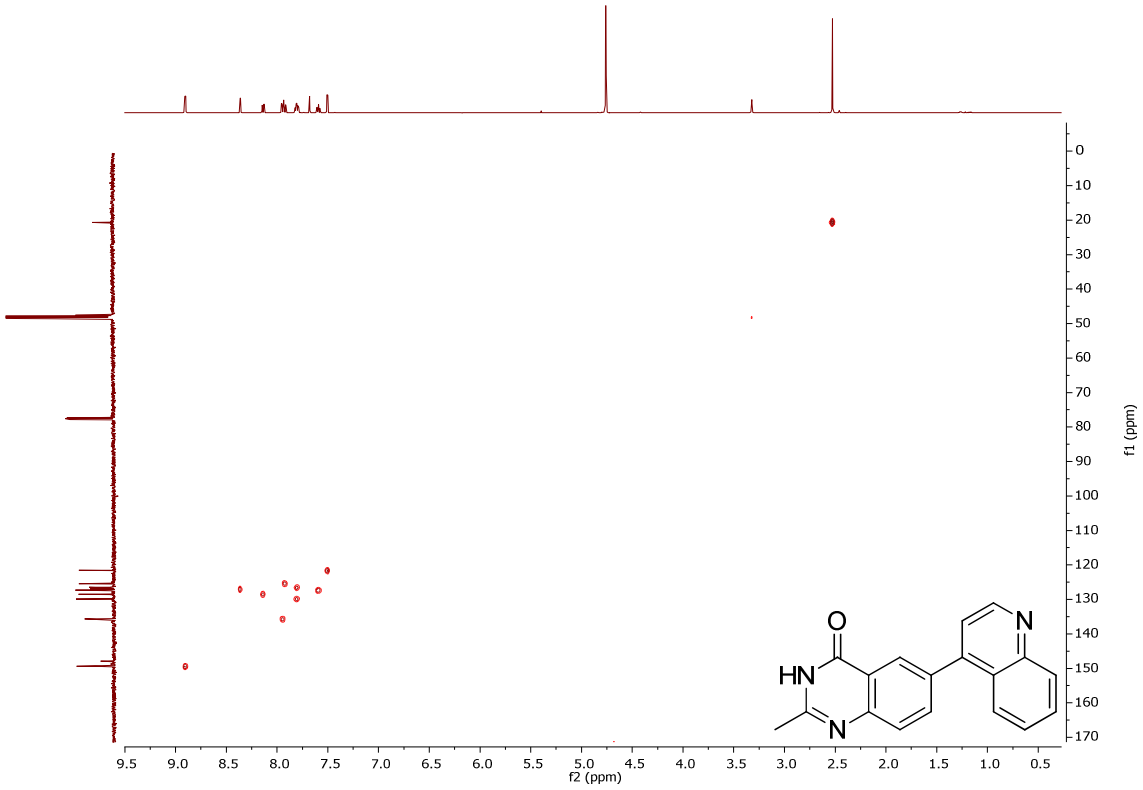
f2 (ppm)
f1 (ppm)
O
HN
N
N

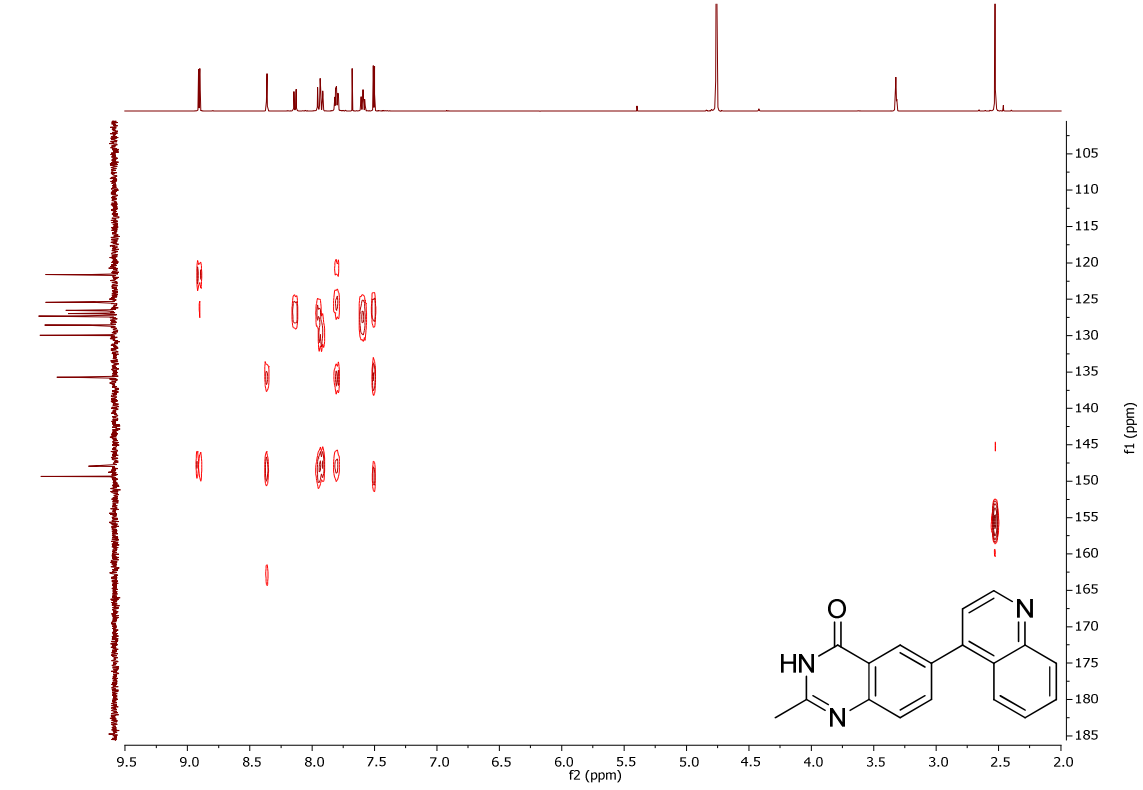
f2 (ppm)
f1 (ppm)
O
HN
N
N

2-Methyl-6-(quinolin-5-yl)quinazolin-4(3*H*)-one, 15

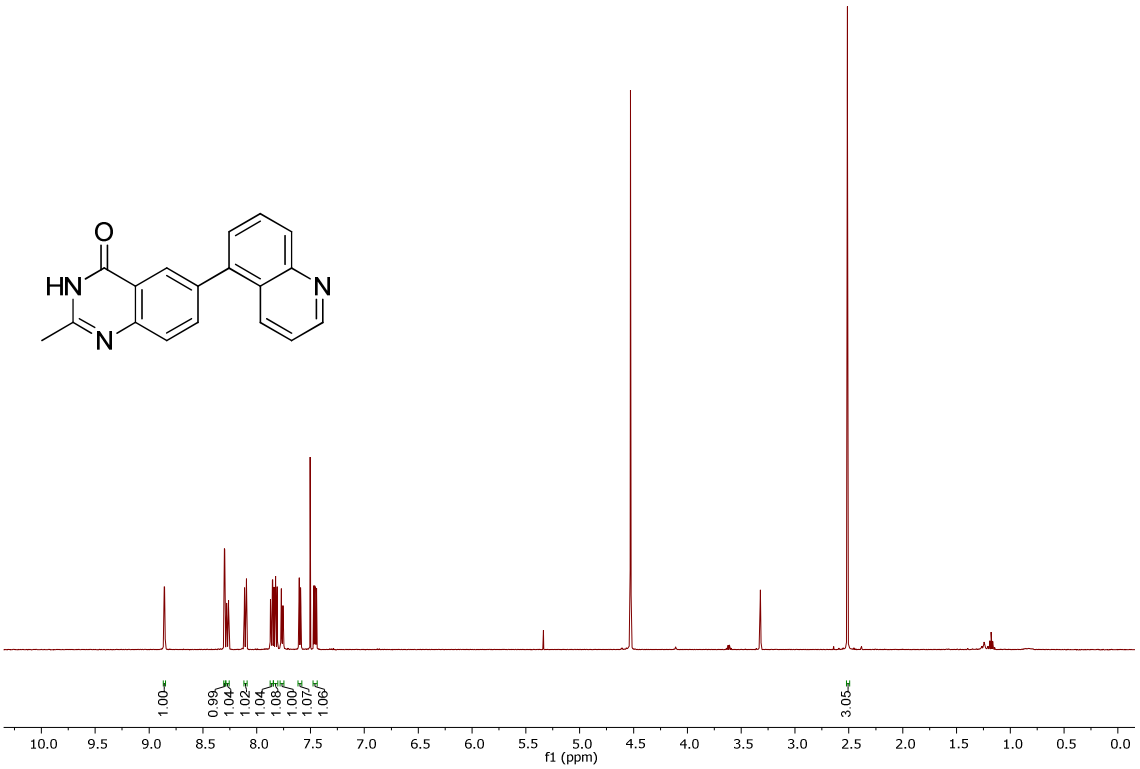

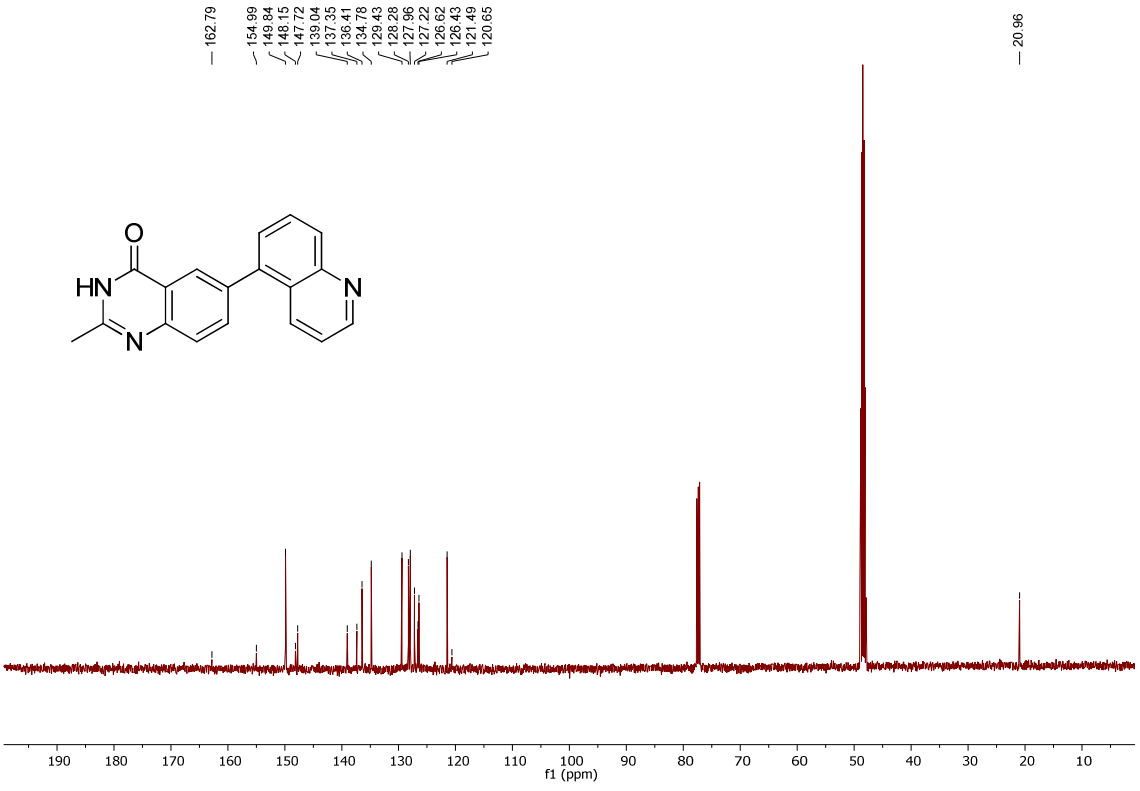

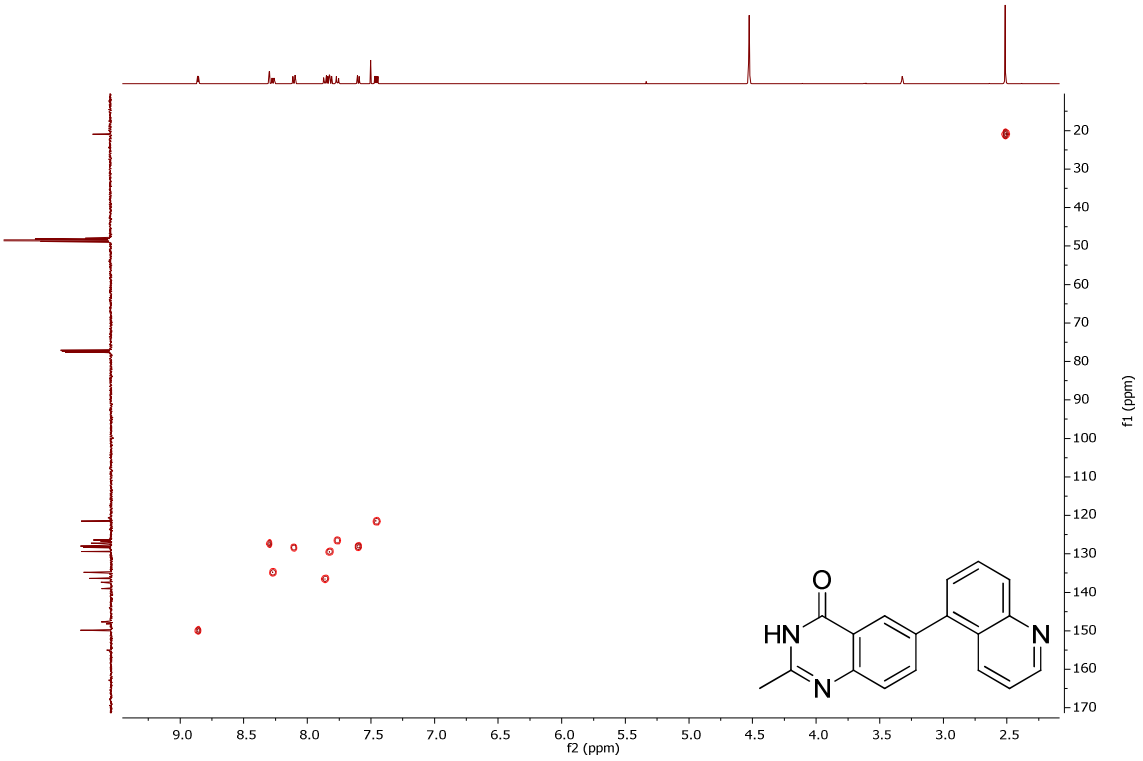
f2 (ppm)
f1 (ppm)
HN
O
N
N

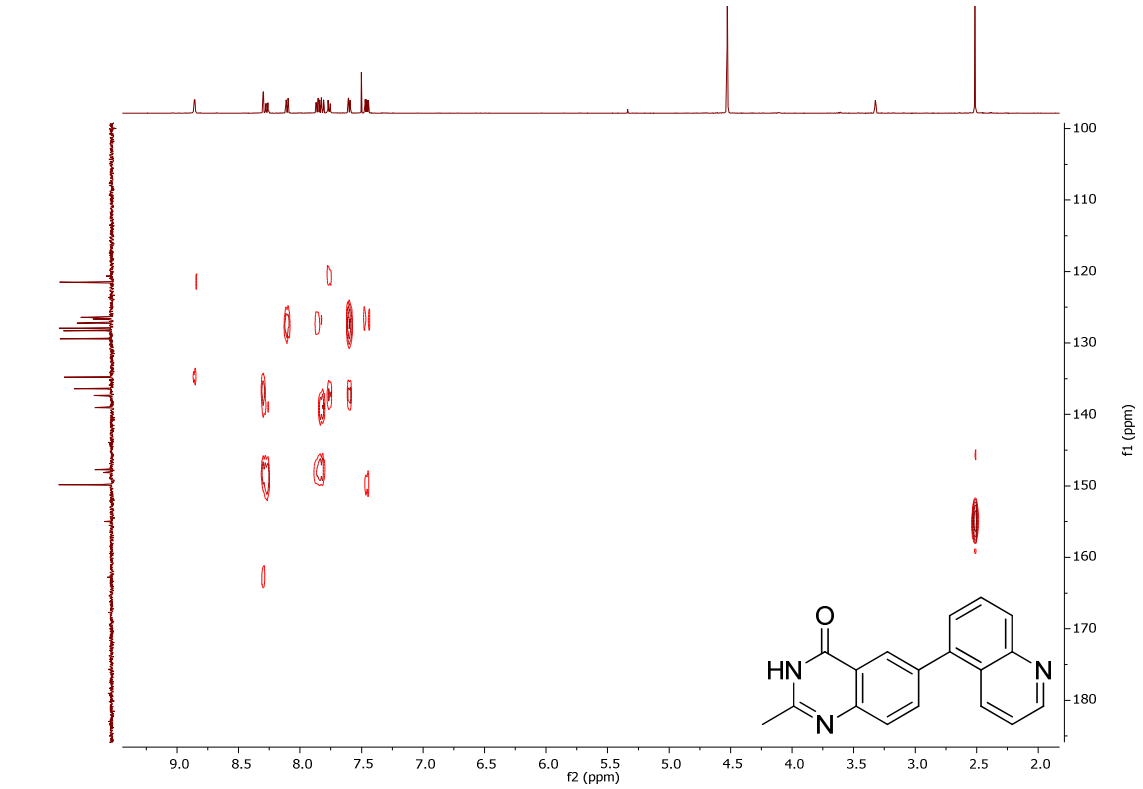
f2 (ppm)
f1 (ppm)
HN
O
N
N

3-(4-Morpholinophenyl)-6-(quinolin-4-yl)quinazolin-4(3*H*)-one, 16

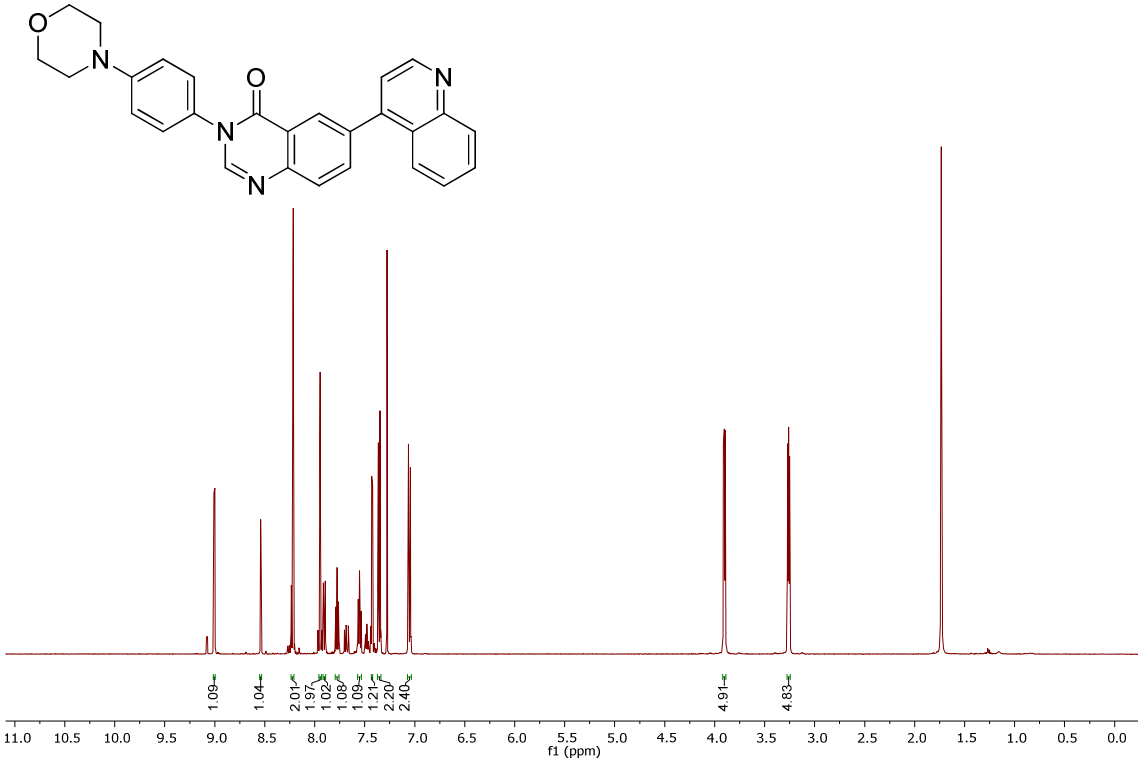

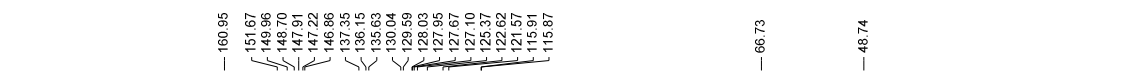

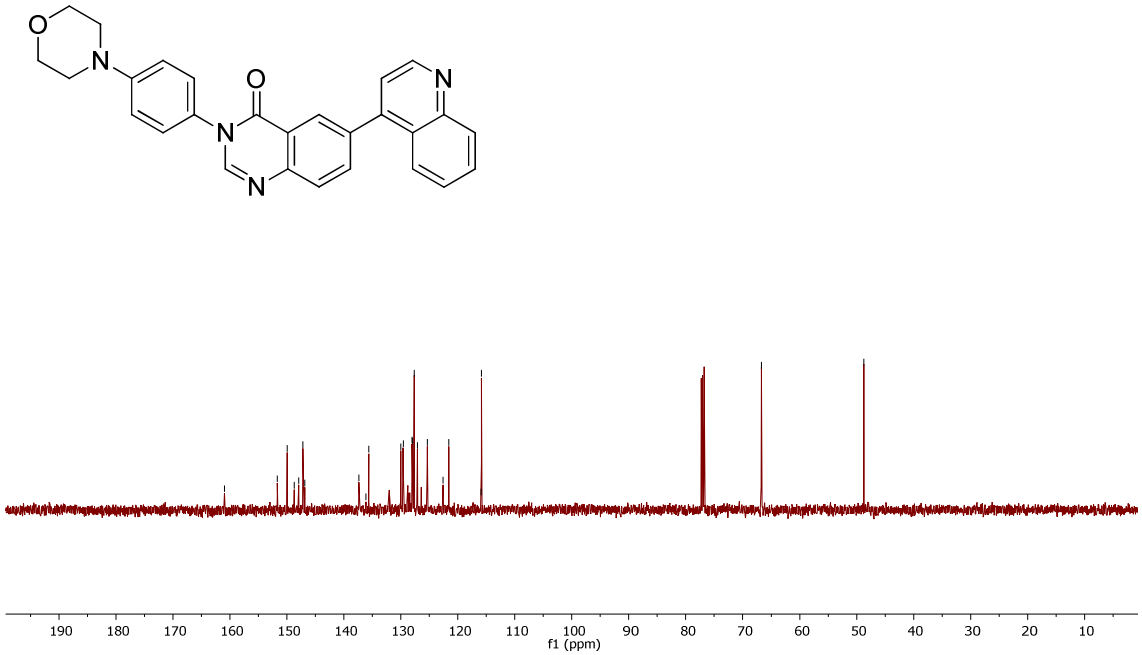

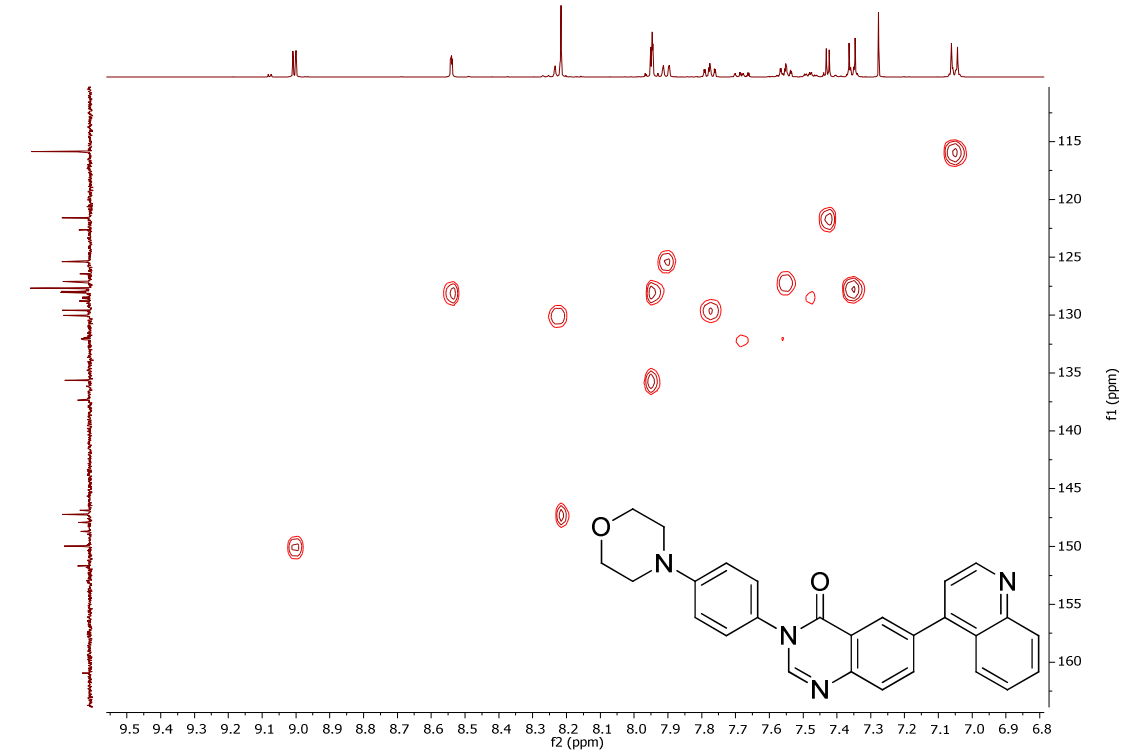
f2 (ppm)
f1 (ppm)

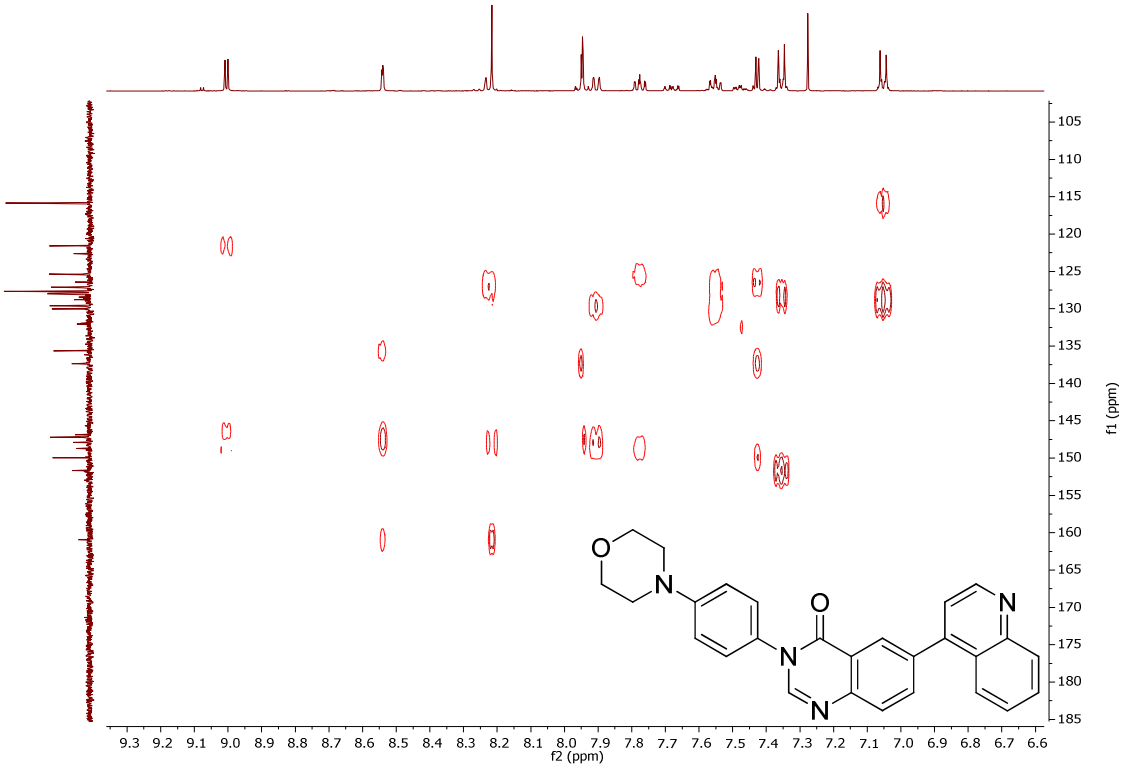
f2 (ppm)
f1 (ppm)

3-Phenyl-6-(quinolin-4-yl)quinazolin-4(3*H*)-one, 17

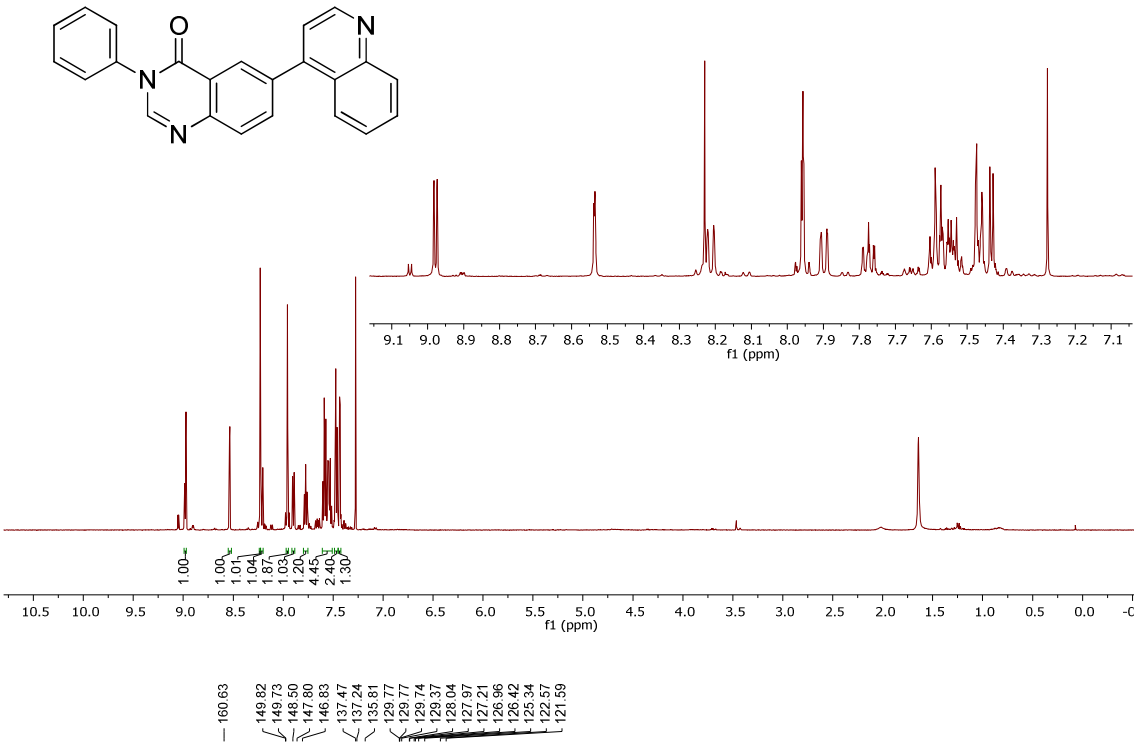

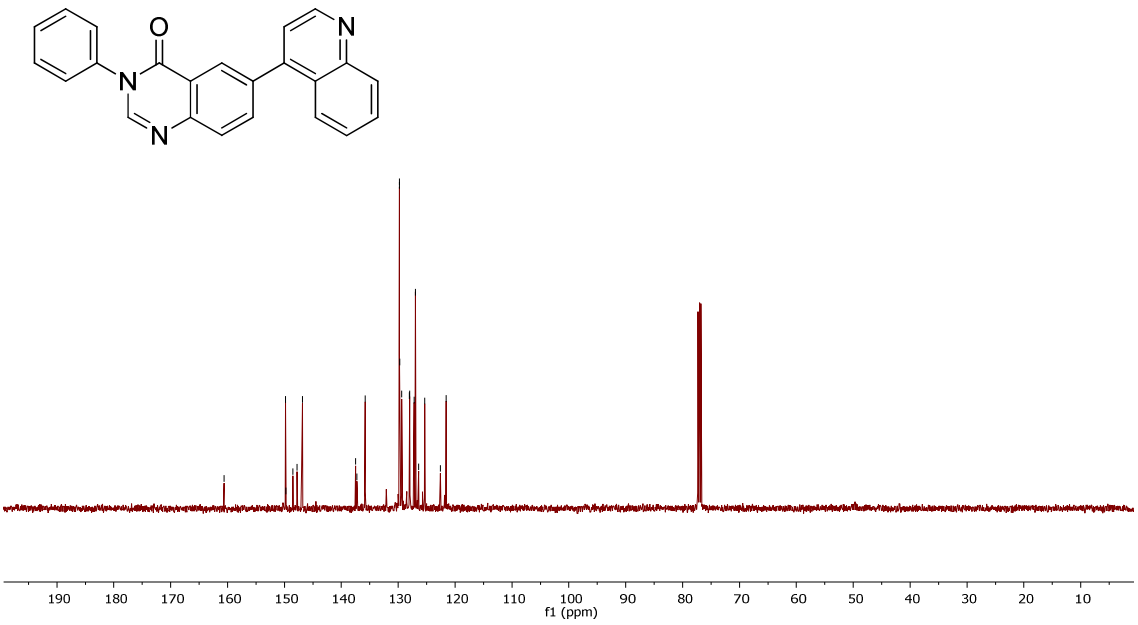

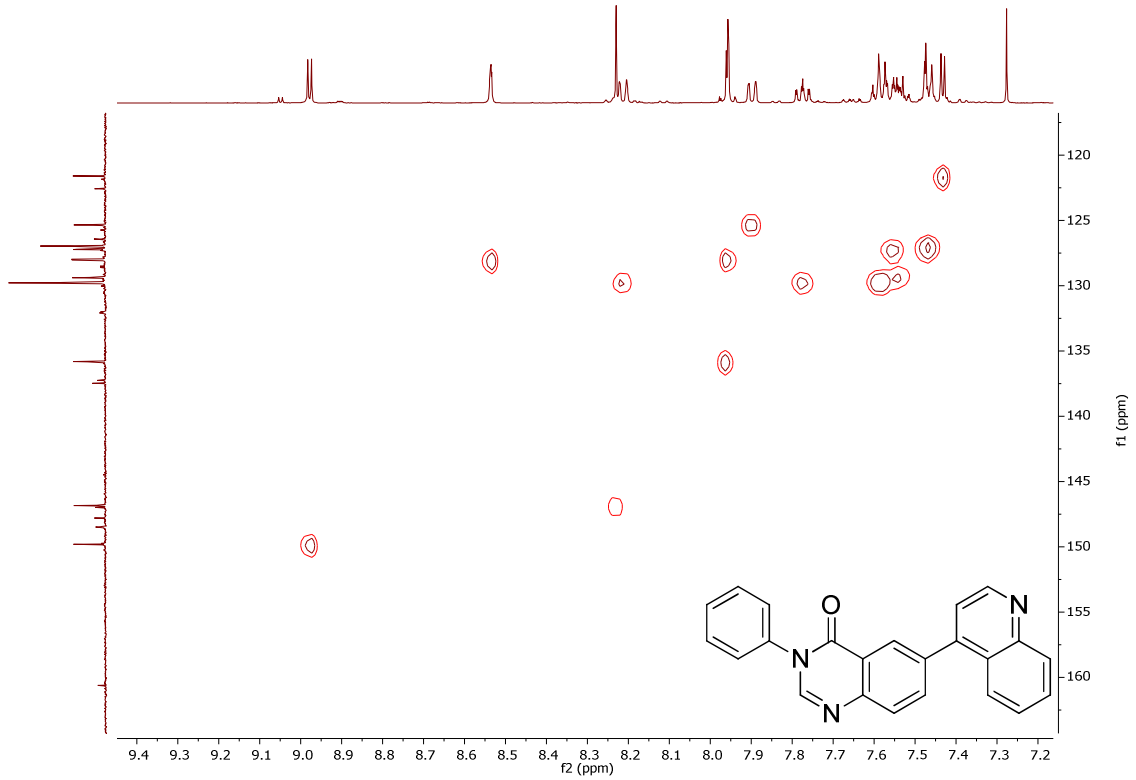
f2 (ppm)
f1 (ppm)
O
N
N
N

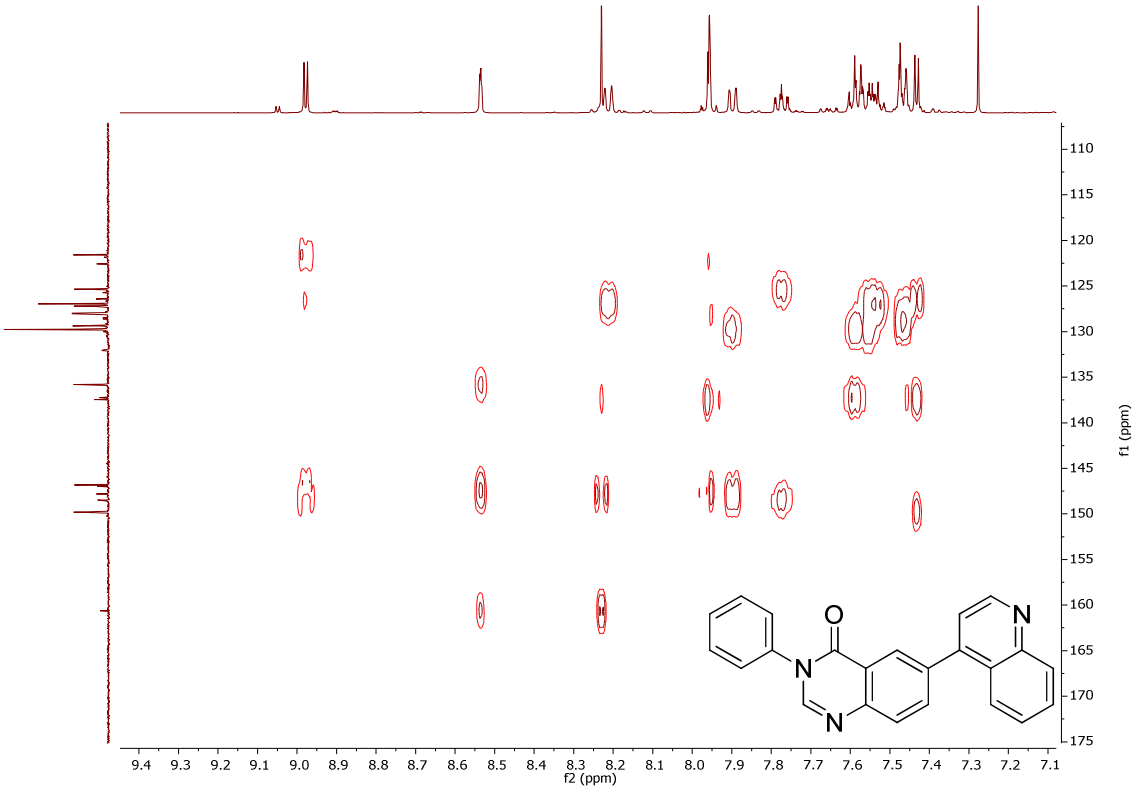
f2 (ppm)
f1 (ppm)
O
N
N
N

3-Cyclohexyl-6-(quinolin-4-yl)quinazolin-4(3*H*)-one, 18

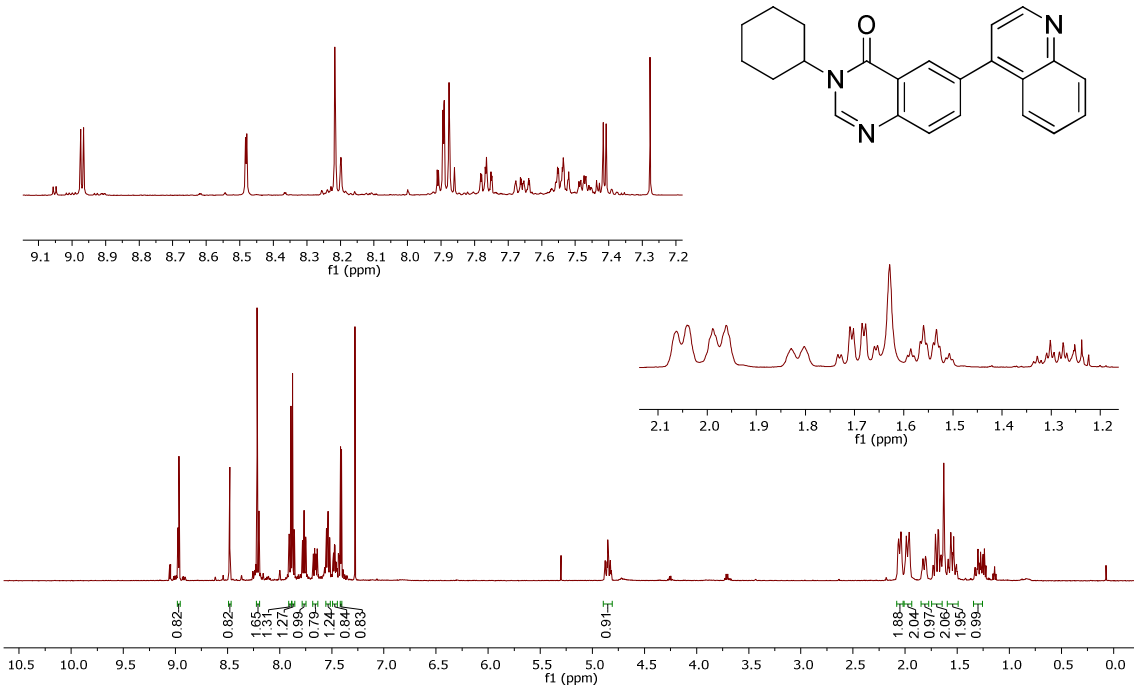

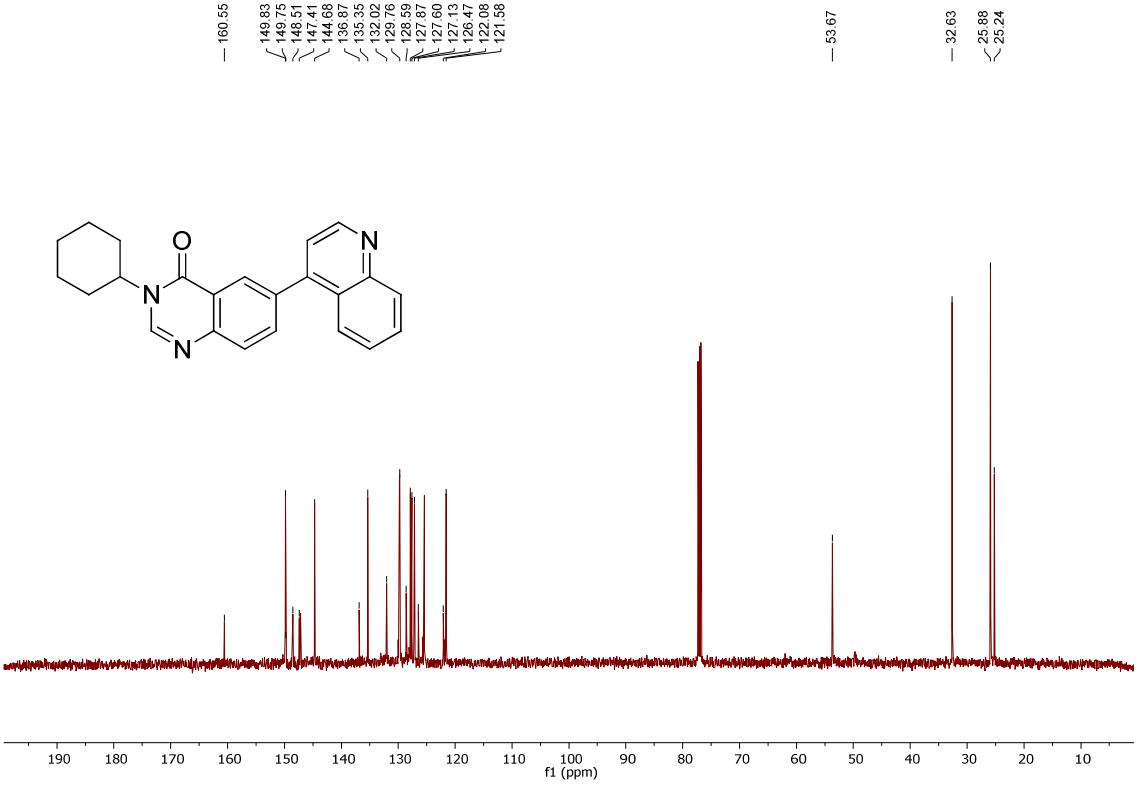

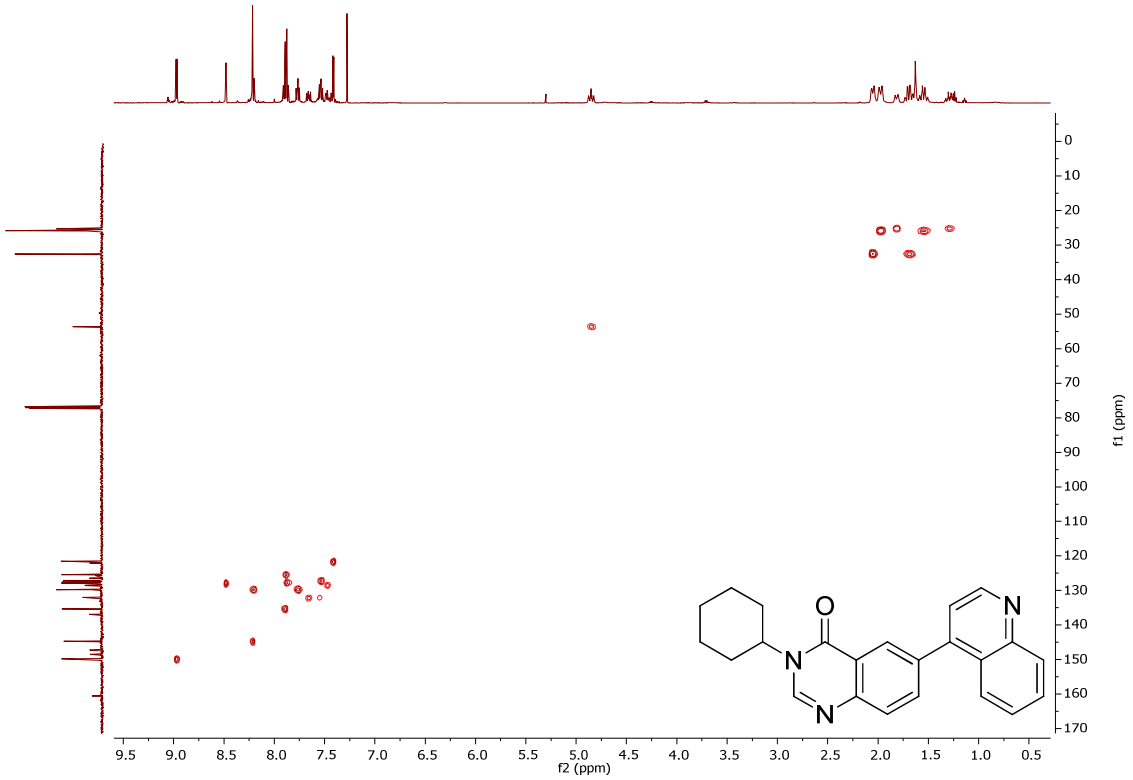
f2 (ppm)
f1 (ppm)
O
N
N
N

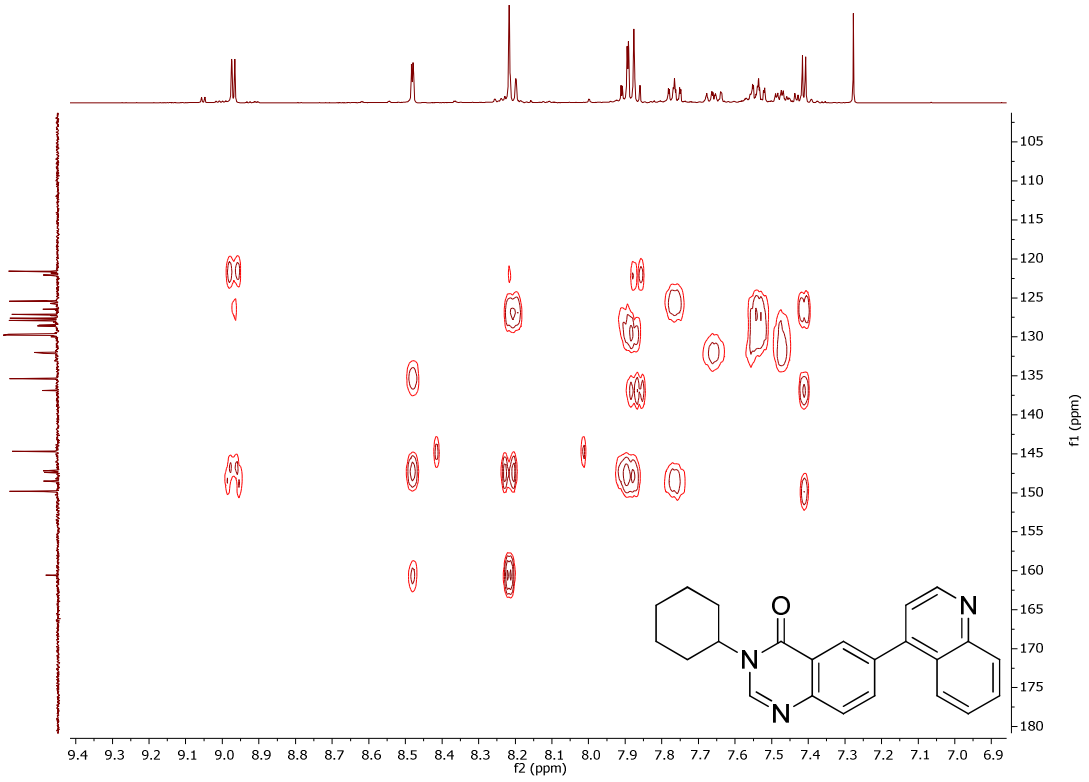
f2 (ppm)
f1 (ppm)
O
N
N
N

3-(3-Morpholinopropyl)-6-(quinolin-4-yl)quinazolin-4(3*H*)-one, 19

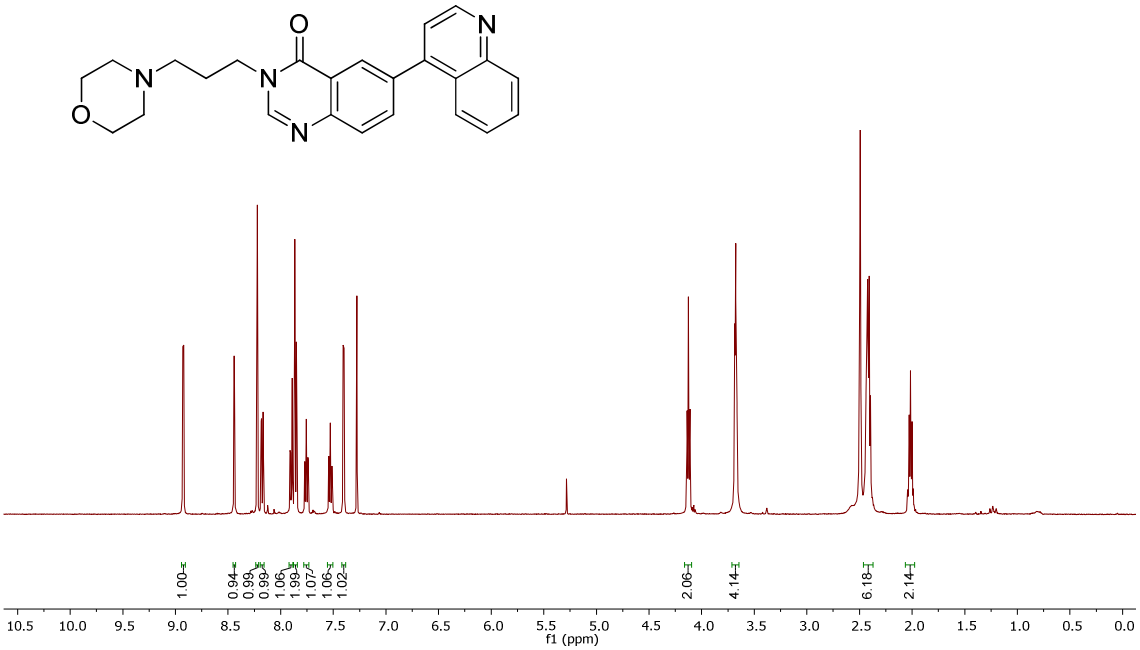

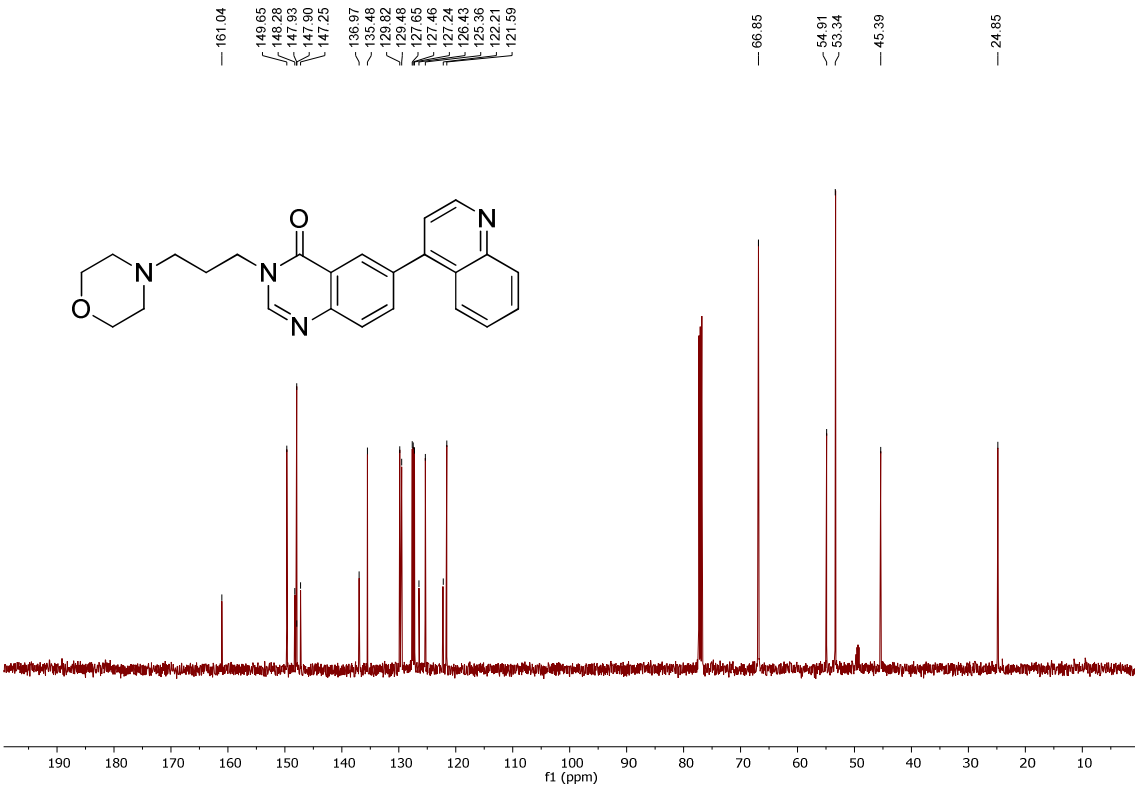

3-(4-(Dimethylamino)phenyl)-6-(quinolin-4-yl)quinazolin-4(3*H*)-one, 20

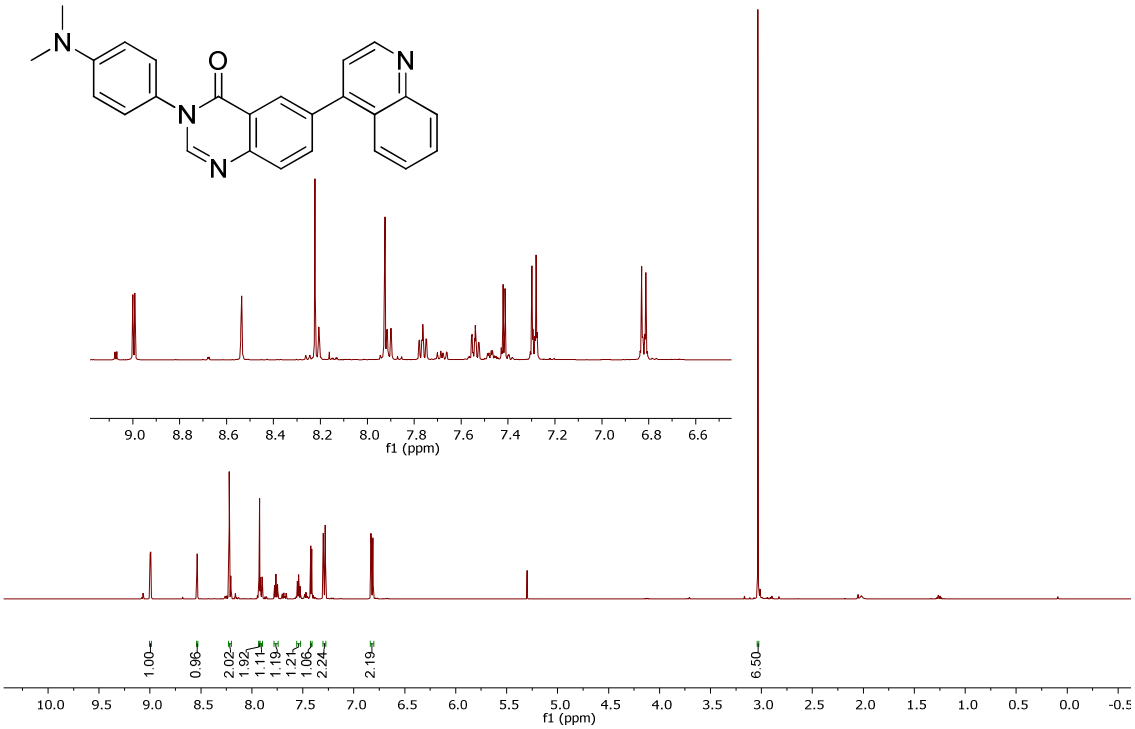

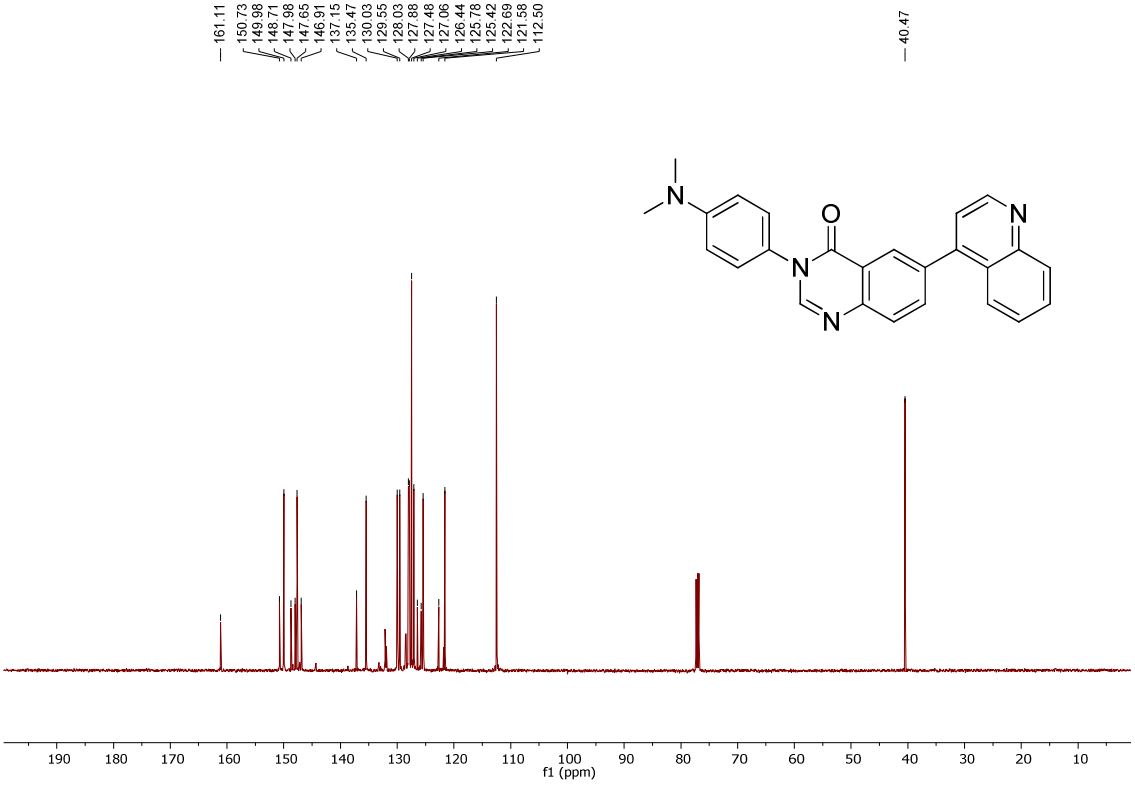

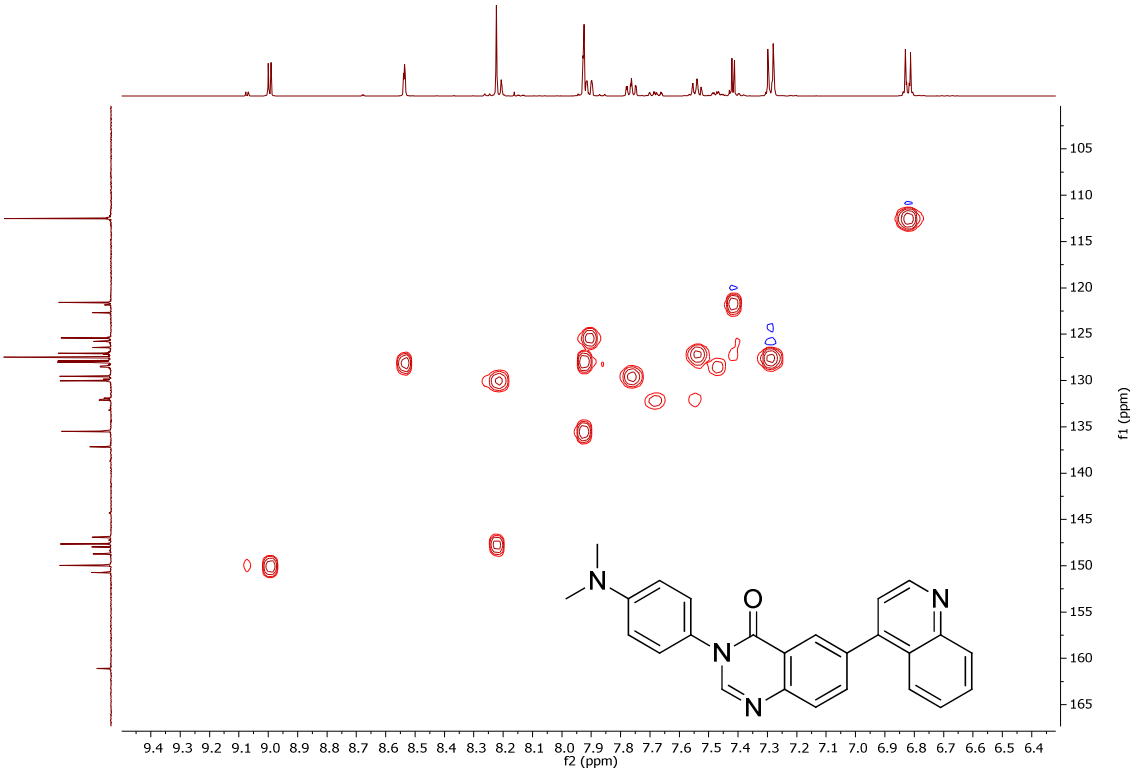
f2 (ppm)
f1 (ppm)
N
O
N
N

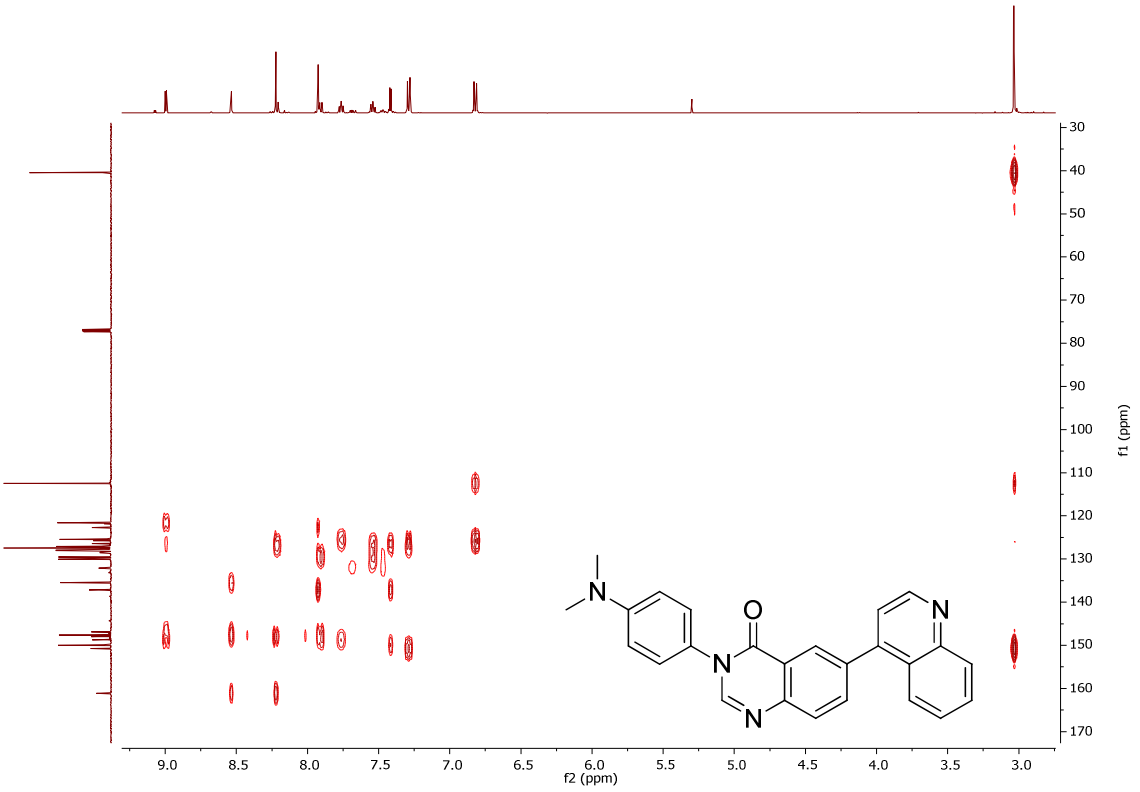
f2 (ppm)
f1 (ppm)
N
O
N
N

2,5-Dimethyl-6-(quinolin-4-yl)quinazolin-4(3*H*)-one, 21

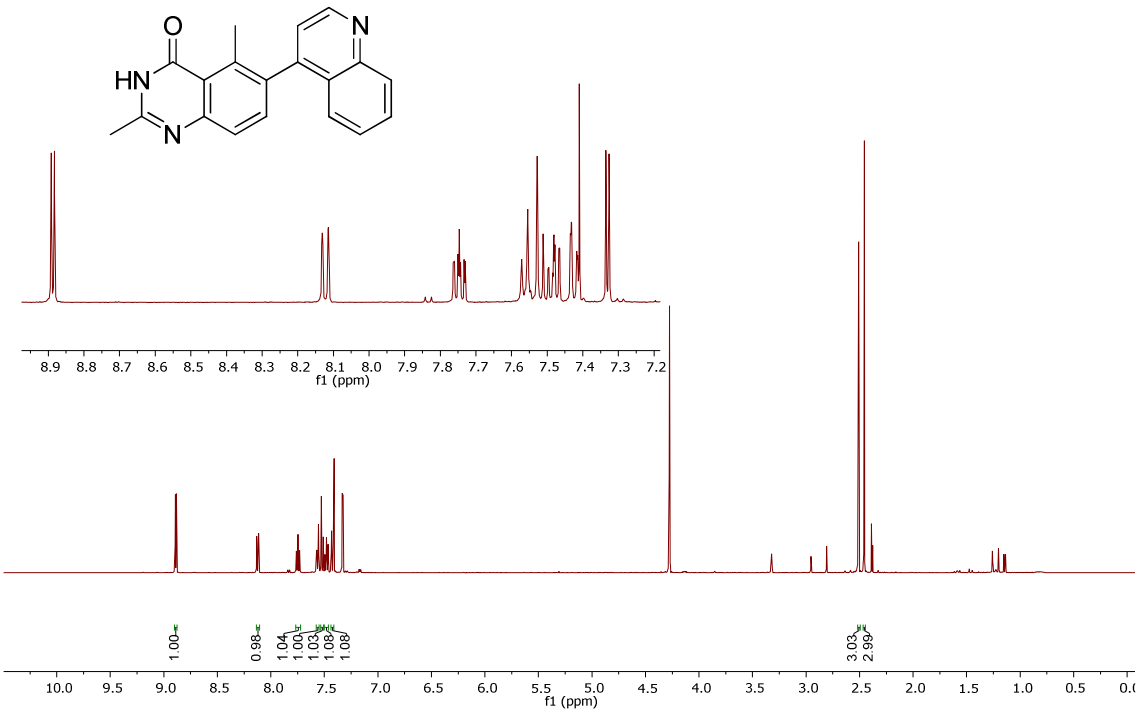

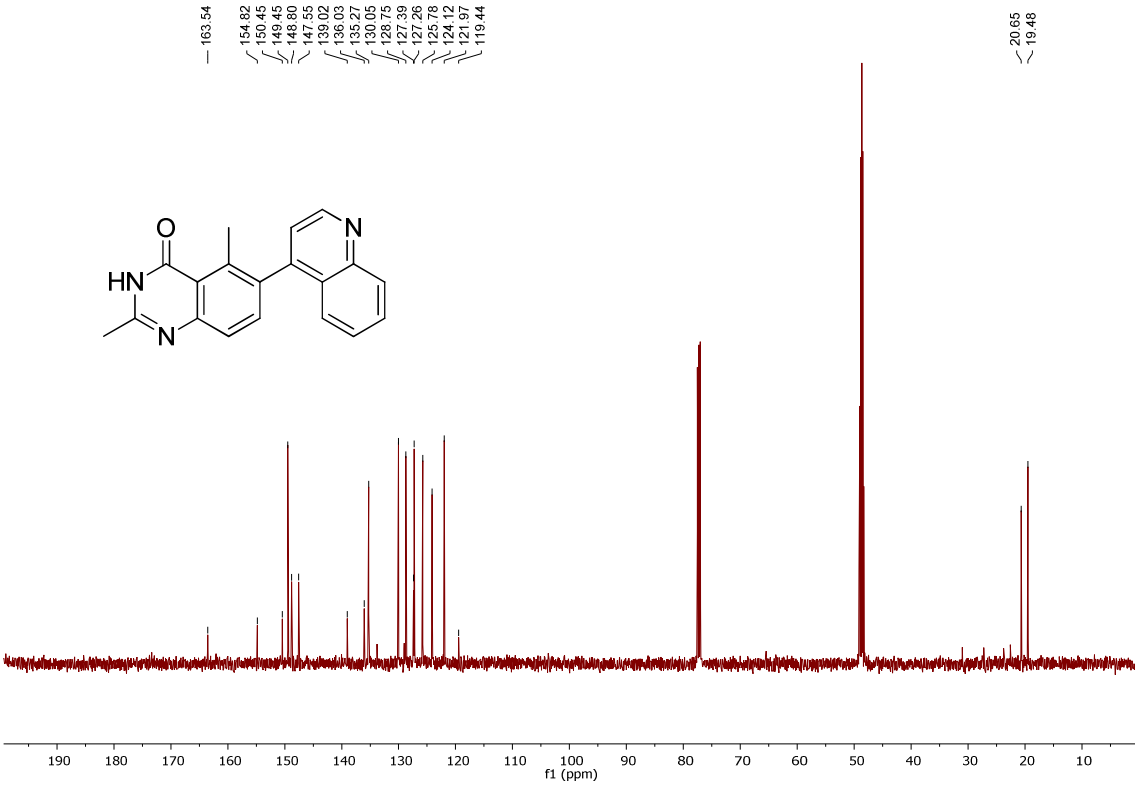

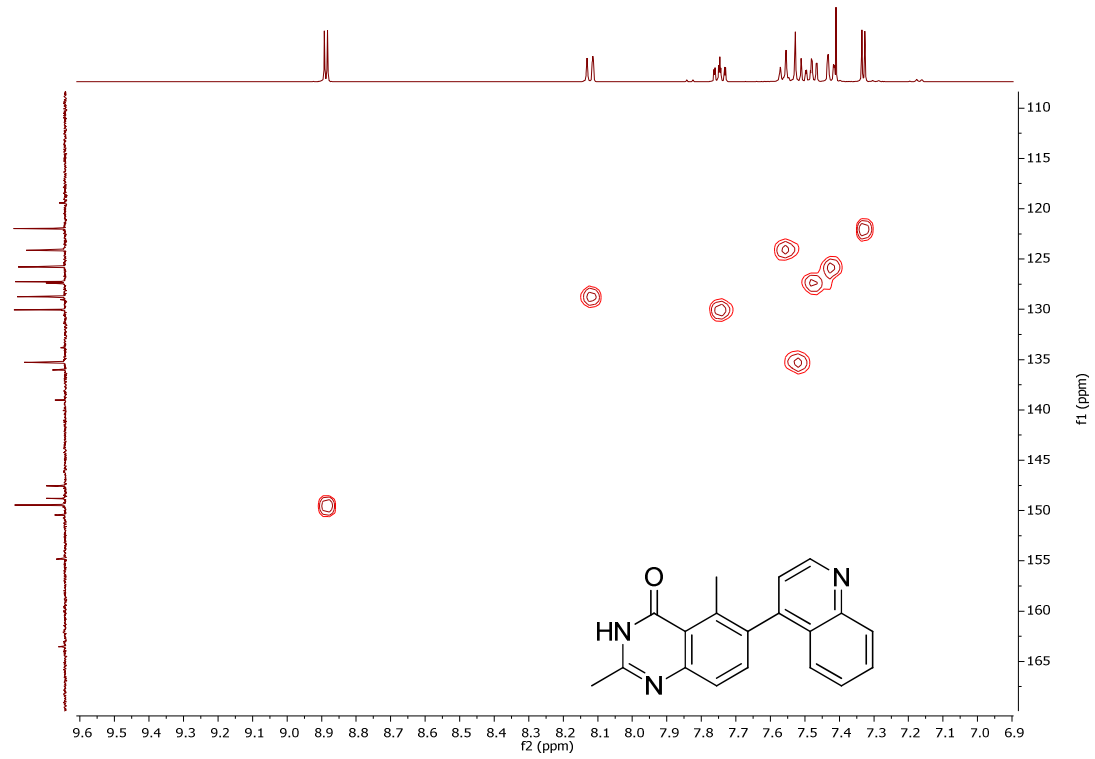
f2 (ppm)
f1 (ppm)
O
HN
N
N

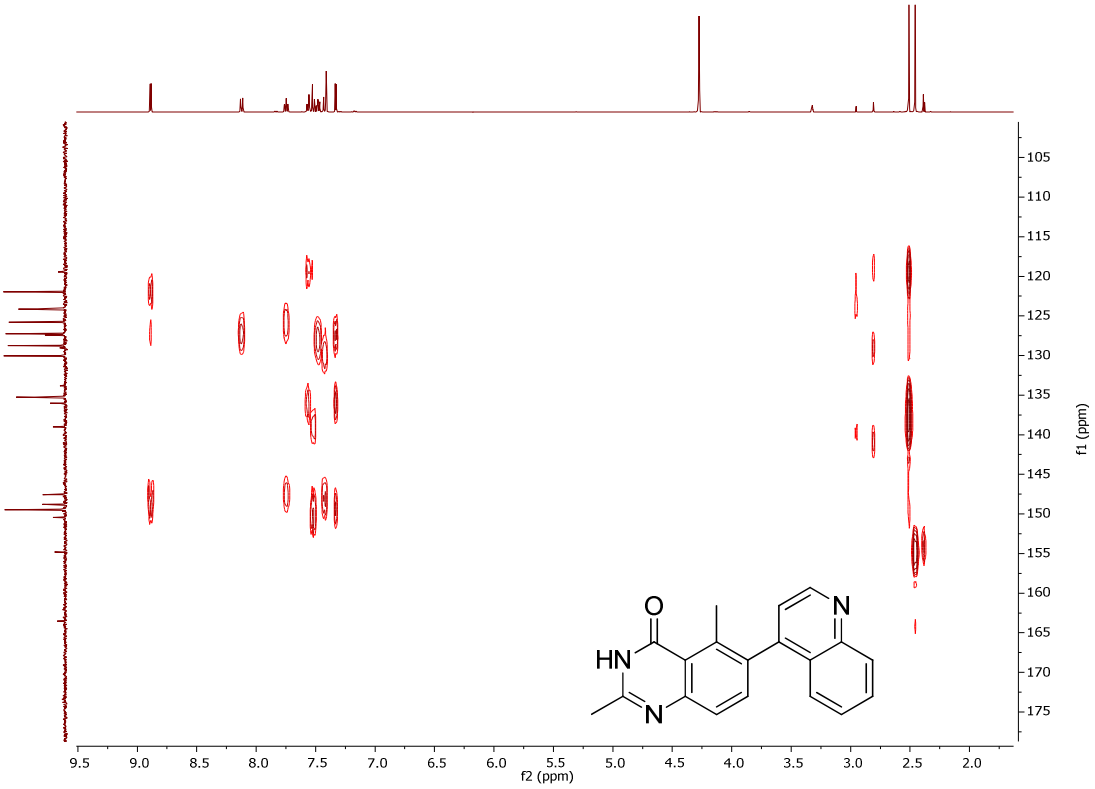
f2 (ppm)
f1 (ppm)
O
HN
N
N

2-Ethyl-5-methyl-6-(quinolin-4-yl)quinazolin-4(3*H*)-one, 22

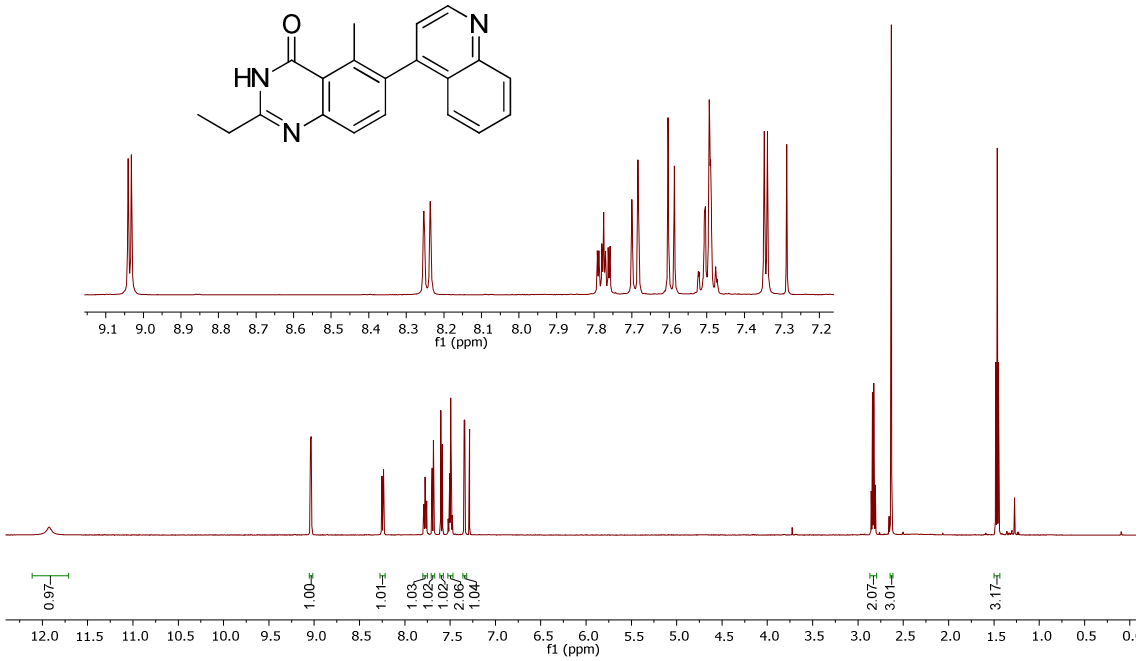

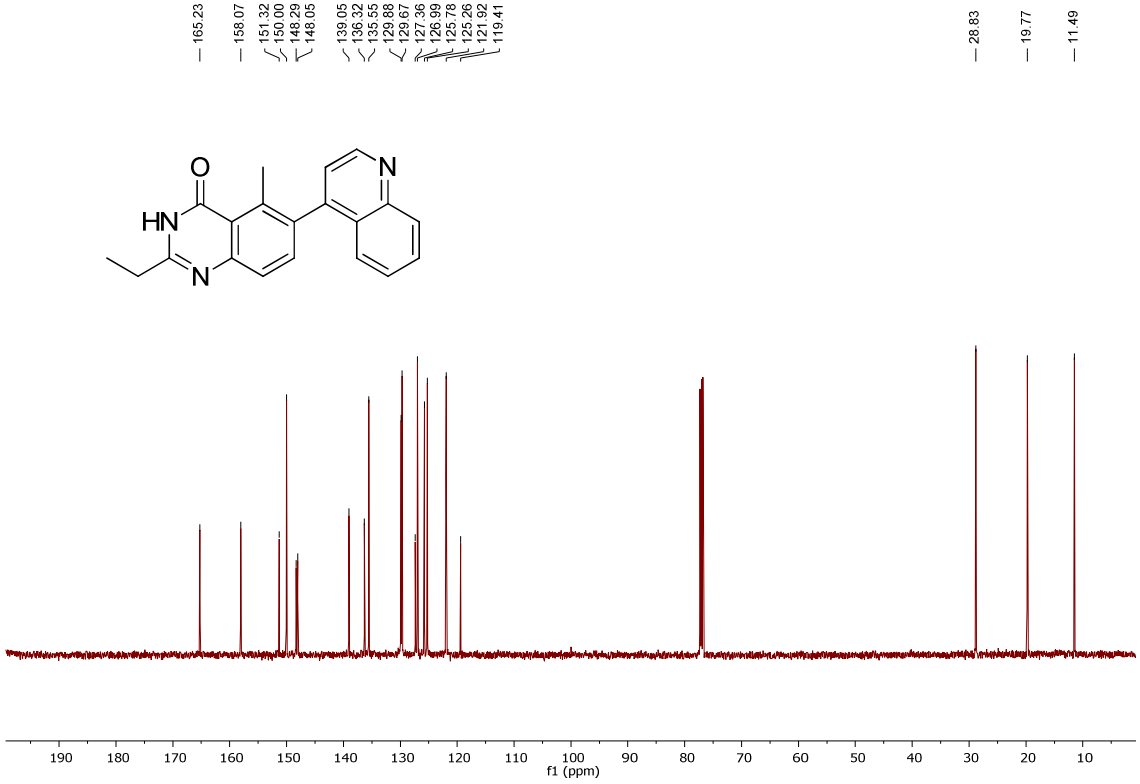

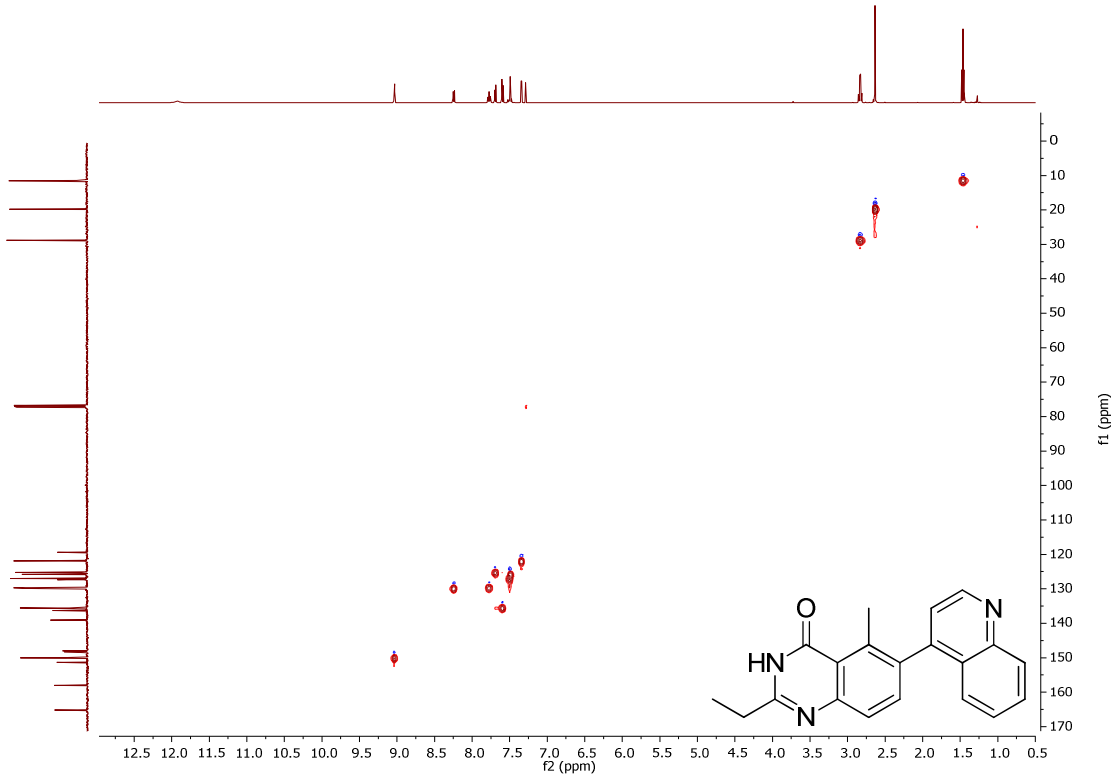
f2 (ppm)
f1 (ppm)
O
HN
N
N

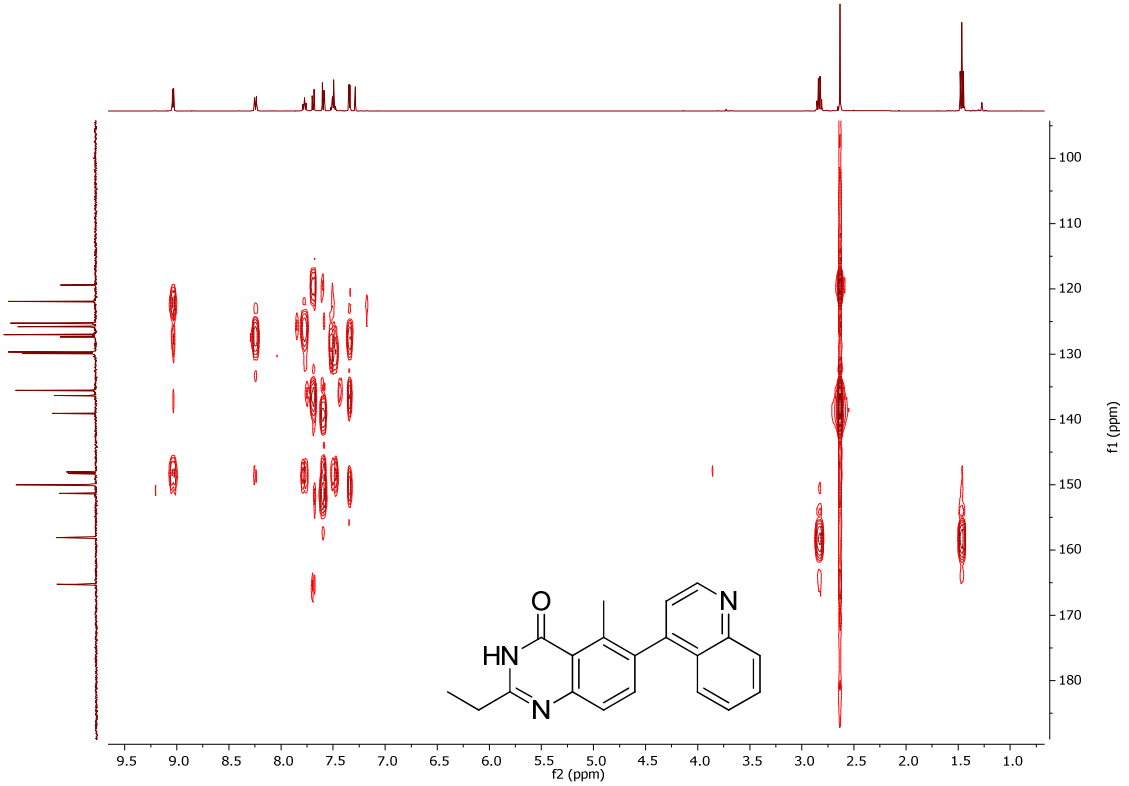
f2 (ppm)
f1 (ppm)
O
HN
N
N

2-Benzyl-5-methyl-6-(quinolin-4-yl)quinazolin-4(3*H*)-one, 23

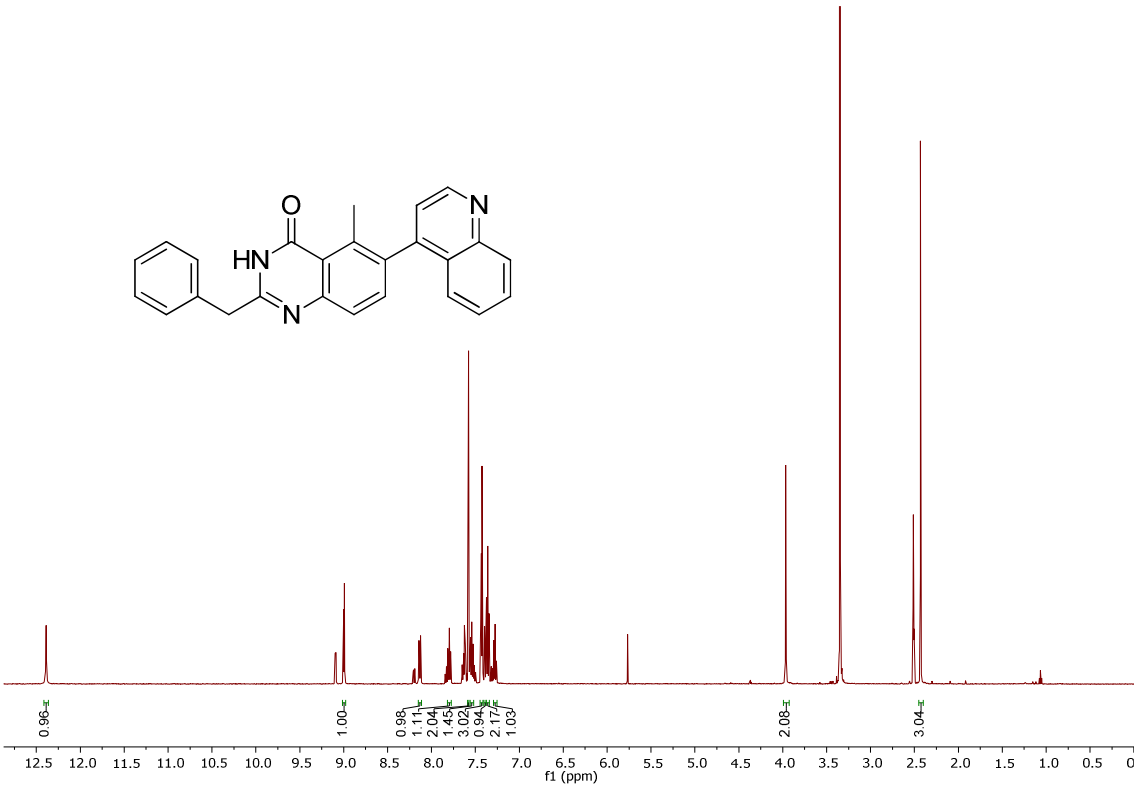

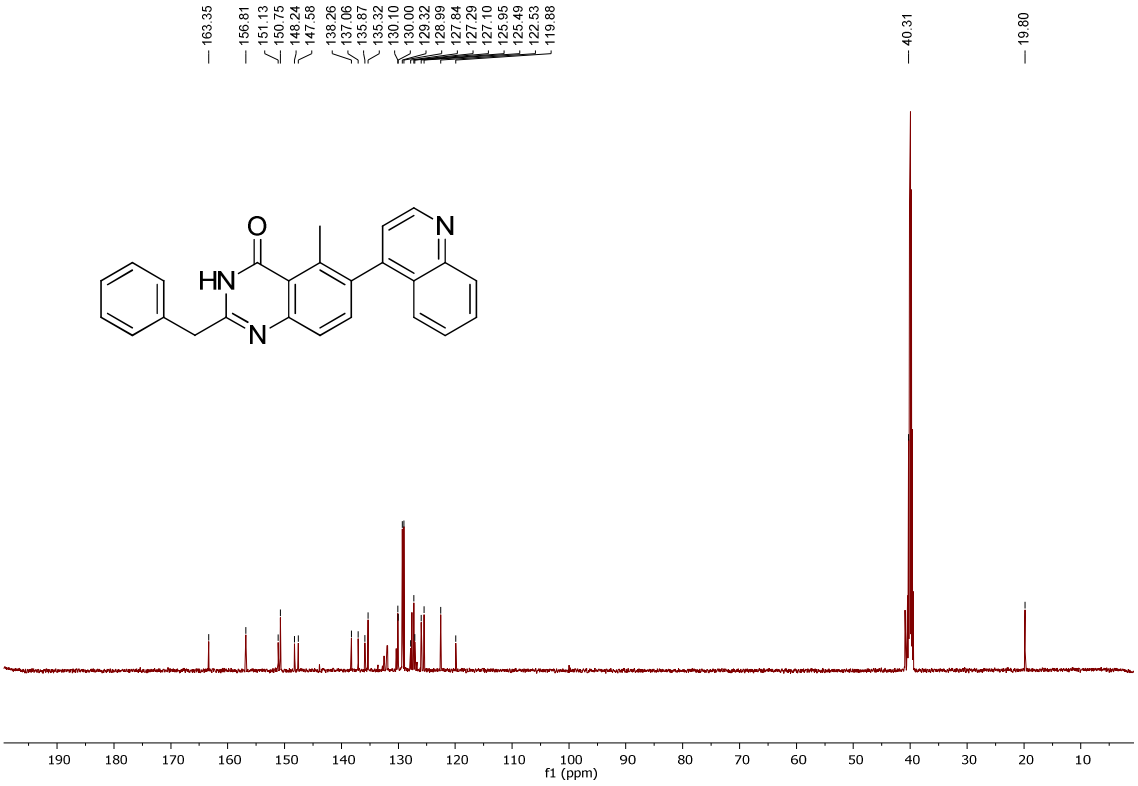

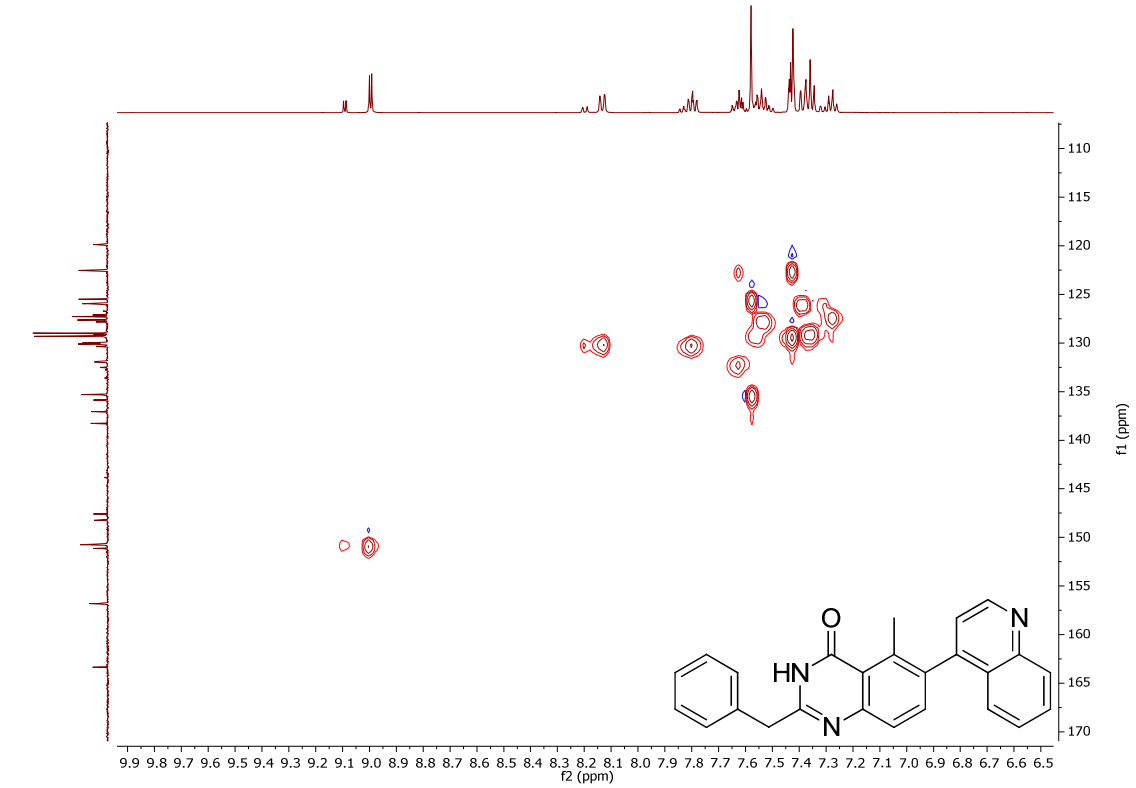
f2 (ppm)
f1 (ppm)
O
HN
N
N

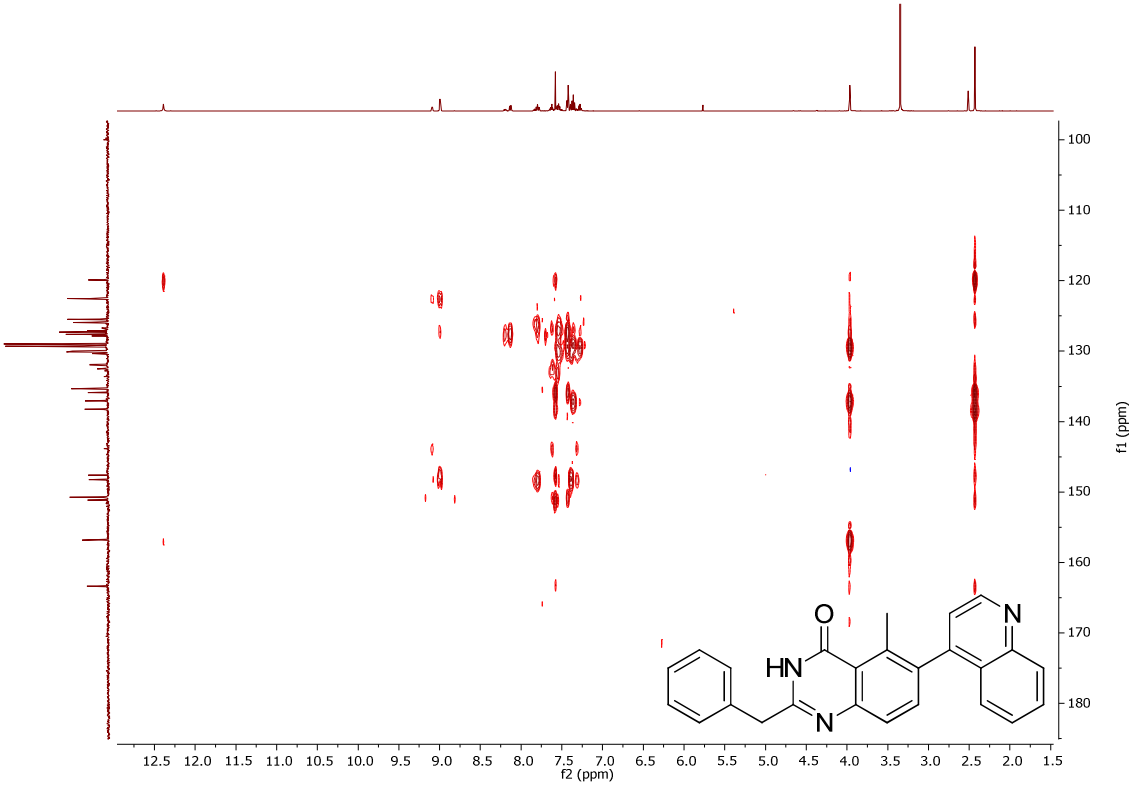
f2 (ppm)
f1 (ppm)
O
HN
N
N

3,8-Dimethyl-7-(quinolin-4-yl)isoquinolin-1(2*H*)-one, 24

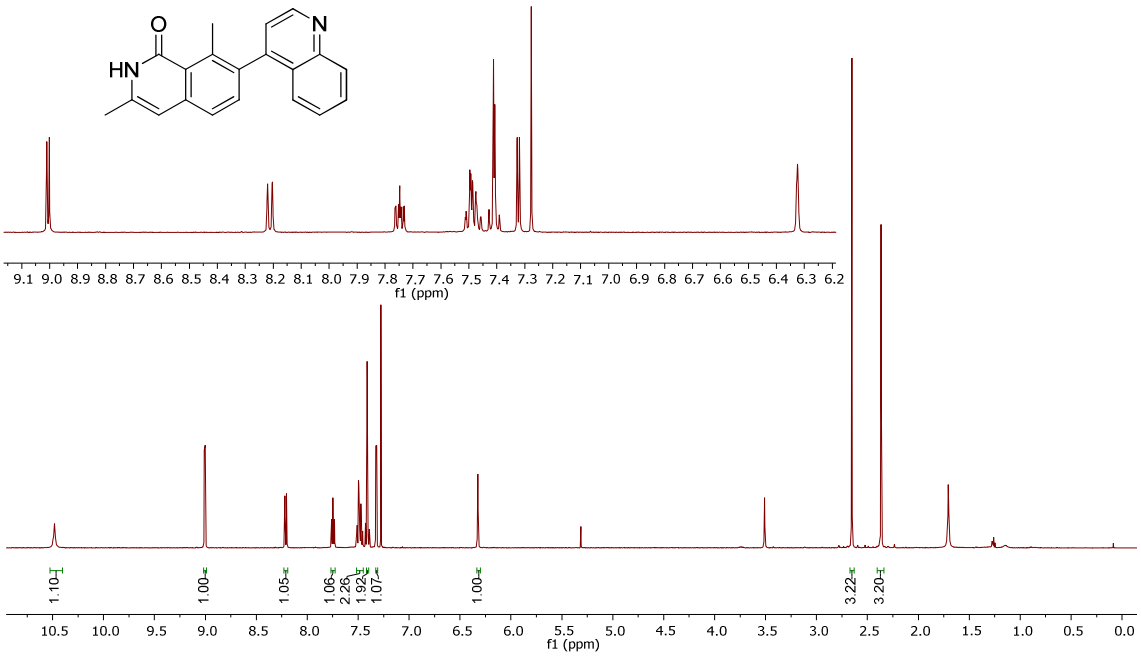

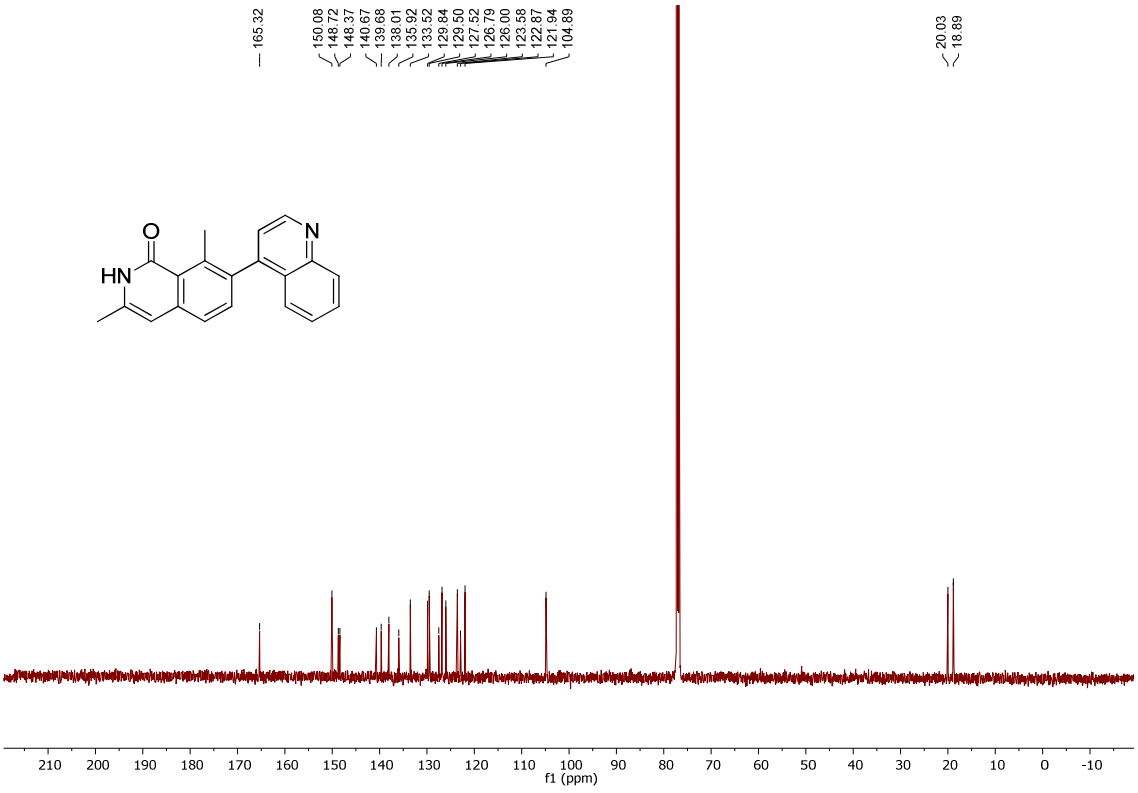

2-Benzyl-6-bromo-5-methylquinazolin-4(3*H*)-one, 26

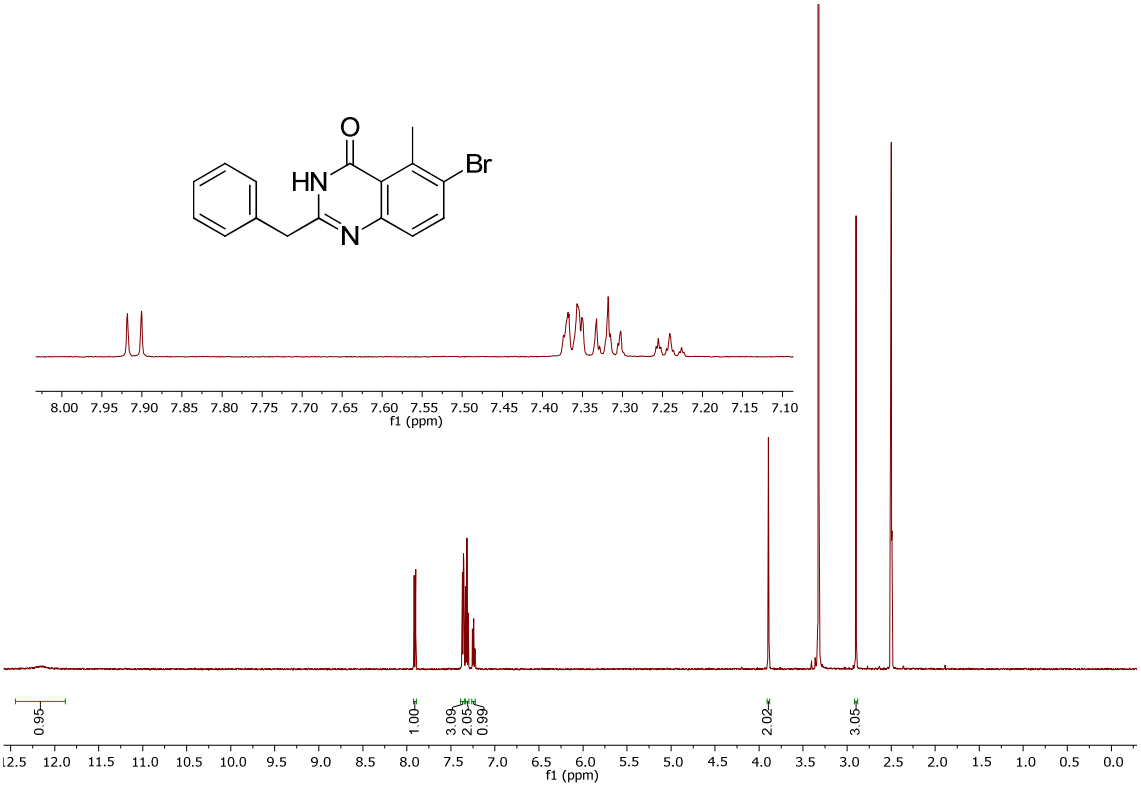

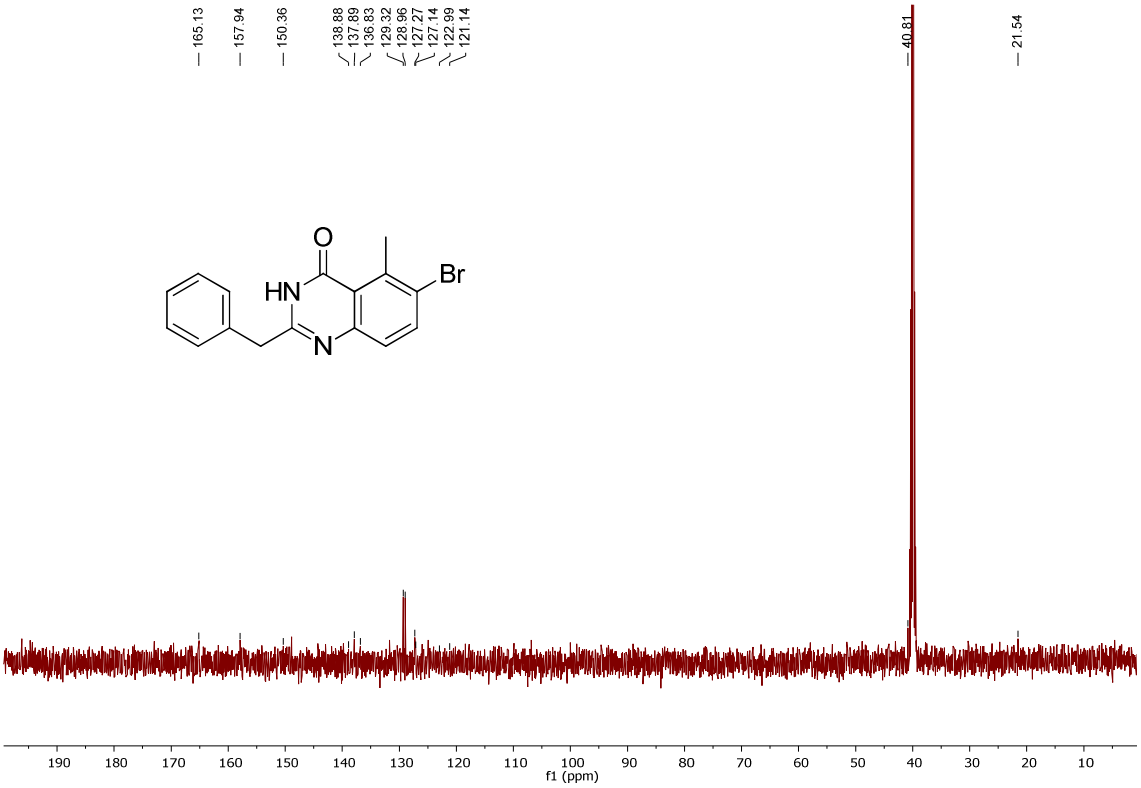

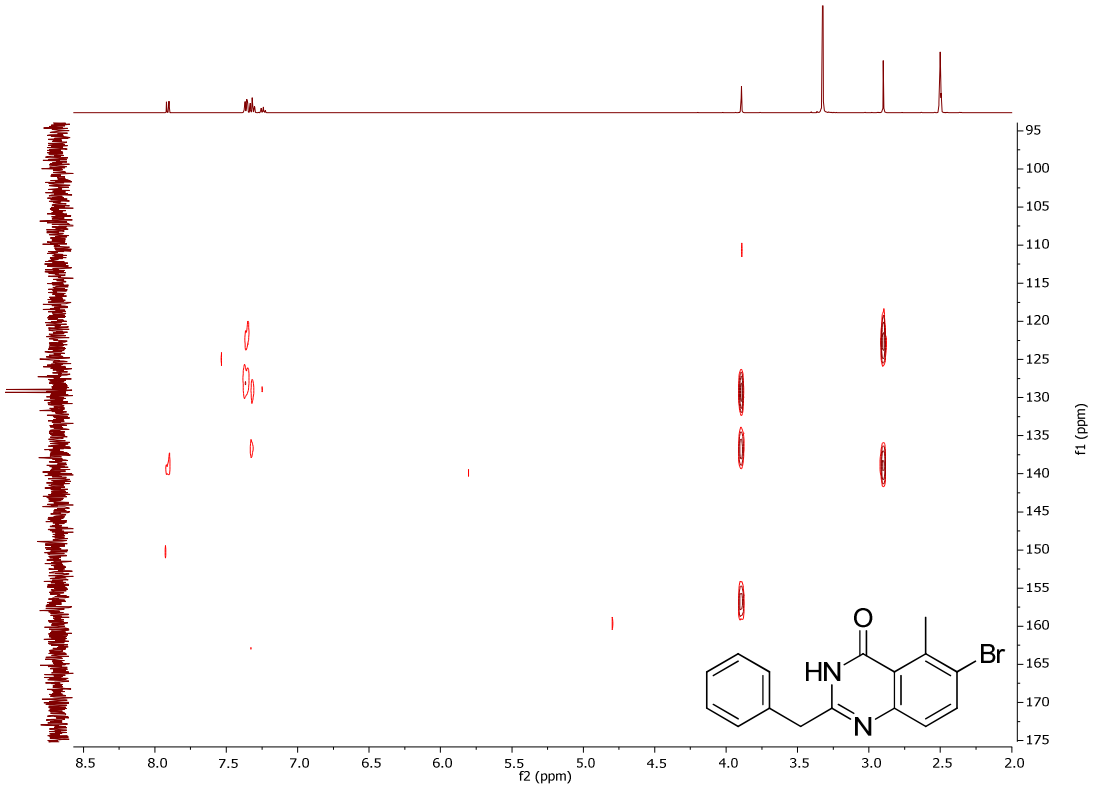

3-(4-Bromo-3-methylphenyl)-2-methylacrylic acid, 27

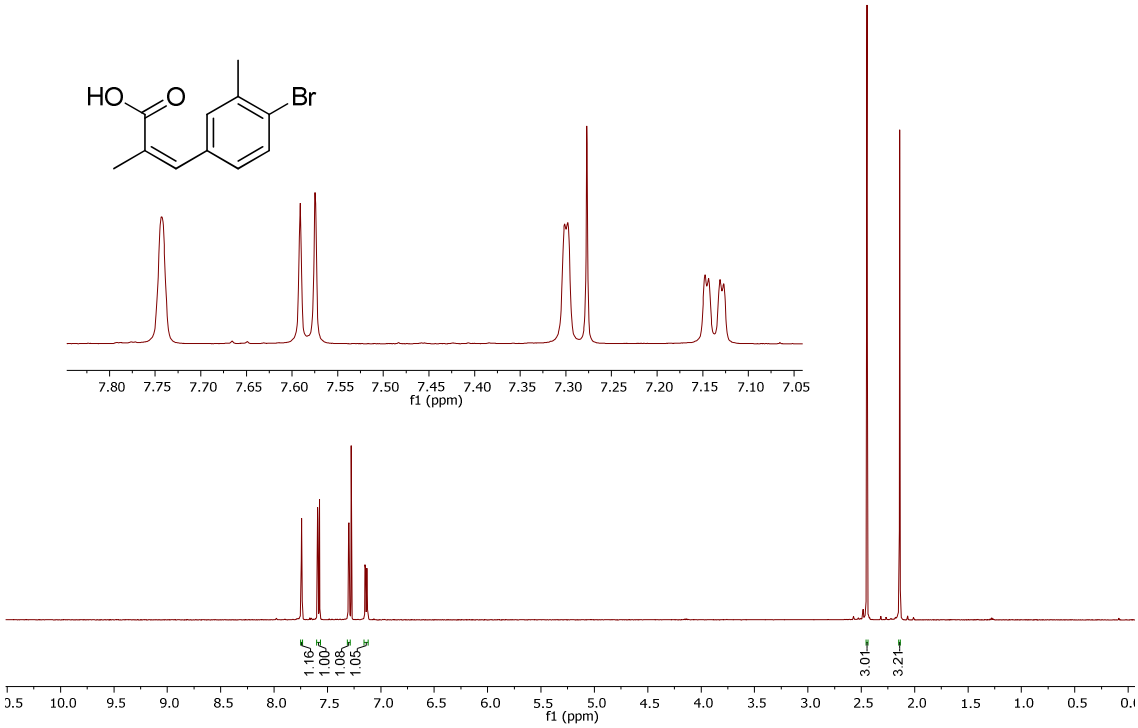

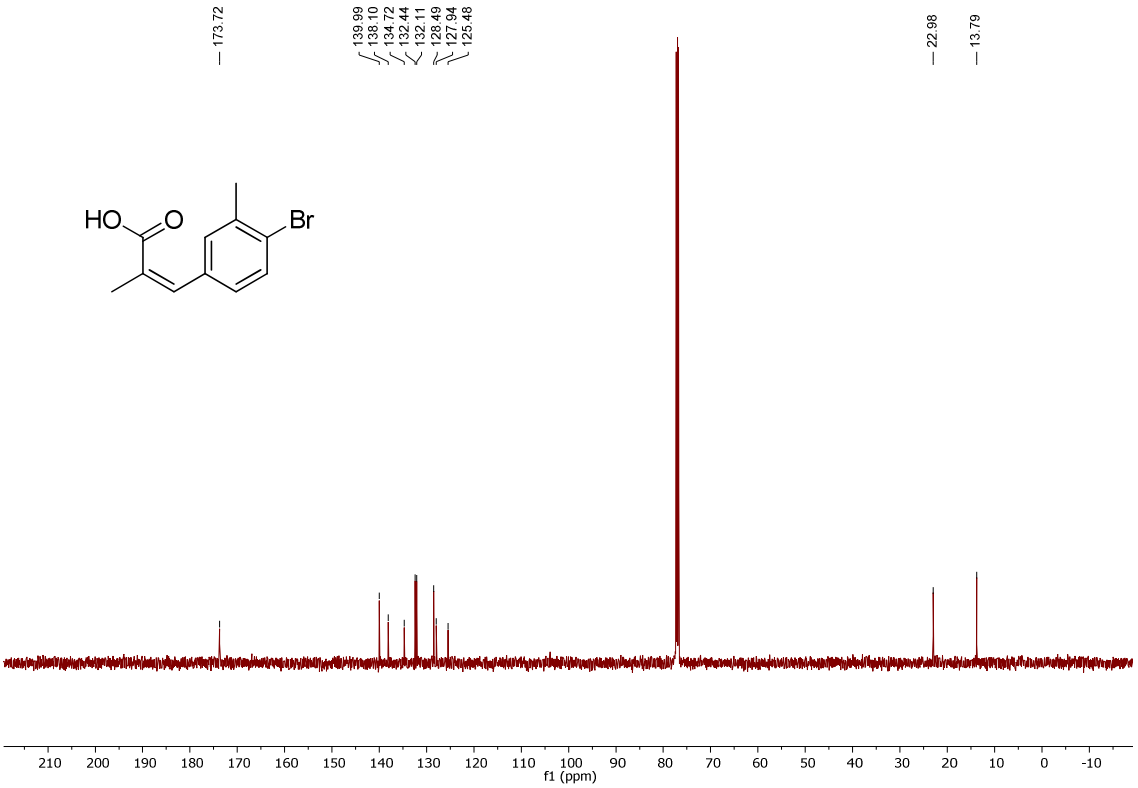

3-(4-Bromo-3-methylphenyl)-2-methylacryloyl azide, 28

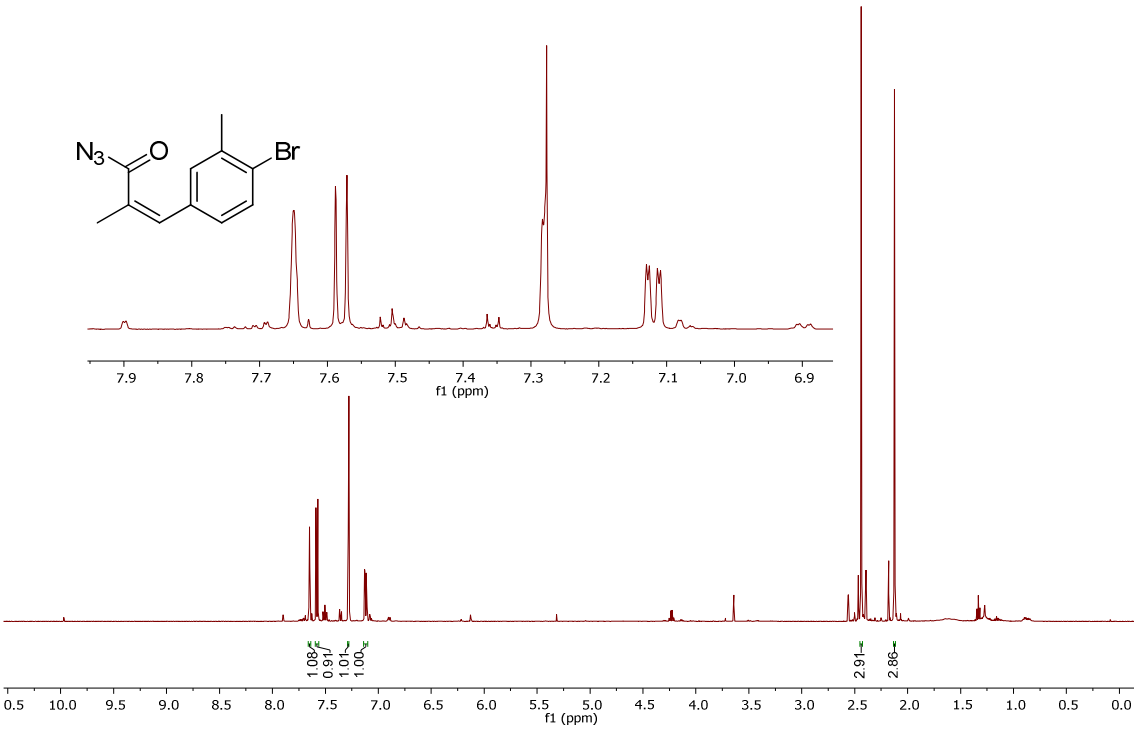

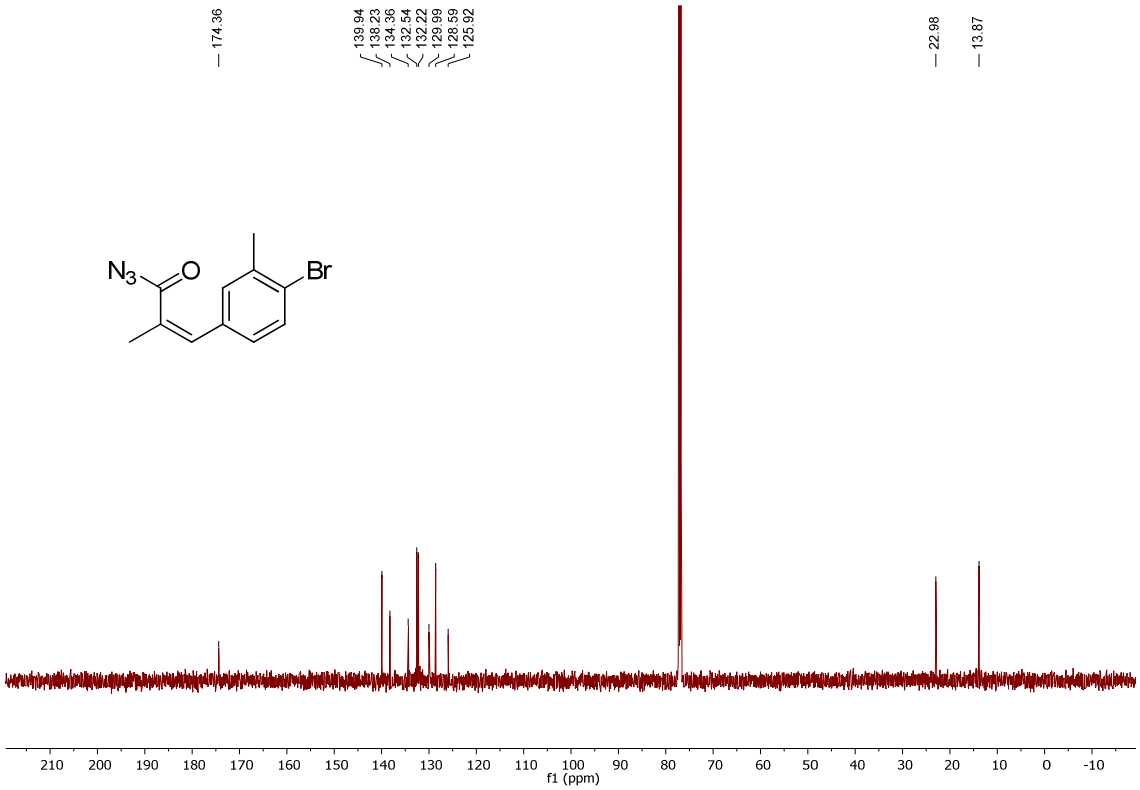

7-Bromo-3,8-dimethyl-2*H*-isoquinolin-1-one, 29

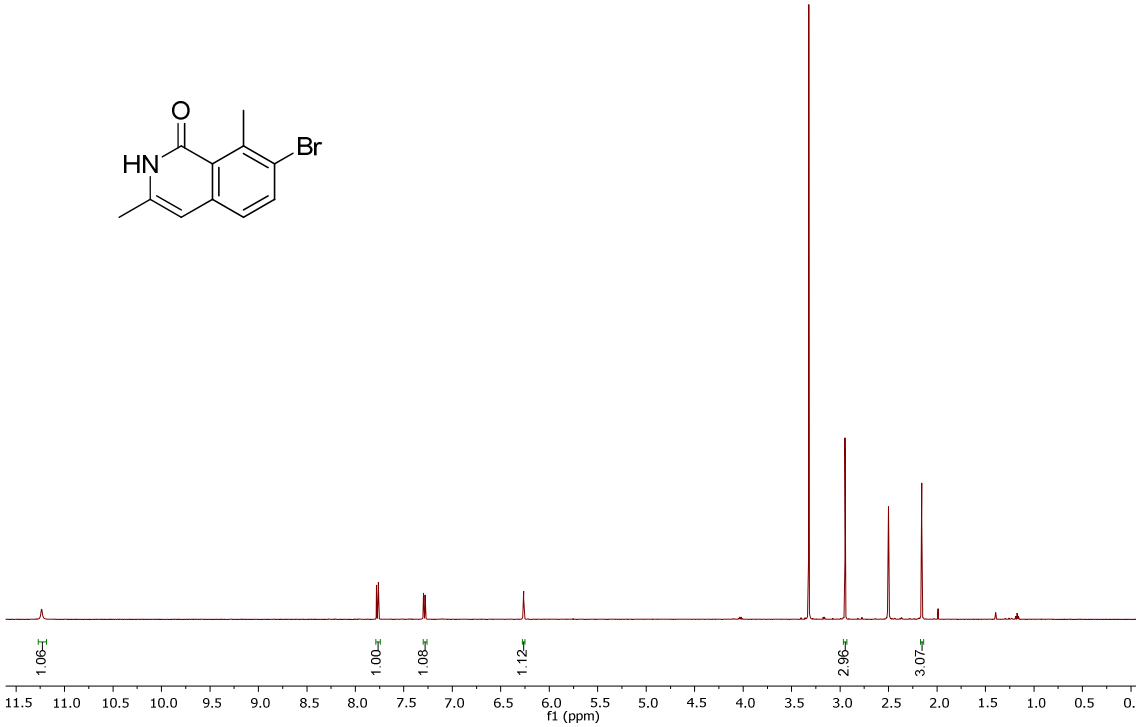

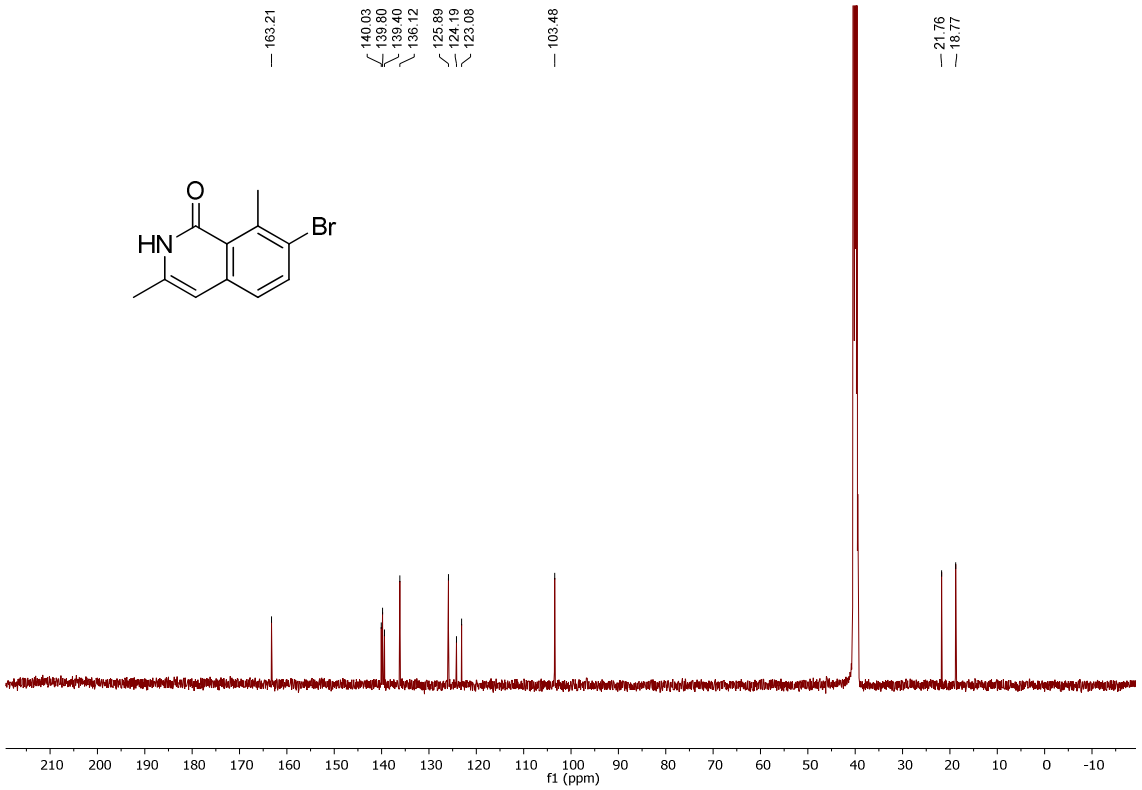
163.21
140.03
139.80
139.40
136.12
125.89
124.19
123.08
103.48
21.76
18.77
O
HN
Br
210 200 190 180 170 160 150 140 130 120 110 100 90 80 70 60 50 40 30 20 10 0 -10
f1 (ppm)

5. References

[1] Sanvitale, C. E.; Kerr, G.; Chaikuad, A.; Ramel, M.-C.; Mohedas, A. H.; Reichert, S.; Wang, Y.; Triffitt, J. T.; Cuny, G. D.; Yu, P. B.; Hill, C. S.; Bullock, A. N. A new class of small molecule inhibitor of BMP signalling. *PLoS One* **2013**, *8* (4), e62721.

[2] Battye, T. G. G.; Kontogiannis, L.; Johnson, O.; Powell, H. R.; Leslie, A. G. W. iMOSFLM: a new graphical interface for diffraction-image processing with MOSFLM. *Acta Crystallogr. Sect. D Biol. Crystallogr.* **2011**, *67* (4), 271-281.

[3] Winn, M. D.; Ballard, C. C.; Cowtan, K. D.; Dodson, E. J.; Emsley, P.; Evans, P. R.; Keegan, R. M.; Krissinel, E. B.; Leslie, A. G. W.; McCoy, A.; McNicholas, S. J.; Murshudov, G. N.; Pannu, N. S.; Potterton, E. A.; Powell, H. R.; Read, R. J.; Vagin, A.; Wilson, K. S. Overview of the CCP4 suite and current developments. *Acta Crystallogr. Sect. D Biol. Crystallogr.* **2011**, *67* (4), 235-242.

[4] McCoy, A. J.; Grosse-Kunstleve, R. W.; Adams, P. D.; Winn, M. D.; Storoni, L. C.; Read, R. J. Phaser crystallographic software. *J. Appl. Crystallogr.* **2007**, *40* (4), 658-674.

[5] Emsley, P.; Lohkamp, B.; Scott, W. G.; Cowtan, K. Features and development of Coot. *Acta Crystallogr. Sect. D Biol. Crystallogr.* **2010**, *66* (4), 486-501.

[6] Murshudov, G. N.; Vagin, A. A.; Dodson, E. J. Refinement of Macromolecular Structures by the Maximum-Likelihood Method. *Acta Crystallogr. Sect. D Biol. Crystallogr.* **1997**, *53* (3), 240-255.

[7] Afonine, P. V.; Grosse-Kunstleve, R. W.; Echols, N.; Headd, J. J.; Moriarty, N. W.; Mustyakimov, M.; Terwilliger, T. C.; Urzhumtsev, A.; Zwart, P. H.; Adams, P. D. Towards automated crystallographic structure refinement with phenix.refine. *Acta Crystallogr. Sect. D Biol. Crystallogr.* **2012**, *68* (4), 352-367.

[8] Painter, J.; Merritt, E. A. Optimal description of a protein structure in terms of multiple groups undergoing TLS motion. *Acta Crystallogr. Sect. D Biol. Crystallogr.* **2006**, *62* (4), 439-450.

[9] Davis, I. W.; Leaver-Fay, A.; Chen, V. B.; Block, J. N.; Kapral, G. J.; Wang, X.; Murray, L. W.; Arendall, W. B.; Snoeyink, J.; Richardson, J. S.; Richardson, D. C. MolProbity: all-atom contacts and structure validation for proteins and nucleic acids. *Nucleic Acids Res.* **2007**, *35* (SUPPL.2), 375-383.